Tarik Hubana, MSc

Artificial Neural Networks Application for Station Protection

DOCTORAL THESIS

to achieve the university degree of

Doktor der technischen Wissenschaften

submitted to

Graz University of Technology

Supervisor

em. Univ. Prof. Dipl.-Ing. Dr. techn., Lothar Fickert

Institute of Electrical Power Systems

Graz, July 2020

AFFIDAVIT

I declare that I have authored this thesis independently, that I have not used other than the declared sources/resources, and that I have explicitly indicated all material which has been quoted either literally or by content from the sources used. The text document uploaded to TUGRAZonline is identical to the present doctoral thesis.

Date

Signature

Institute of Electrical Power Systems

IEAN

Artificial Neural Networks Application for Station Protection

A Dissertation by
Tarik Hubana

Supervisor
em. Univ. Prof. Dipl.-Ing. Dr. techn. Lothar Fickert

Reviewer
Prof. Dr.-Ing. habil. Krzysztof Rudion

July 2020

Graz University of Technology
Institute of Electric Power Systems
Inffeldgasse 18/I
8010 Graz
Austria

Head of Institute
Univ.-Prof. Dipl.-Ing. Dr.techn. Robert Schürhuber

Supervisor
em. Univ. Prof. Dipl.-Ing. Dr. techn. Lothar Fickert

Reviewer
Prof. Dr.-Ing. habil. Krzysztof Rudion

A Dissertation by
Tarik Hubana

July 2020

Statutory Declaration

I declare that I have authored this thesis independently, that I have not used other than the declared sources / resources, and that I have explicitly marked all material which has been quoted either literally or by content from the used sources.

Graz, 27.04.2020.

Tarik Hubana

Tarik Hubana

Eidesstattliche Erklärung

Ich erkläre an Eides statt, dass ich die vorliegende Arbeit selbstständig verfasst, andere als die angegebenen Quellen/Hilfsmittel nicht benutzt, und die den benutzten Quellen wörtlich und inhaltlich entnommenen Stellen als solche kenntlich gemacht habe.

Graz, am 27.04.2020.

Tarik Hubana

Tarik Hubana

Confirmations of the share of the doctoral candidate in the publications

Paper A: Artificial Intelligence based Station Protection Concept for Medium Voltage Microgrids

I, as an author of the publication: "*T. Hubana, "Artificial Intelligence based Station Protection Concept for Medium Voltage Microgrids," 2020 19th International Symposium INFOTEH-JAHORINA (INFOTEH), East Sarajevo, Bosnia and Herzegovina, 2020, pp. 1-6.",* confirm that my share is 100% in this publication.

_____
Tarik Hubana

_____
Date

Paper B: New Approach for Fault Identification and Classification in Microgrids

I, as a co-author of the publication: "*T. Hubana, M. Šarić, S. Avdaković, „New Approach for Fault Identification and Classification in Microgrids" In: Avdaković S., Mujčić A., Mujezinović A., Uzunović T., Volić I. (eds) Advanced Technologies, Systems, and Applications IV. IAT 2019. Lecture Notes in Networks and Systems, vol 83. Springer, Cham 2020",* confirm that the share of the co-author and the doctoral candidate Tarik Hubana is at least 50% in this publication.

_____	_____	_____
Tarik Hubana	Mirza Šarić	Samir Avdaković

_____
Date

Paper C: Willingness to Pay for Reliable Electricity: A Contingent Valuation Study in Bosnia and Herzegovina

I, as a co-author of the publication: "*T. Hubana, N. Ljevo, „Willingness to Pay for Reliable Electricity: A Contingent Valuation Study in Bosnia and Herzegovina" In: Avdaković S., Mujčić A., Mujezinović A., Uzunović T., Volić I. (eds) Advanced Technologies, Systems, and Applications IV. IAT 2019. Lecture Notes in Networks and Systems, vol 83. Springer, Cham 2020",* confirm that the share of the co-author and the doctoral candidate Tarik Hubana is at least 50% in this publication.

_____	_____
Tarik Hubana	Nerman Ljevo

_____
Date

Paper D: Classification of Distribution Network Faults Using Hilbert-Huang Transform and Artificial Neural Network

I, as a co-author of the publication: "*T. Hubana, M. Šarić, S. Avdaković, "Classification of Distribution Network Faults Using Hilbert-Huang Transform and Artificial Neural Network", In: Avdaković S. (eds) Advanced Technologies, Systems, and Applications III. IAT 2018. Lecture Notes in Networks and Systems, vol 59. Springer, Cham 2019",* confirm that the share of the co-author and the doctoral candidate Tarik Hubana is at least 50% in this publication.

_____	_____	_____
Tarik Hubana	Mirza Šarić	Samir Avdaković

_____

Date

Paper E: Transmission lines fault location estimation based on artificial neural networks and power quality monitoring data

I, as an author of the publication: "*T. Hubana, "Transmission lines fault location estimation based on artificial neural networks and power quality monitoring data", 2018 IEEE PES Innovative Smart Grid Technologies Conference Europe (ISGT-Europe), Sarajevo, 2018, pp. 1-6.",* confirm that my share is 100% in this publication.

_____

Tarik Hubana

_____

Date

Paper F: High-impedance fault identification and classification using a discrete wavelet transform and artificial neural networks

I, as a co-author of the publication: "*T. Hubana, M. Šarić, S. Avdaković, "High-impedance fault identification and classification using a discrete wavelet transform and artificial neural networks", Elektrotehniški Vestnik 85(3): 109-114, 2018",* confirm that the share of the co-author and the doctoral candidate Tarik Hubana is at least 50% in this publication.

_____	_____	_____
Tarik Hubana	Mirza Šarić	Samir Avdaković

_____

Date

Paper G: Approach for Identification and Classification of HIFs in Medium Voltage Distribution Networks

I, as a co-author of the publication: "*T. Hubana, M. Saric, S. Avdakovic, "Approach for Identification and Classification of HIFs in Medium Voltage Distribution Networks", IET Generation, Transmission & Distribution Journal, ISSN 1751-8687, DOI: 10.1049/iet-gtd.2017.0883, November, 2017",* confirm that the share of the co-author and the doctoral candidate Tarik Hubana is at least 80% in this publication.

_____	_____	_____
Tarik Hubana	Mirza Šarić	Samir Avdaković

_____

Date

Acknowledgements

I would first like to thank my thesis advisor em. Univ. Prof. Dipl.-Ing. Dr. techn Lothar Fickert from Institute of Electric Power Systems, Graz University of Technology. Prof. Lothar Fickert always had enough time for me, and he was a huge support whenever I had questions about my research. Throughout his mentoring, he advised me in the best possible way, and steered me to the right direction, while letting this be my personal project and my own work. Prof. Lothar Fickert is the advisor that every student wishes to have, and I could not have imagined a better thesis advisor for my research.

I would also like to acknowledge Prof. Dr.-Ing. habil. Krzysztof Rudion from Institute of Power Transmission and High Voltage Technology, University of Stuttgart, as the second reader of this thesis, and I am thankful for the time he took to read this thesis and provide the useful feedback.

Finally, I must thank to my parents, grandma, brothers and sister and of course to my spouse for providing the selfless support over these years. Their sacrifice, continuous support and encouragement was my driving motivation to finish this thesis. This thesis would not be possible without them.

Thank you!

Author

Abstract

The high level of distributed generation penetration in the distribution systems is changing the traditional operation of the distribution system. Consequently, the concept of microgrid has emerged as a remarkable way of integrating sustainable energy sources in the electric network. The possibility of microgrid systems and deliberate islanding of sections of the network requires highly flexible distribution management systems and a redesign of protection strategies. Since the currently developed protection schemes already use microprocessor-based relays or industrial computers, an implementation of an advanced artificial intelligence station protection scheme that takes standard measurements as inputs (voltages, currents, circuit breaker states, etc.) and provides improved protection decisions seems like a natural upgrade. Usage of signal processing and artificial intelligence algorithms such as artificial neural networks can help to make decisions that lead to the successful fault isolation. Based on the previous authors research, this thesis is an outcome of the previous work that leads all these researches towards the final step: artificial neural network-based station protection. The objective of this research is to demonstrate the capabilities of the artificial neural networks paired with different signal preprocessing methods in station protection field. The presented results show the applicability of the proposed methodologies that contribute to the existing body of knowledge by designing, testing and verifying these new protection concepts.

Kurzfassung

Der hohe Durchdringungsgrad der Verteilnetze mit dezentraler Erzeugung verändert die traditionelle Funktionsweise des elektrischen Energiesystems. Folglich hat sich das Konzept des Microgrids als eine interessante Möglichkeit zur Integration nachhaltiger Energiequellen in das elektrische Netz herauskristallisiert. Die Ermöglichung von Microgrid-Systemen und die bewusste Trennung von Netzabschnitten vom Verbundnetz erfordert hochflexible Managementsysteme für die Stromverteilung und eine Neugestaltung der Schutzstrategien. Da die derzeit entwickelten Schutzsysteme bereits mikroprozessorgestützte Relais oder Industriecomputer verwenden, scheint eine Implementierung eines fortschrittlichen Stationsschutzes von elektrischen Anlagen unter Verwendung künstlicher Intelligenz eine natürliche Verbesserung zu sein, wobei Standardmessungen als Eingangsgrößen (Spannungen, Ströme, Leistungsschalterzustände usw.) verwendet werden und verbesserte Schutzentscheidungen ermöglichen. Die Verwendung von Signalverarbeitungsverfahren und Algorithmen der künstlichen Intelligenz, wie z.B. künstliche neuronale Netze, können dabei helfen, Entscheidungen zu treffen, die zur erfolgreichen Fehlerabschaltung führen. Basierend auf den bereits vorliegenden Forschungsergebnissen anderer Autoren führt diese Dissertation als Ergebnis der vorhergehenden Arbeiten zu einem letzten Schritt: dem Stationsschutz von elektrischen Anlagen mittels künstlicher neuronaler Netzen. Das Ziel dieser Forschung ist es, die Anwendungsmöglichkeiten und das Leistungsvermögen der neuronalen Netze, gepaart mit verschiedenen Signalvorverarbeitungsmethoden, im Bereich des Stationsschutzes zu demonstrieren. Die vorgestellten Ergebnisse zeigen die Anwendbarkeit der vorgeschlagenen Methoden, die durch Entwurf, Prüfung und Verifizierung dieser neuen Schutzkonzepte einen Beitrag zum bestehenden Stand der Wissenschaft leisten.

List of Symbols

A(t)	Instantaneous amplitude
a_j	Weighted sum of the inputs
E_i	Actual artificial neural network output
E_o	Output of the artificial neural network model
$e^{i\omega t}$	Sinusoidal waves
f	Function
$\hat{f}(\omega)$	Fourier transform
L^2	Lebesgue vector space
N	Set of neurons
MSE	Mean squared error
PV	Cauchy's principle value integral
R	Set of real numbers
t_k	Corresponding target of the input
V	Set of connections
w	Neural network function
w_{ij}	Weight of connection between neuron i and neuron j
x_i	Artificial neural network inputs
y_k	Activation output of unit k
z_j	Artificial neural network activation unit
δ_k	Derivative of the error at a k-th neuron
θ(t)	Phase function
Ω	Ohm

List of Abbreviations

ABCE	Three-phase to earth fault
ABE	Phase-phase-earth fault
AE	Single-phase-earth fault
ANN	Artificial Neural Network
BB	Busbar
CB	Circuit breaker
CT	Current transformer
dB	Decibel
DC	Direct current
DFT	Discrete Fourier transform
DG	Distributed generation
DWT	Discrete wavelet transform
EMD	Empirical mode decomposition
FFT	Fast Fourier transform
HHT	Hilbert–Huang transform
HV	High voltage
IAT	International Symposium on Innovative and Interdisciplinary Applications of Advanced Technologies
IEC	International Electrotechnical Commission
IEEE	Institute of Electrical and Electronics Engineers
IET	Institution of Engineering and Technology
IMF	Intrinsic mode functions
kV	Kilovolt
kW	Kilowatts
log	Logarithm
LV	Low voltage
ms	Millisecond

MV	Medium voltage
MW	Megawatts
PCC	Place of common coupling
PES	Power & Energy Society
PhD	Doctor of Philosophy
PQ	Power quality
PQM	Power quality monitor
PV	Photovoltaic
RMU	Ring main unit
RQ	Research question
SHPP	Small hydro power plant
SNR	Signal to noise ratio
THD	Total harmonic distortion
VT	Voltage transformer
WT	Wavelet transform

Table of Figures

Table of Contents

1 Introduction

1.1 Motivation

The artificial intelligence was always a fantasy of many scientists and engineers. That moment when computers start to mimic cognitive functions that were usually associated with the human brain as learning and problem solving always seemed too far away. However, with the advances of technology, we came to the point where an artificial intelligence can be utilized. The application of artificial intelligence is almost limitless, and therefore it finds its application in the field of power engineering too. Considering the power system as a complex and dynamic system, it seems to be the perfect place where artificial intelligence can be applied. Motivated by this, these new methods had to be tested for solving problems in power engineering, primarily in the field of protection. The dynamic behaviour of the power system during the failures, with the appropriate measurement equipment to record these events, present a perfect place for artificial intelligence application, more specifically the artificial neural network application. So, the research started. The detection, classification, location and fault estimation in various power systems was conducted using different methods of data preparation for artificial neural networks. For years, focusing on exactly where traditional methods of protection had challenges, this research led to the protection on the basis of a whole substation using artificial neural networks.

1.2 Objective and Research Questions

During the last decade, the high level of distributed generation penetration in the distribution systems is changing the traditional operation of the distribution system. Consequently, the concept of microgrid has emerged as a new concept of integrating renewable energy sources in the electric network. Its main benefit lies in that it supplies power locally, reduces operation costs and losses, shaves the peak load and increases reliability [1].

Looking in the future, the possibility of microgrid systems in form of islanding of sections of the network will require highly flexible distribution management systems and a redesign of the protection strategies [2]. Designing an appropriate station protection for microgrid is problematic, since microgrids are particularly dynamic networks, because they can operate in both parallel and islanded modes with different short-circuit currents. Therefore, an appropriate protection scheme should be capable of protecting the network in both modes.

There are numerous challenges when it comes to microgrid protection, and one of the most important ones are changes in the short-circuit level, false tripping signals when using the traditional protection approaches, blindness of protection, coordination of automatic reclosing, are unsynchronized reclosing [3], [4]. Since the currently developed protection schemes already use microprocessor-based relays or industrial computers, an implementation of an advanced artificial intelligence station protection scheme that takes standard measurements as inputs (voltages, currents, circuit breaker states, etc.) and

provides improved protection decisions seems like a natural upgrade. Simultaneously, it is possible to implement a pattern recognition algorithm that could learn while the microgrid operates and make even more precise decisions when the fault occurs. There has been a steady increase of the use of artificial intelligence and computer-based detection methods over the last decade [5], and in that manner this research presents an upgrade to the existing protection schemes. Usage of signal processing and artificial intelligence algorithms such as artificial neural networks (ANNs) can help to make decisions that lead to the successful fault isolation. Therefore, following research questions arise:

RQ1 How can advanced protection algorithms based on artificial intelligence improve present protection schemes?

RQ2 How is microgrid protection seen in terms of sustainability?

RQ3 What socioeconomic, technical and financial factors justify the usage of the advanced protection schemes in microgrids?

RQ4 How the proposed methods deal with changes in the short-circuit levels, dynamic changes of the other distribution system parameters and different network topologies?

RQ5 How does the noise level in measured signals affect the accuracy of the protection system?

RQ6 How does the size of the moving time frame affects the accuracy of the protection system?

Based on the previous authors research [6]–[15], this thesis can be seen as a final outcome of the previous work that connects all of these publications into one story, and leads towards the final step: artificial neural network based station protection. Papers that are directly related to this PhD research are:

Paper A: **T. Hubana**, "Artificial Intelligence based Station Protection Concept for Medium Voltage Microgrids," 2020 19th International Symposium INFOTEH-JAHORINA (INFOTEH), East Sarajevo, Bosnia and Herzegovina, 2020, pp. 1-6.

Paper B: **T. Hubana**, M. Šarić, S. Avdaković, „New Approach for Fault Identification and Classification in Microgrids" In: Avdaković S., Mujčić A., Mujezinović A., Uzunović T., Volić I. (eds) Advanced Technologies, Systems, and Applications IV. IAT 2019. Lecture Notes in Networks and Systems, vol 83. Springer, Cham 2020

Paper C: **T. Hubana,** N. Ljevo, „Willingness to Pay for Reliable Electricity: A Contingent Valuation Study in Bosnia and Herzegovina" In: Avdaković S., Mujčić A., Mujezinović A., Uzunović T., Volić I. (eds) Advanced Technologies, Systems, and Applications IV. IAT 2019. Lecture Notes in Networks and Systems, vol 83. Springer, Cham 2020

Paper D: **T. Hubana**, M. Šarić, S. Avdaković, "Classification of Distribution Network Faults Using Hilbert-Huang Transform and Artificial Neural Network", In: Avdaković S. (eds) Advanced Technologies, Systems, and Applications III. IAT 2018. Lecture Notes in Networks and Systems, vol 59. Springer, Cham 2019

Paper E: **T. Hubana**, “Transmission lines fault location estimation based on artificial neural networks and power quality monitoring data“, 2018 IEEE PES Innovative Smart Grid Technologies Conference Europe (ISGT-Europe), Sarajevo, 2018, pp. 1-6.

Paper F: **T. Hubana**, M. Šarić, S. Avdaković, “High-impedance fault identification and classification using a discrete wavelet transform and artificial neural networks“, Elektrotehniški Vestnik 85(3): 109-114, 2018

Paper G: **T. Hubana**, M. Saric, S. Avdakovic, “Approach for Identification and Classification of HIFs in Medium Voltage Distribution Networks”, IET Generation, Transmission & Distribution Journal, ISSN 1751-8687, DOI: 10.1049/iet-gtd.2017.0883, November, 2017

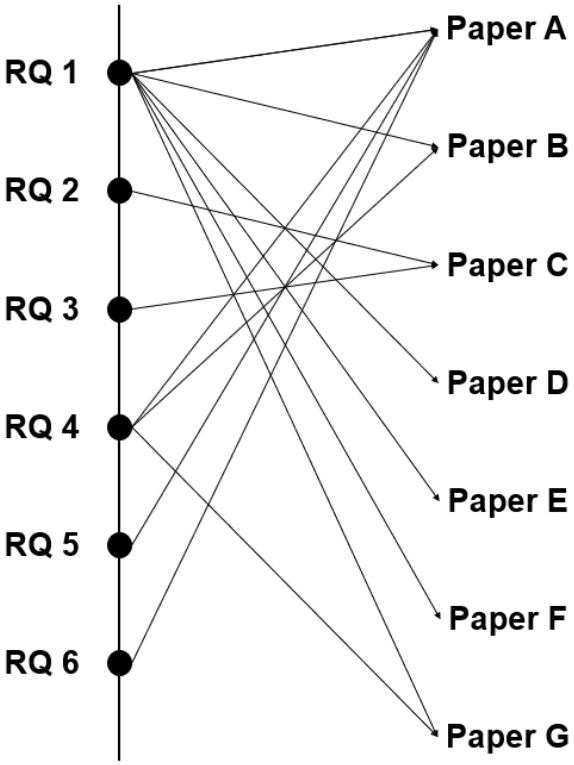

Figure 1: Research questions and related papers

Each of these papers, together with the results presented in the thesis, answer the research questions of this thesis. The objective of this research is to demonstrate the capabilities of the ANNs paired with different signal preprocessing methods in station protection field. This ultimate research should contribute to the existing body of knowledge by designing, testing and verifying these new protection concepts.

1.3 Structure

This research work of the thesis is organized as follows:

- The chapter 2 will give a theoretical background. Firstly, the distribution networks and the new challenges that come with the distributed generation will be explained. After that the

fundamental theory of ANNs and signal processing methods that will be used in this research will be presented (wavelet, Hilbert-Huang and Fourier transform).

- In Chapter 3, five different yet connected research methodologies based on ANNs will be presented. In each of these subsections an experimental setup, the data preprocessing methodology and the outline of the computational procedure for each methodology will be presented.

- Chapter 4 will present the obtained results from each methodology presented in Chapter 3, with the discussion of each method.

- Finally, the conclusions will be given in Chapter 5. The outline of this thesis is shown in Figure 2. Full sized diagram is given in Appendix.

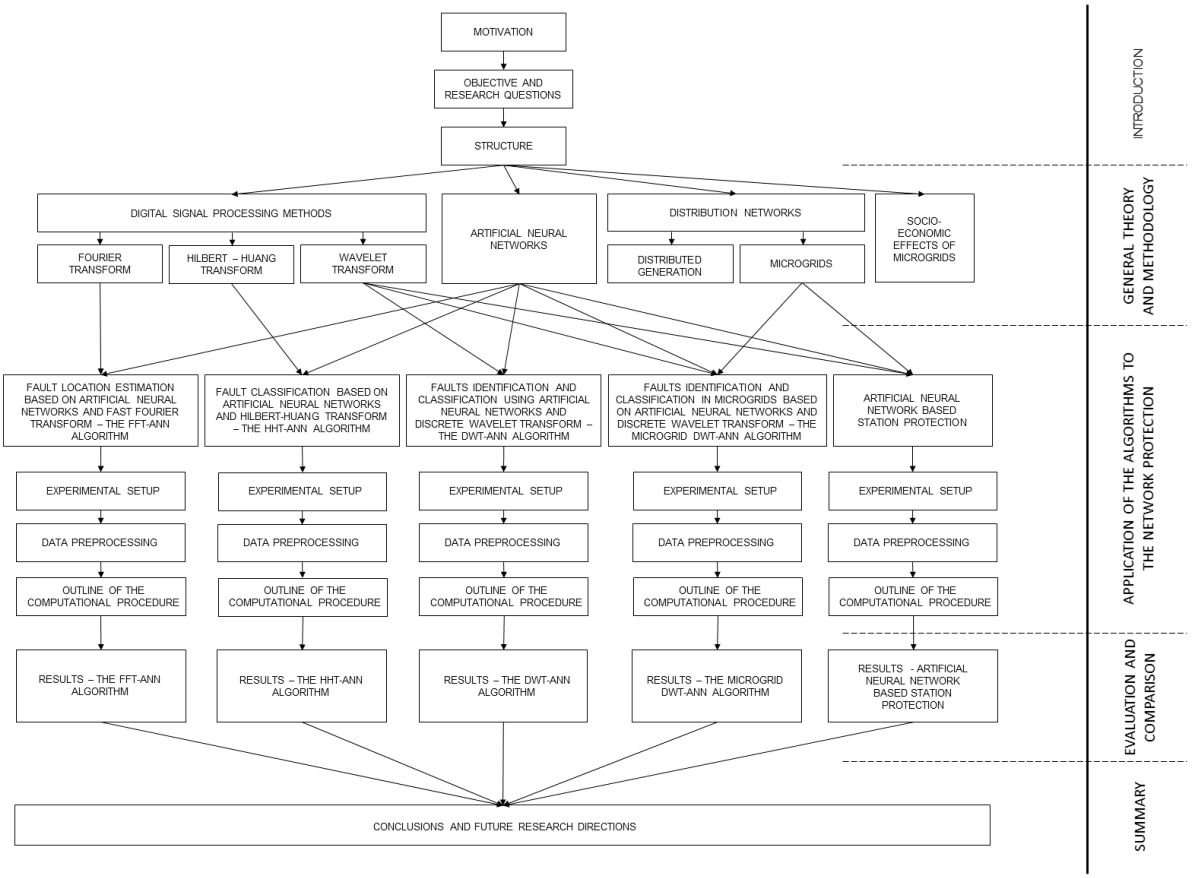

Figure 2: Thesis outline

As mentioned in previous section, this thesis is based on papers A to G. The additional work that relies on the research published through these papers is the main contribution of this thesis. Because of that, research questions that are part of this research are mostly answered in these papers. Other related and non-related papers are given in Appendix. First significant results are published in paper G, therefore answering research questions RQ1 and RQ4. After that, papers D, E and F are published, resulting in more detailed answer of the research question RQ1. Results published in Paper C give an answer to research questions RQ2 and RQ3. Paper B gives answers to research questions RQ1 and RQ4. Research questions RQ5 and RQ6 will be answered in this thesis, by presenting the research

results in section 4.5., while they are also published in the Paper A. Many of other published papers listed in section 7 support and complement the listed papers A to G, by analysing the wider research area and topics that are indirectly related to this research. The diagram that shows the relations between the research questions and papers A to G is shown in Figure 1.

2 General Theory and Methodology

This section will give a theoretical and mathematical background for each ANN-based methodology that has been used throughout this research for faults detection, classification and location estimation. The general theory and methodology will be presented in subsections that follow the development of the research through five sequentially published methodologies.

2.1 Theoretical Background of the Fault location estimation method based on artificial neural networks and Fast Fourier transform – The FFT-ANN algorithm

2.1.1 Artificial Neural Networks

Artificial intelligence has always been an interesting part of the computer engineering science. One of the problems that computers always lacked to solve are problems that cannot be described by a flow chart or algorithm of any sort. On the other hand, the human brain can overcome this and find an approximate solution based on different input factors, experience and the ability to learn. The ability to learn is still the main advantage of data processing when it comes to the human brain, while computers still can perform challenging calculations in a very short time.

The science of artificial neural networks is motivated by the biological neural systems. These systems have many neurons that can work together in parallel and have the capability to deal with large number of data, problems and finally, the ability to learn. Artificial neural networks work in a similar manner, only with mathematically described neurons and connections between them. This allows them to learn from the prepared data, and afterwards be able to solve problems that they were not precisely prepared for [16].

The artificial neural networks (ANNs) could be described as the number of neurons organized in layers, designed to take after the real biological neural networks. Neurons, the key parts of the neural networks, can be described as single units that perform the simple operation and provide an output based on the specific input. Each neuron is characterized by the weight, which is being accordingly adjusted in the process of learning. As a result of the learning process all weights are being adjusted according to the learning dataset which is necessary for the process [7].

When it comes to the mathematical representation of the ANNs, the following definition is commonly used:
A neural network is a sorted triple (N, V, w) with two sets N, V and a function w, where N is the set of neurons and V a set {(i, j) | i, j ∈ N} whose elements are called connections between neuron i and neuron j. The function w: V → R defines the weights, where w((i, j)), the weight of the connection between

neuron i and neuron j, is shortened to $w_{i,j}$ [16]. *Depending on the point of view it is either undefined or 0 for connections that do not exist in the network* [16].

The simple and common representation of the ANN structure is shown in Figure 3. It can be seen that the neuron layers are clearly separated. The ANNs have input and output layers that can be seen from the outside, and one or many inside layers called hidden layers. Connections between neurons that represent weights are usually permitted only between the neighbouring layers [16].

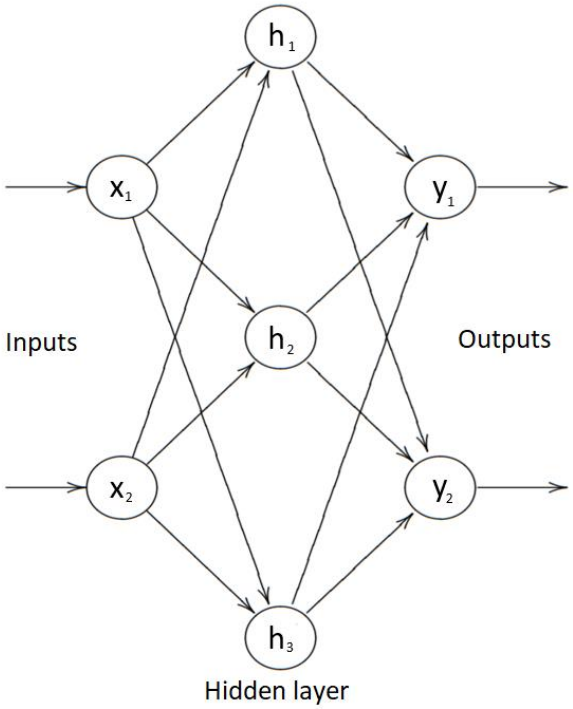

Figure 3: A feedforward network with three layers: two input neurons, three hidden neurons and two output neurons

When it comes to calculation procedure, the dataset with outputs and inputs is used to adjust the values of the weights. The values of the weights are chosen randomly at the beginning of the procedure in order to prevent bias to any of the outputs [17]. The procedure is described by the following equations:

$$a_j = \sum_{i}^{m} w_{ji}^{(1)} x_i \tag{1}$$

$$z_j = f(a_j) \tag{2}$$

$$y_j = \sum_{i}^{M} w_{kj}^{(2)} z_j \tag{3}$$

Where a_j is the weighted sum of the inputs, w_{ij} the weight that represents a connection, x_i the input, z_j the activation function and finally the y_i the corresponding output.

The second step is a calculation of the output difference [17]:

$$\delta_k = y_k - t_k \tag{4}$$

where δ_k represents the derivative of the error at a k-th neuron, y_k the output of the activation of the unit k and where t_k represents the fitting target of the input.

The next step is back propagation for hidden layers [17]:

$$\delta_j = (1 - z_j^2) \sum_{k=1}^{K} w_{kj} \delta_k \tag{5}$$

where δ_j is the derivative of error w_{kj} to a_j.

Afterwards, the error gradient is calculated, and propagated back in order to calculate the weights. The mean square error is given by the following equation [17]:

$$MSE = \frac{1}{N} \sum_{1}^{N} (E_i - E_o)^2 \tag{6}$$

where:
N presents the iterations number,
E_i the actual model output and
E_o the desired model output.

By following the previous equations, the weights are updated in every iterative process. The iterative process is repeated by using all of the available inputs and outputs form the learning data set until the ANN converges according to the predefined error tolerance [17].

2.1.2 Digital Signal Processing Methods

In order to use the analogue signals that are usually obtained in the measurement process in digital devices, these signals need to be converted to a discrete signal. The easiest method for analogue signal f(t) discretization is to record discrete samples $\{f(ns)_{n \in Z}\}$ at fixes interval s. In order to turn it back to the analogue signal, the signal f(t) for any $t \in R$ can be reconstructed by using the standard interpolation methods [18].

2.1.3 Fourier Transform

The Fourier transform is a popular mathematical tool in both mathematics and physics due to its properties of diagonalization of the time invariant convolution operator and since it controls the linear time invariant signal processing [19]. The Fourier transform reconstructs any finite analogue function f(t) as a sum of sine waves $e^{i\omega t}$ [19]:

$$f(t) = \frac{1}{2\pi}\int_{-\infty}^{\infty} \hat{f}(\omega) e^{i\omega t} d\omega \tag{7}$$

The amplitude $\hat{f}(\omega)$ (or the Fourirer transform) of each sinusoidal wave $e^{i\omega t}$ is proportional to the relation with $f(t)$ [19]:

$$\hat{f}(\omega) = \int_{-\infty}^{\infty} f(t) e^{-i\omega t} dt \tag{8}$$

For more regular signal $f(t)$, the sine wave amplitude $|f(t)|$ decay is faster when frequency rises.

2.1.3.1 Fast Fourier Transform

A Fast Fourier Transform (FFT) is a common and more efficient method to calculate the Discrete Fourier Transform (DFT). The DFT, just like the FFT with analogue signals, deals with the decomposition process of the discrete signals, in a way to obtain the range of different frequency components. However, even though the DFT is practical and useful in many engineering fields, the calculation process is too slow to be practical [20]. A FFT is a way to compute the same result more quickly and can reduce the computation time by several orders of magnitude [20].

If the signal of N points is considered, the calculation procedure is described by the following equation [19]:

$$\hat{f}[k] = \sum_{n=0}^{N-1} f[n] \exp\left(\frac{-i2\pi kn}{N}\right), \quad for\ 0 \le k < N \tag{9}$$

This calculation process requires N^2 complex mathematical operations. On the other hand, the FFT algorithm reorganizes these calculations and reduces the number to O(*N log₂N*). Additionally, when the index group of the frequency is even, two groups can be obtained [19]:

$$\hat{f}[2k] = \sum_{n=0}^{N/2-1} (f[n] + f[n+N/2]) \exp\left(\frac{-i2\pi kn}{N/2}\right) \tag{10}$$

However, in the case of odd index of the frequency, the following equations stand [19]:

$$\hat{f}[2k+1] = \sum_{n=0}^{N/2-1} \exp\left(\frac{-i2\pi n}{N}\right) (f[n] - f[n+N/2]) \exp\left(\frac{-i2\pi kn}{N/2}\right) \tag{11}$$

Therefore, the equation (10) proves that the even frequencies can be calculated by using the DFT of the signal with the period of *N/2* [19]:

$$f_e[n] = f[n] + f[n+N/2] \tag{12}$$

The odd frequencies can be calculated from the equation (11) by calculating the Fourier transform [19]:

$$f_O[n] = \exp\left(\frac{-i2\pi n}{N}\right)(f[n] - f[n + N/2]) \quad (13)$$

Previos equations demonstrated that the DFT of the signal with size N can be calculated by using two DFTs, while reducing the total size. The inverse FFT is calculated by using the following equation [19]:

$$f^*[n] = \frac{1}{N}\sum_{k=0}^{N-1} \hat{f}^*[k]\exp\left(\frac{-i2\pi kn}{N}\right) \quad (14)$$

2.1.3.2 Harmonics monitoring in power systems

The measurement process in the high voltage (HV) power system includes voltage and current transformers (VTs and CTs). The power quality measurement is carried out by power quality meters, whether with portable or stationary power quality meters. In the measurement process, the sine wave of the HV side of the voltage and current transformers will be converted to the low voltage (LV) side with the error in both the signal amplitude and angle [13].

However, these transformers have some frequency limitations. The construction parameters and the operating and environmental conditions can have a significant impact on the frequency characteristic of the VTs and CTs [21].

Network	Voltage level	Harmonics		
		2nd to 7th	8th to 20th	21st to 50th
MV	10 kV	OK	OK	OK
	20 kV	OK	OK	Uncertain
	30 kV	OK	NO	NO
	60 kV	OK	OK	Uncertain
HV	110 kV	OK	Uncertain	NO
	220 kV	Uncertain	NO	NO

Table 1: Reliability of harmonics measurements in different voltage levels

Many researchers [21]–[23] have analysed the impact of the frequency to the voltage and current transformers characteristics. They implicate that the measurements in the HV power systems can lead to errors in the high frequency range. Also, authors in [23] have proposed the recommendations for the reliable measurement in specific frequency ranges for each voltage level, as shown in Table 1.

2.2 Theoretical Background of the Fault classification algorithm based on artificial neural networks and Hilbert-Huang transform – The HHT-ANN algorithm

2.2.1 Distribution networks

Electric power systems present a great example of the largest technical systems ever created by a man. Generally, the power system can be described as a complex, dynamic systems whose main goal is to safely, reliably and economically supply consumers with appropriate amount of quality electric energy. One part of these complex systems are the distribution systems. Distribution systems are physically closest to the end consumers and present a part of the power system that distributes the electrical energy from the supply points (usually from the HV grid) to the end consumers. The common concept of the traditional European distribution system is following. The distribution system is usually supplied from the HV grids, usually over a 400/110 kV (or 400/220 kV) transformers. This presents a HV to medium voltage transformation (HV/MV). Medium voltage (MV) levels are usually 10kV, 20kV and 35 kV. However, the remains of 35 kV voltage level is in process of transition to 20 kV. MV lines (feeders), start from the MV busbars and create a mainly radial topology. However, these feeders can be connected to other ones for the reconfiguration needs in cases of the distribution system overload or faults. The typical distribution system is shown in Figure 4.

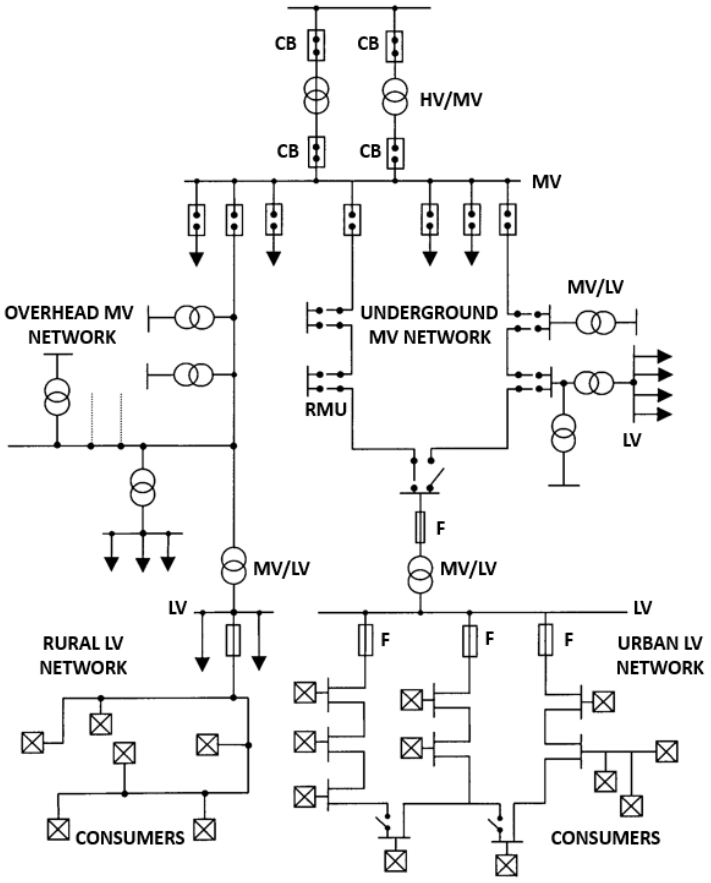

Figure 4: Typical distribution network topology

2.2.2 Isolated neutral point medium voltage networks

In the isolated neutral point MV networks, the neutral point is disconnected from the earth. However, the coupling is obrained throung lines and cables capacieties. Modern distribution systems tend to switch to different neutral point treatments due to the disadvatnages of the isolated neutral point systems. During the earth fault, currents flow through earth capacities of healthy phases (Figure 5). Neglecting draining and longitudinal impedances, the fault current depends on the network capacities and the fault resistance [14].

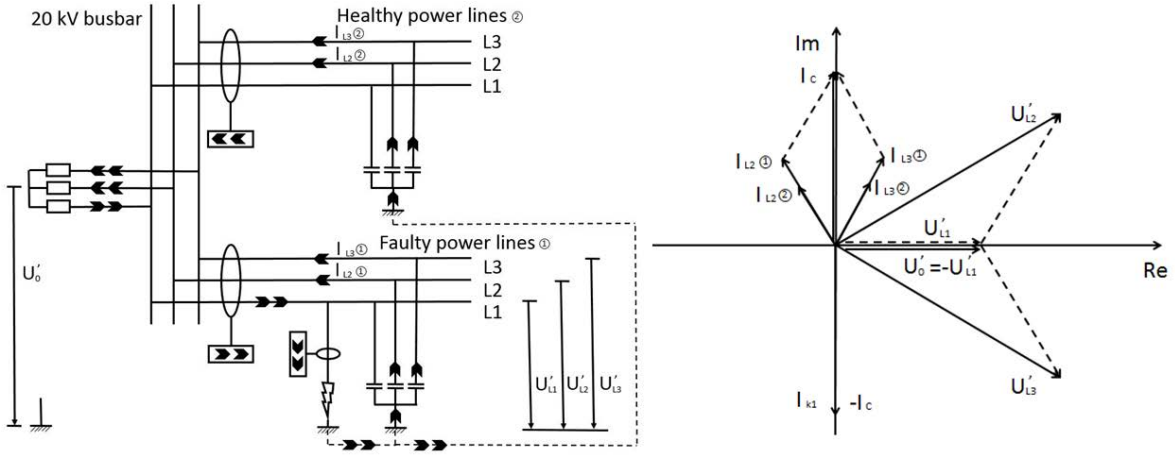

Figure 5: Isolated neutral point medium voltage networks during fault (right) and the phasor diagram (left)

The phasor diagram shown in Figure 5 is valid for so-called metallic earth faults. At low values of fault resistance, the voltage in the isolated neutral point as almost as same as the phase to ground voltage. There are many advantages of the networks with isolated neutral point [14]. During earth faults, which statistically represent the most frequent faults, transient faults get self-extinguished if the current has low capacitance, and in that manner improve the power quality. However, there are some disadvantages of isolated neutral point medium voltage networks as well [14]. In these networks, intermittent overvoltage can occur, with relatively high overvoltage factors. The fault detection is more challenging also, and the improved resiliency can lead to overvoltages. The problematic part also occurs if the fault with high capacitive currents occur, since in that scenario there is no self-extinguishing property that can clear the fault.

2.3 Hilbert – Huang Transform

The Hilbert–Huang transform (HHT) is a methodology used to decompose a signal into intrinsic mode functions (IMFs) and in the same time obtain the instantaneous frequency [24]. Unlike the Fourier transform that presents the pure mathematical tool, the HHT presents an algorithm. The algorithm is composed of two parts: the empirical mode decomposition (EMD) and Hilbert Spectral Analysis (HSA). By using the EMD the signal is being processed in order to obtain the IMFs, while the HSA is used to obtain the time-frequency spectrum [25].

2.3.1 Hilbert Spectral Analysis

The HHT is used as an alternative tool to existing methods that deal with spectral analysis of the signals [26]. This methodology aims to give a local description of the nonstationary data, and it is described by the following equations (the PV denotes Cauchy's principle value integral) [26]:

$$H[x(t)] \equiv \hat{y}(t) = \frac{1}{\pi} PV \int_{-\infty}^{\infty} \frac{x(t)}{t-\tau} d\tau \tag{15}$$

$$z(t) = x(t) + i\hat{y}(t) = A(t)e^{i\theta(t)} \tag{16}$$

Where:

$$A(t) = \sqrt{x^2 + \hat{y}^2} \tag{17}$$

$$\theta(t) = arctg\left(\frac{\hat{y}}{x}\right), \text{ and} \tag{18}$$

$$i = \sqrt{-1} \tag{19}$$

$A(t)$ presents instantaneous amplitudes, while the $\theta(t)$ presents phase functions. If this phase function is derived over time, as shown in the following equation, the instantaneous frequency can be obtained [26]:

$$\omega = \frac{d\theta(t)}{dt} \tag{20}$$

By applying this methodology to all IMFs, a number of functions and frequencies can be calculated.

2.3.2 Empirical Mode Decomposition

As previously mentioned, the EMD algorithm is one component of the HHT methodology. By using this algorithm, the goal is to decompose a signal into IMFs [8]. The EMD algorithm uses sifting process in order to extract the local mean from the original signal [27], and this process is repeated until the IMF is obtained by a definition that states that the IMF is the signal that has a zero mean, and where number of zero crossings and extrema do not differ more than by one [29].

When the IMF is obtained, this new function is extracted from the signal, and the previously described iterative process is repeated on the original signal residue [28]. The iterative process is performed until the final residue after the last IMF extraction becomes a monolithic function. Since the last extracted IMF has the lowest frequency due to the decay of the mean values as the order of IMD increases, it is considered as the trendline of the original signal.

After the procedure of IMFs extraction is completed, the original signal $D(t)$ can be written as a sum of the final residue and all extracted IMFs from the iterative procedure, as shown in the following equations:

$$D(t) = R_n(t) + \sum_{j=1}^{n} IMF_j(t) \tag{21}$$

Using previous equations, the analytic function can be formed as shown in equation (22) [26].

$$D(t) - R_n(t) = Re\left[\sum_{j=1}^{n} A_j(t) e^{i\int \omega_j(t)dt}\right] \tag{22}$$

For comparison purposes, the analytic function that is formed by using the Fourier transform is shown in the following equation:

$$D(t) = Re\left[\sum_{j=1}^{n} A_j e^{i\omega jt}\right] \tag{23}$$

Compared to the Fourier decomposition, the EMD is more generalized since it decomposes a signal to IMFs that have amplitudes and frequencies that can change in time [29].

2.4 Theoretical Background of the Faults identification and classification algorithm using artificial neural networks and discrete wavelet transform – The DWT-ANN algorithm

2.4.1 Wavelet Transform

The wavelet transforms emerged as a novel mathematical tool for multiresolution decomposition of continuous-time signals with potential applications in computer vision, signal processing, etc. Nowadays, the wavelet transform is used in numerous engineering applications. It is regarded as a mathematical tool that has numerous advantages when compared with traditional methods in a stochastic signal-processing application, mainly because waveform analysis is performed in a time scale region [30]. Wavelet transform of a signal $f\ (t) \in L^2(R)$, where L^2 is the Lebesgue vector space, can be defined by the following equation [30]:

$$WT\ (f, a, b) = \frac{1}{\sqrt{a}} \int_{-\infty}^{+\infty} f(t)\, \Psi\left(\frac{t-b}{a}\right) dt \tag{24}$$

2.4.1.1 Discrete wavelet transform

The discrete wavelet transform (DWT) presents a wavelet transform that has discrete wavelets, i.e. whose wavelets are sampled discreetly. The main advantage compared to the Fourier transform is that it records both frequency and location information. The mathematical representation is given by the equations bellow [30]:

$$DWT\ (f,m,n) = \frac{1}{\sqrt{a_0^m}} \sum_k f(t)\, \Psi \left(\frac{n - k a_0^m}{a_0^m} \right) \tag{25}$$

If the equation (25) is compared with the equation (24), it can be seen that the values a and b are replaced by values a_0^m and ka_0^m, where k and m are integer values. In the most common applications, these values are set to $a_0 = 2$ and $b_0 = 1$, while yielding to $a_0^0 = 1$, $a_0^{-1} = 2^{-1}$, etc. [30].

2.5 Theoretical Background of the Faults identification and classification in microgrids based on artificial neural networks and discrete wavelet transform – The Microgrid DWT-ANN algorithm

2.5.1 Distributed generation

Distribution system is a much wider term than just a distribution network, since it also incorporates the distributed generation (DG). The DGs present a smaller scale power plants that are connected directly to distribution networks. The power range of the DG power plants can be from couple kW to hundreds of MW.

It is about the continuing environmental pollution, intensive climate change and sustainability of the renewable sources since they are in most cases based on renewable energy sources. Therefore, they are commonly associated to the group of renewable energy sources (RES). Because of this, there is a continuously increasing exploitation of renewable energy DG. However, their integration into the distribution systems is not an easy task since their presence changes the traditional unidirectional power flow that was common for many years in the distribution systems [31].

The penetration of DGs into the distribution networks has both positive and negative impacts on the operation, protection and control of the distributions systems. Of course, these impacts depend on the on its utility system interfaced, the size of DG units, the amount of capacity of the DG relative to the system and the feeder voltage regulation practice [32], [33].

Positive effects of DGs are improved voltages, reduces power losses, capability of utilizing the ancillary services and improved reliability [34]. On the other hand, the negative impacts include possible islanding, power quality issues, protection coordination and stability problems [34]. In order to regulate

these effects and possibly boost the scenarios where DGs have positive impact to the system, various regulations are being imposed throughout the world [34].

The research [10] evaluated the effect of photovoltaic DG penetration on power losses in the LV distribution network, since the losses mitigation is one of the key strategies in the process of system operation and control, and directly affects the system efficiency.

2.5.2 Microgrids

By definition: *A microgrid is a group of interconnected loads and distributed energy resources within clearly defined electrical boundaries that acts as a single controllable entity with respect to the grid* [35].

Therefore, the microgrid presents a dynamic distribution network, with various DGs, controllable loads and energy storage devices [3]. Due to its controllability, in a case of a fault in the main grid, a microgrid can island and continue to operate in the islanded mode. In the normal operating scenario, the microgrid operates in a grid-connected mode [36]. The capacity of the microgrids can vary from couple of kW to tens of MW, depending on the main grid connection (LV or MV) [37].

Utilization and forming of the microgrids can bring many benefits, both from the grid and user perspective. From the grid point of view, a microgrid can be seen as a single controllable entity and in that manner operated as a load or energy source [3]. From the customer point of view, the microgrids can improve the reliability, power quality and efficiency. Also, important part of the microgrid utilization is the environmental point of view, where microgrids reduce pollution and global warming by increasing efficiency and local energy production that is mainly based on the renewable energy sources [3].

However, the microgrid set up requires investments. On the other hand, to the distribution system operator the investments may be related to benefits related to rewards or penalties in accordance to the total non-delivered energy when individual standards of quality of service are not met [15]. This is a point where consumers need to take part in the process. In order to have a more reliable supply of energy, consumers can pay for an improved service. Research [15] estimates this value that presents a key parameter that can be used to analyse the investments in distribution systems and future microgrids in order to target exactly those investments that will improve the reliability of that part of the distribution system.

2.6 Theoretical Background of the Artificial Neural Network based Station Protection algorithm

Since the ANN-based station protection algorithm presents an improved and advanced microgrid DWT-ANN algorithm, the theoretical background for this methodology is as well described in detail in section 2.5.

2.6.1 Socio-economic effects of microgrids

Electricity supply interruptions are less and less accepted by both consumers and regulators, making the requirements for the reliability of supply higher than ever. This is the perfect place for microgrids to fit in, with all the benefits that microgrid bring. However, distribution system operators struggle to achieve these requirements, mainly because of the infeasibility of the investments. On the other hand, if the consumers were willing to pay for the increased reliability of supply that can come from the upgrade of the conventional distribution system to microgrid, these requirements could be achieved.

Using a sample of residential and business consumers in Bosnia and Herzegovina, a willingness to pay (WTP) for an improved electricity service for both residential and business consumers is estimated by using the contingent valuation method (CVM) in paper B (section 1.2). The research results presented the average WTP of domestic and business consumers for avoiding one-hour interruption. Generally, majority of the respondents are willing to pay more for increased supply reliability (74.4% of domestic consumers, and 97.2% of business consumers). Socio-economic parameters that affect this decision for domestic consumers can be ranked in the following way (from the highest to the least important parameter): electric heating, employment and time spent in the house. When it comes to business consumers' willingness to pay depends on the following parameters: size of enterprise, business sector, back-up system possession and the size of the electricity bill.

The obtained information can be used to analyse the investments in distribution systems and future microgrids in order to target exactly those investments that will improve the reliability of that part of the distribution system. In that way, consumers that are willing to pay more for more reliable electricity could have a special designed pricing tariff that would justify the additional investments in the reliability.

3 Application of the algorithms to the network protection

This section will give an outlook of different ANNs-based methodologies that have been used throughout this research for faults detection, classification and location estimation. The methods evolved over the years finally leading to the station protection algorithm presented in section 3.5.

3.1 Fault location estimation based on artificial neural networks and Fast Fourier transform – The FFT-ANN algorithm

The following research was conducted in order to test the capability of the ANNs for fault location and resistance estimation in HV power network. The input data for the ANN are the harmonic components of the voltage and current, obtained with the FFT from the measured voltages and currents from the power quality meters in the system. The following section will give the experimental setup, the data preprocessing methodology and the outline of the computational procedure.

3.1.1 Experimental setup of the FFT-ANN algorithm

For this purpose, an 8-bus system is developed. The power quality meters installed in the system are set to record the voltages and currents up to the 9th harmonic (including the DC component) [13]. The fault resistance is simulated in the range of 0 – 100 Ω, for various fault locations. Test system is developed in MATLAB Simulink software, and represents a power system with 8 busbars, while the power quality meters are installed in 4 busbars in 8-bus system. Test system is shown in Figure 6. The red busbars are the ones with the installed power quality meters. In the 8-bus system the power quality meters are installed in the busbars: BB1, BB4, BB7 and BB8. The power quality algorithm developed in MATLAB calculates harmonics in the 200 ms time frame. The procedure of harmonics calculation is carried out according to the IEC 61000-4-7 standard [38].

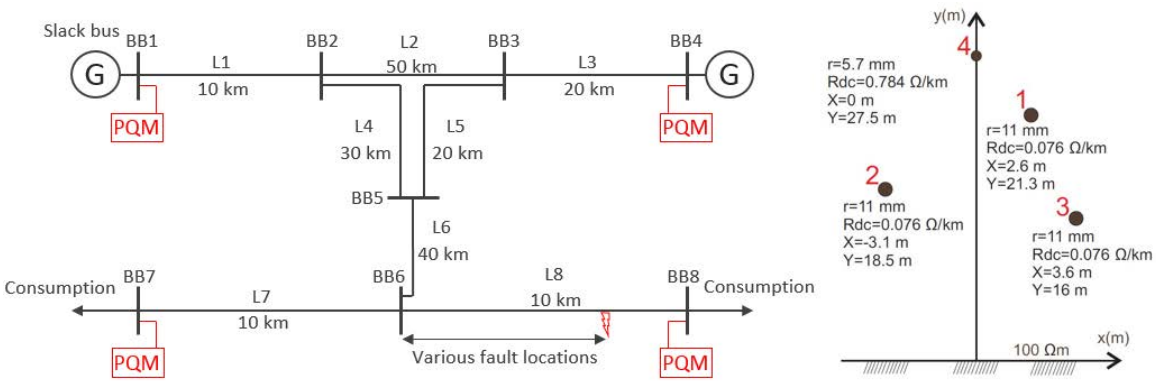

Figure 6: The 8-bus power system model (left) and the transmission lines parameters (right) [13]

Faults are simulated in different locations in the line, in the range of 0% to 100% length of the line L8.

3.1.2 Data preprocessing for the FFT-ANN algorithm

As a result of simulations, the voltage and current harmonics in three phases up to 9th harmonic, with DC component in 4 measuring points are calculated by using the FFT, which results in 240 values. These values are converted to a vector that will present an input for the ANN. This means that an ANN receives a vector of 240 values as inputs that are associated with two appropriate outputs – the fault location and the fault resistance. Each input vector corresponds to one pair of outputs. The total of 573 fault scenarios are simulated.

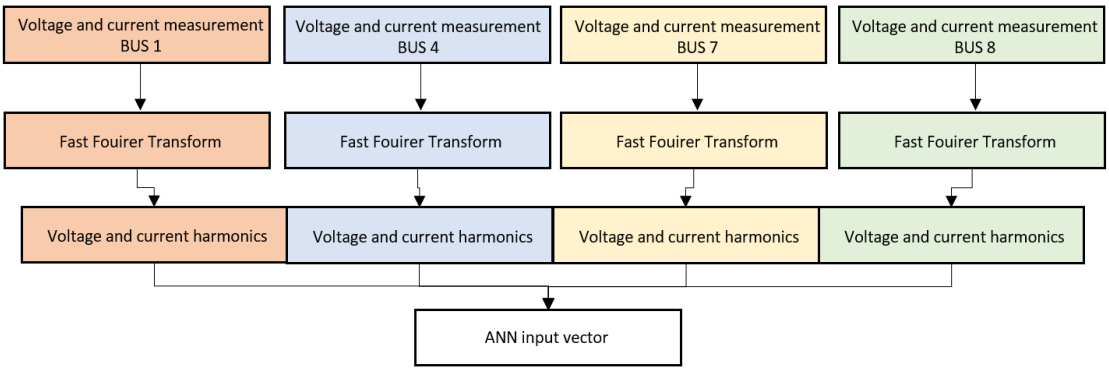

Figure 7: The FFT preprocessing flowchart

3.1.3 Outline of the computational procedure for the FFT-ANN algorithm

After simulating the fault, for each fault and different values of fault location and resistance, the voltage and current waveforms are measured. The fault is sustained during the entire simulation interval. When the voltage and current waveforms are generated and collected, the power quality devices calculate the voltage and current harmonics. The input vector gives a good insight into system behaviour during the fault conditions. Once trained ANN is ready to be used for fault location estimation, according to the algorithm shown in Figure 8.

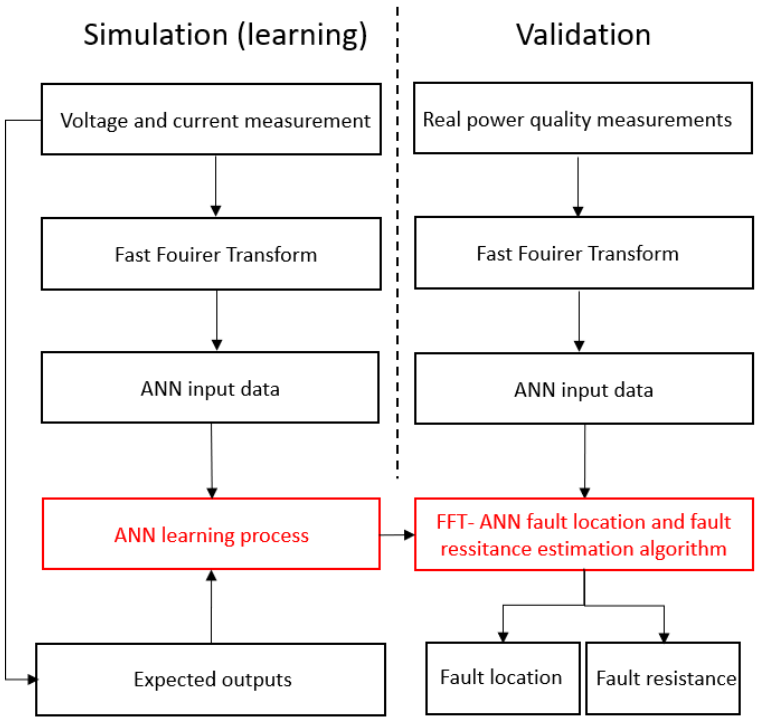

Figure 8: Proposed method algorithm [13]

With the power quality devices installed in power system, voltage and current harmonics can be measured, and sent to postprocessing unit with the installed algorithm for the fault location estimation.

3.2 Fault classification based on artificial neural networks and Hilbert-Huang transform – The HHT-ANN algorithm

The HV power systems protection is well researched and developed in the past decades. Besides that, the HV power lines are already well protected since the fault usually presents a large loss of supplied energy and money. However, the distribution system protection, especially with the rise of the DG penetration, electric vehicles and storage systems presence is becoming challenging from the protection point of view. Also, since the distribution consumers are less sensitive to the power outage, the additional investment in the protection of MV feeders is not always feasible. The research that will be presented in this section was conducted in order to test the capability of the ANNs for fault identification and classification in a MV distribution network. The input data for the ANN are the measured substation voltages pre-processed with the HHT. The following section will give the experimental setup, the data preprocessing methodology and the outline of the computational procedure.

3.2.1 Experimental Setup for the HHT-ANN algorithm

The test system developed for this purpose presents a modified real distribution from Bosnia and Herzegovina by adding the renewable resources that can generate enough power for the system to work in islanded mode. The DGs rated powers are the common rated powers of small hydro power

plants (SHPP) and photovoltaic (PV) DGs that occur in the Bosnia and Herzegovina distribution network [11].

Consumers are fed over 35/10 kV transformer, via 10 kV underground cables, 10/0.4 kV distribution transformers and finally over 0.4 kV LV network [7]. The single line diagram of the test system is shown in Figure 9.

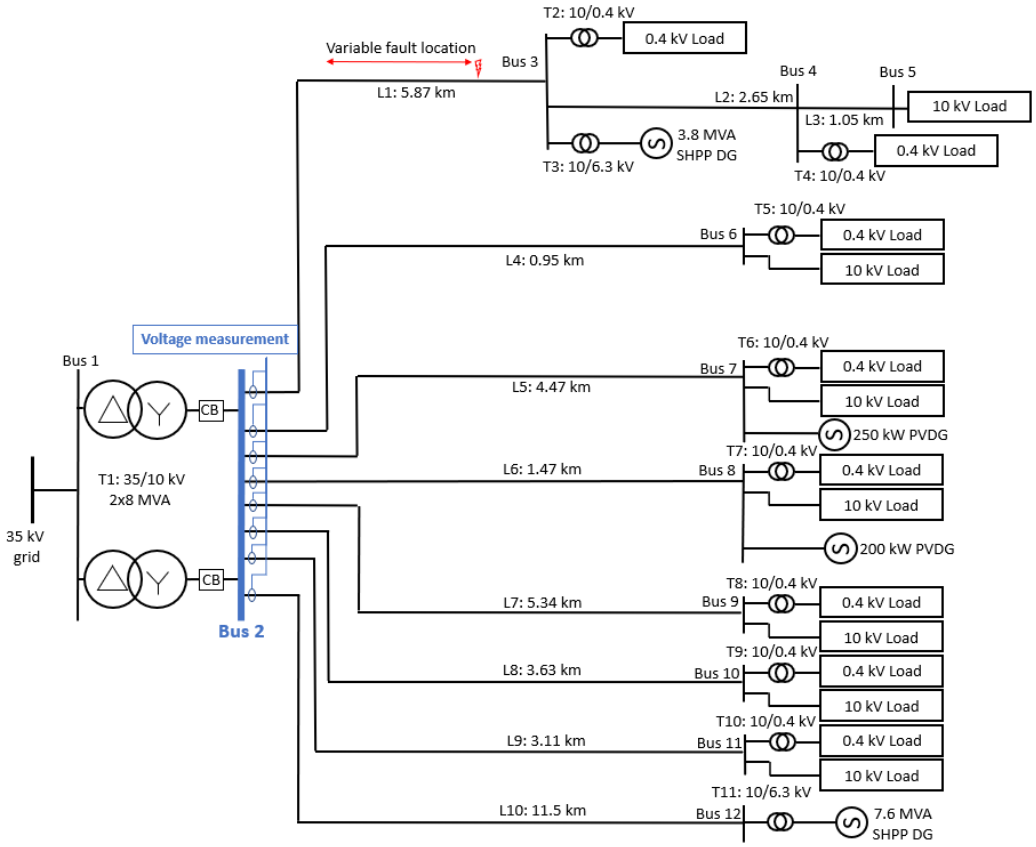

Figure 9: The developed test system for the algorithm testing

Faults are simulated on the 5.87 km long 10 kV feeder, over various fault locations (in the range from 20 to 600 Ω) [7]. The single-phase-earth faults (AE), phase-phase-earth faults (ABE) and three-phase faults (ABCE) are simulated. Voltage measurements devices are connected to the 10 kV busbar of the 10/0.4 kV transformer.

3.2.2 Data Preprocessing for the HHT-ANN algorithm

After measuring the voltages, in order get the characteristic signature of each fault, the voltages are processed with HHT. High-frequency signals that are generated when a fault occurs reside in IMF1, so the instantaneous frequency of IMF1 will mutate as soon as the short-circuit fault takes place [7]. In this part of a research, high frequency IMF components are chosen to be the characteristic quantity for the further analysis. The HHT is applied to the measured voltage signals in order to obtain a characteristic behaviour during each fault [7]. Since the classifier is based on ANN, it is necessary to create appropriate ANN inputs. However, the number of IMF components depends of the signal complexity, and in various fault scenarios, different number of IMF components occur [7].

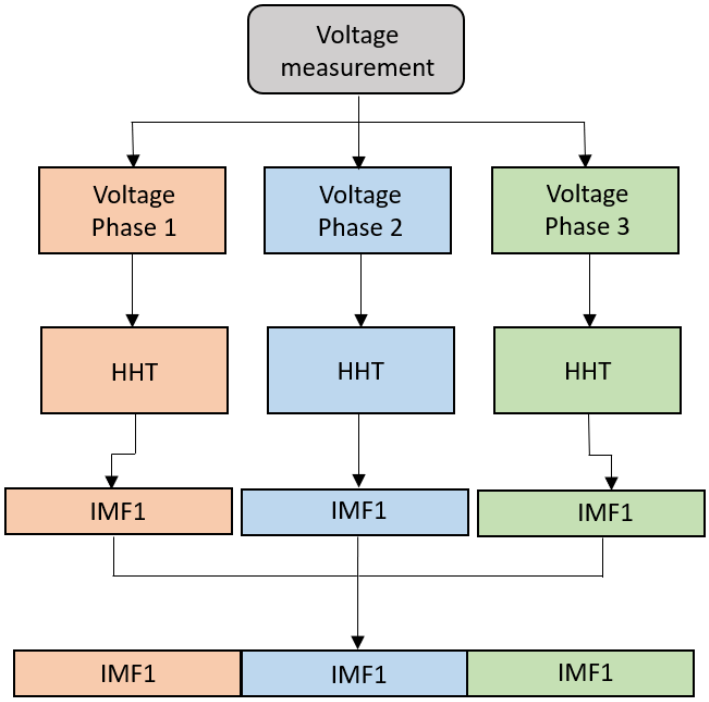

Figure 10: The HHT preprocessing flowchart

Because of that, the proposed algorithm works with first IMF components, since the first IMF component is always present in every signal [7]. In order to reflect the system behaviour in the best manner, a unique signal that contains first IMF's of each phase voltages is created. By grouping the signals into one signal, a unique system's signature that responds to specific fault scenario is created.

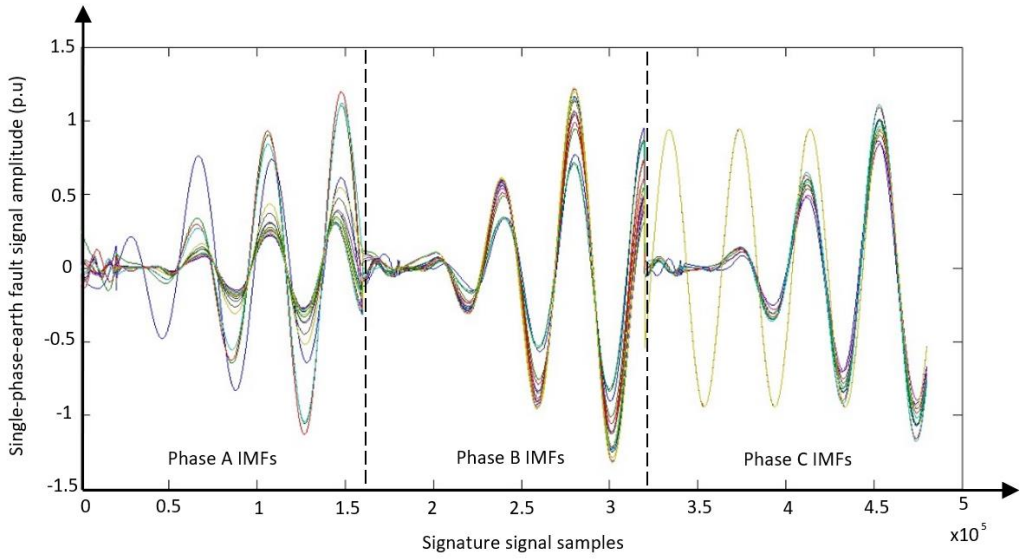

Figure 11: Grouped IMF signal in case of AE fault for various fault resistances

Figure 11 shows the 60 overlapped signature signals in the case of phase A to earth (AE) fault with different fault resistances and fault locations. After the grouped signals are created, the ANN inputs are ready. In this analysis, 180 fault scenarios were simulated and prepared for the ANN input.

3.2.3 Outline of the computational procedure for the HHT-ANN algorithm

The proposed method algorithm is shown in Figure 12. The proposed classifier is completely adjustable, and by simple upgrades it is possible to implement additional parameters and criteria [7]. The voltage in one end of the MV underground cable is measured in various simulated scenarios and by applying the HHT EMD process the IMF's are obtained. Finally, the ANN is trained with the data prepared according to the section 3.2.2. and previously known outputs from the simulation.

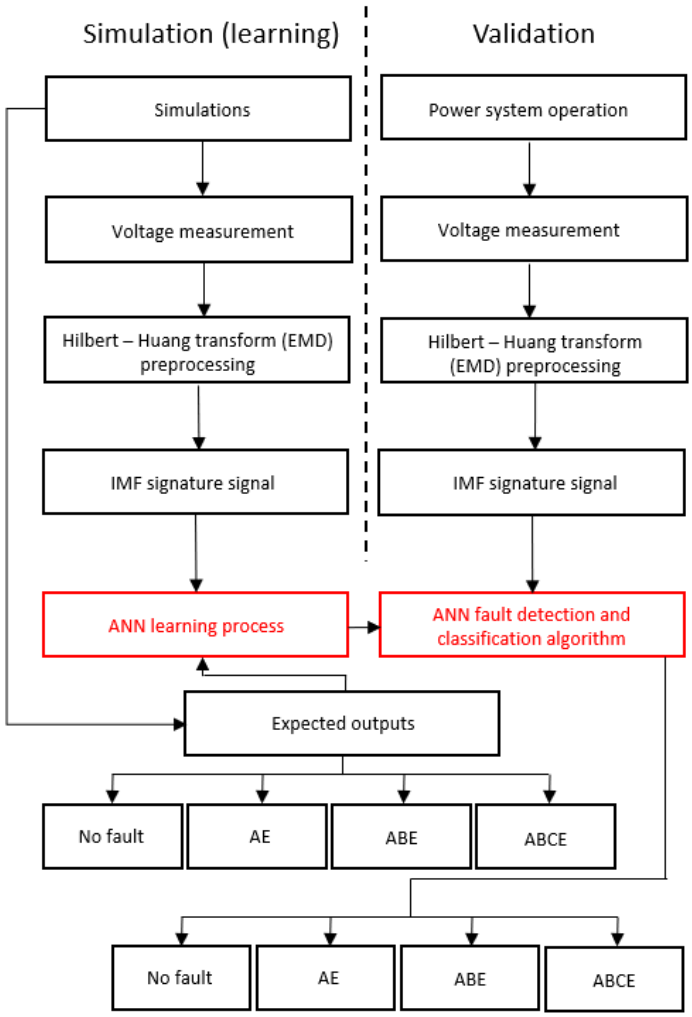

Figure 12: Proposed method algorithm during the data preprocessing

Once created classifier is easy to use and implement in the system. Measured voltages during the faulty conditions can be sent to the HHT-ANN classifier, and after successful classification process, further commands can be undertaken.

3.3 Faults identification and classification using artificial neural networks and discrete wavelet transform – The DWT-ANN algorithm

Even though the HHT preprocessing approach gave great results from the point of fault classification, the number of IMFs that occur in the signal can vary. This means that more complex signals can have valuable information in the higher order of IMFs, which can be omitted if only first IMFs are used as characteristic signals, while the less complex signals will not have a higher order IMFs. Because of that the following research used the DWT as the signal preprocessing method in order to prepare appropriate inputs for the ANN. The DWT signal decomposition is more suitable for extracting the valuable information during the fault. The following section will give the experimental setup, the data preprocessing methodology and the outline of the computational procedure.

3.3.1 Experimental Setup for the DWT-ANN algorithm

The test system that is used in this part of research is shown in Figure 9. Again, the faults and measurements are performed on 10 kV underground cable that feeds the entire load area. Faults are simulated for different fault resistances (in the range of 20 Ω to 600 Ω), and at different fault locations. The single-phase-earth faults (AE), phase-phase-earth faults (ABE) and three-phase faults (ABCE) are simulated, with various fault resistance ranges and fault locations, giving a total of 1600 fault scenarios.

3.3.2 Data Preprocessing for the DWT-ANN algorithm

After simulating the fault, for each fault and different values of fault location and resistance, the voltage waveforms are generated. The fault is sustained during the entire simulation interval, i.e. (0 – 0.08 s) [9], [39]. When the voltage waveforms are generated and collected, DWT can be applied. In this case a Daubechies 4 wavelet is used, resulting in one approximate and 4 details components [9], [39]. The algorithm is also tested by Symlet 4 and Biorthogonal 4.4 wavelet families, and output results are the similar or same [9], [39]. Therefore, it is not necessary to be particularly cautious regarding the choice of wavelet family. The signals shown in the Figure 13, represent a DWT for faulty phase voltage in every fault type (example for one fault location and fault resistance).

The DWT is applied to the measured voltage signals; therefore, one approximation and 4 details are obtained for each voltage [9], [39]. Four levels of decomposition are used in order to get the frequency bands shown in Table 2.

Detail 1	Detail 2	Detail 3	Detail 4	Approximation 4
800 - 1600 Hz	400 - 800 Hz	200 - 400 Hz	100 - 200 Hz	50 - 100 Hz

Table 2: Frequency bands used for the multi scale analysis

The A4 waveform is the base sinusoidal wave that reflects the signal behaviour during each fault. The rest of the DWT waveforms are higher frequency components of the voltage signal, and therefore reflect

the distinctive voltage behaviour during each fault type [9], [39]. After sending these signature signals to the trained ANN, the algorithm should learn how to detect and classify the fault that occurred in the system.

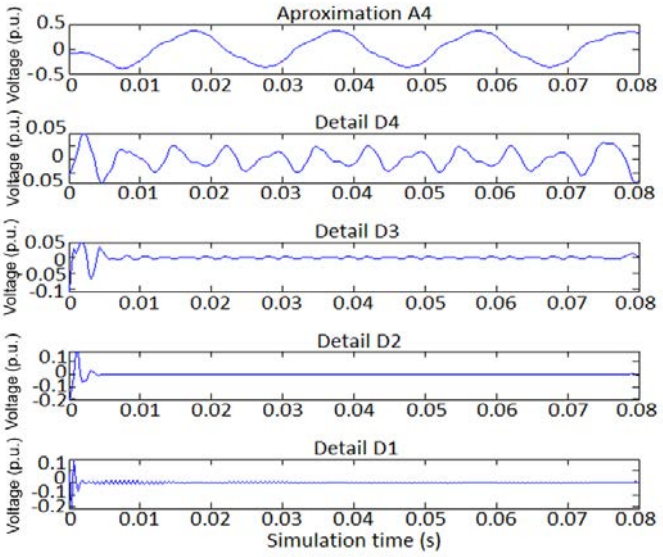

Figure 13: DWT of the phase A voltage in case of AE fault

These signal components give a good insight into system behaviour during the fault conditions. For this reason, they are used as representative signals for each fault type. Afterwards, these signals are used to create the grouped DWT signal, by simply adding the one phase signal components next to the previous ones, for each type of fault, as shown in Figure 14.

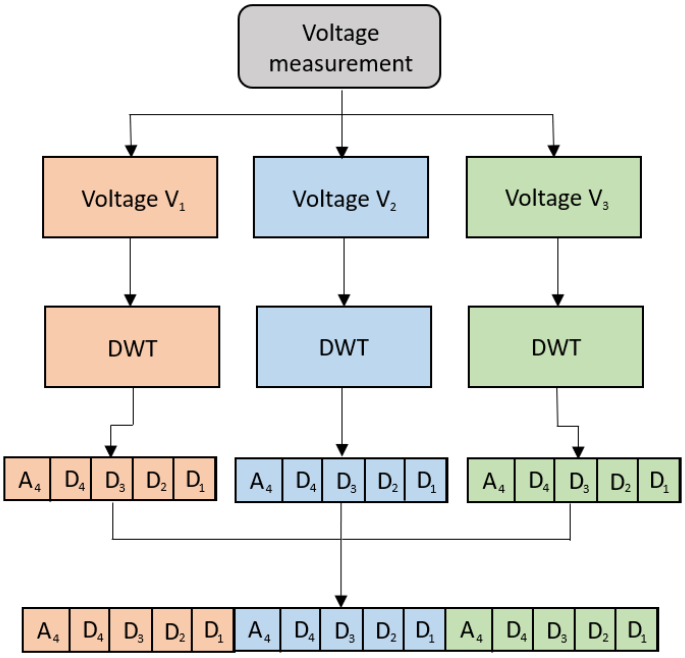

Figure 14: The DWT preprocessing flowchart

These signature signals represent the input to the ANN. After this unique signal for each fault scenario is created, the input set of data for ANN training is ready. The designed ANN takes the input set of 1600 input vectors and 1600 corresponding outputs during a training process. After that, trained ANN has four

possible outputs, where each output notes the normal operating condition and three types of faults. Figure 15 shows an example of the created signature signal.

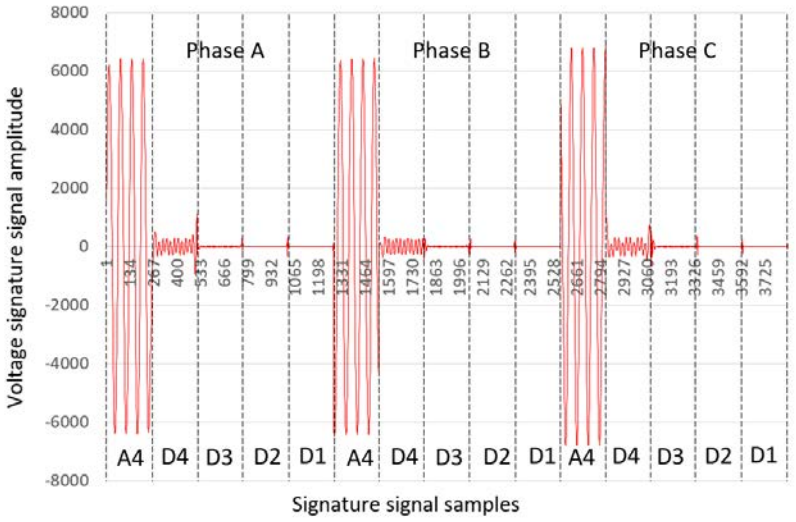

Figure 15: Grouped DWT components signal for *AE HIF fault*

3.3.3 Outline of the computational procedure for the DWT-ANN algorithm

The algorithm proposed in this research is based on DWT signal preprocessing, as shown in Figure 14. The proposed DWT - ANN algorithm needs training in order to accurately detect the fault and distinguish between the three possible categories of faults, regardless of the fault-resistance value and fault location.

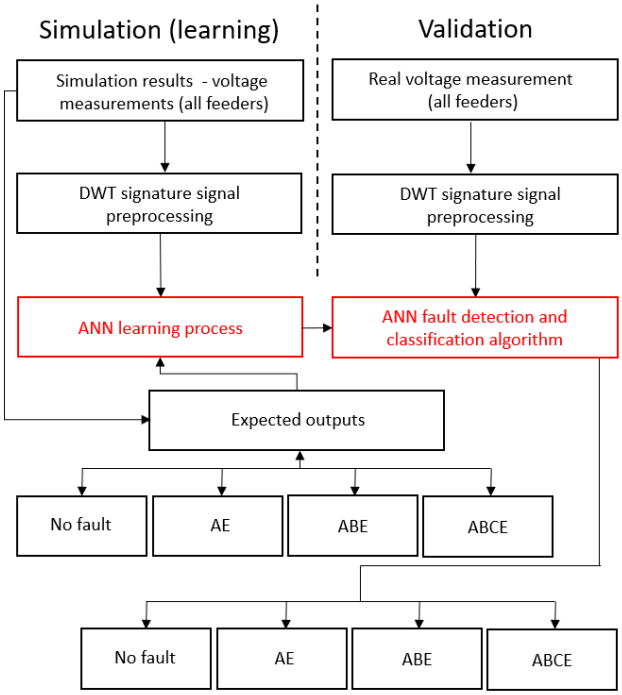

Figure 16: The DWT-ANN algorithm utilization flowchart

After the training and testing process, the created ANN can be used to classify faults in the distribution system. The flowchart of the online working principle of this method is shown in Figure 16.

3.4 Faults identification and classification in microgrids based on artificial neural networks and discrete wavelet transform – The Microgrid DWT-ANN algorithm

Microgrid protection is still a challenge, especially when it comes to operation in the islanded mode where the fault currents are significantly lower. However, motivated by the capability of the previously presented algorithms in terms of high impedance faults detection, these new algorithms could contribute to the solving of this problem. Because of that, the following section will give the experimental setup, the data preprocessing methodology and the outline of the computational procedure of this method.

3.4.1 Experimental setup for the Microgrid DWT-ANN algorithm

The microgrid is supplied from a 35/10 kV two parallel transformers (which presents a place of common coupling – PCC) via 10 kV feeders [11]. In case of the fault in the main grid, the microgrid can be disconnected from the main grid via 10 kV circuit breakers (CBs) that are placed in the 35/10 kV substation. In that case, the DGs supply the 10 kV microgrid [11]. The LV customers are supplied via 10/0.4 kV substations [11]. The simulation model is developed in MATLAB/Simulink software and presents a three-phase model of the previously described microgrid. A single line diagram of the test system is shown in Figure 17.

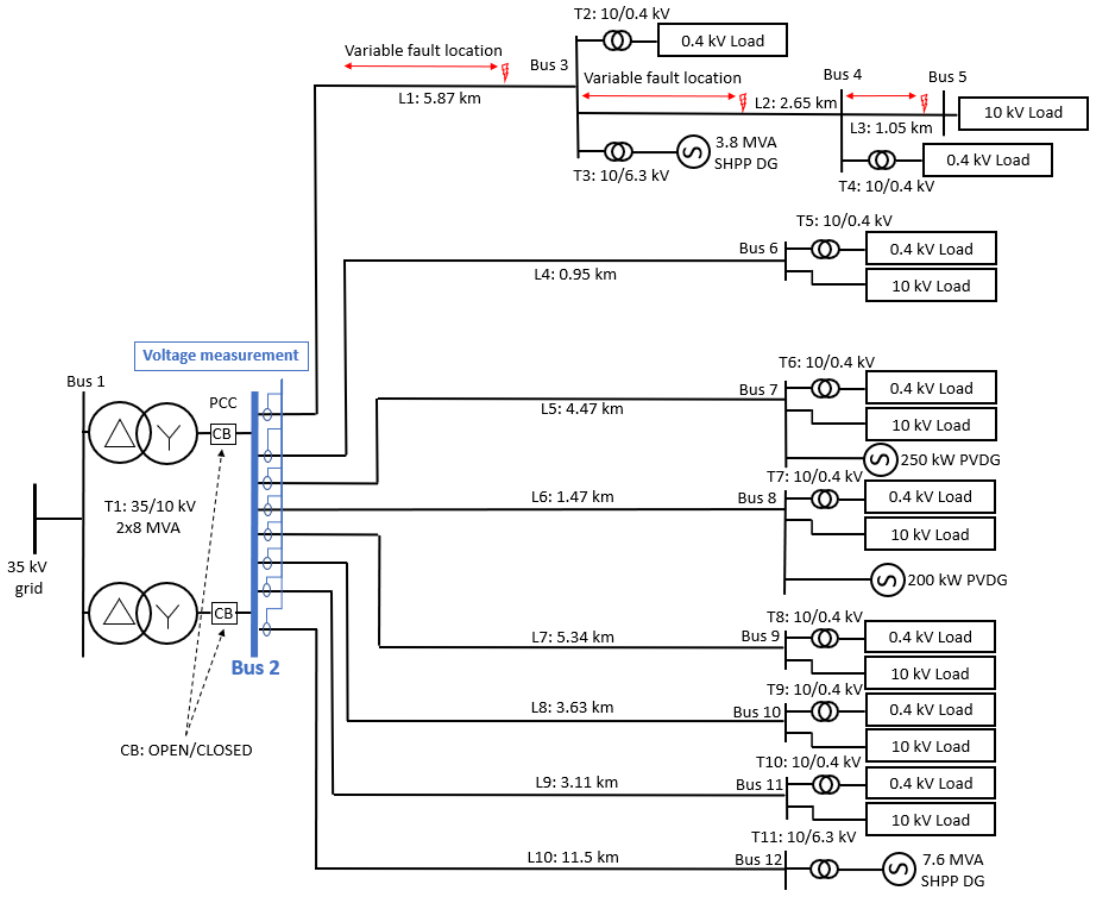

Figure 17: The developed test system for Microgrid DWT-ANN algorithm testing

The faults are simulated on a 10 kV underground cable that feeds the entire consumption area (cable L1) [11]. In order to test the algorithm behaviour in the challenging microgrid scenarios, the fault is simulated in the line between a SHPP and the rest of the consumers. The single-phase-earth faults (AE), phase-phase-earth faults (ABE) and three-phase faults (ABCE) over various resistances (in the range from 0 Ω to 300 Ω) and in different fault locations are simulated. The measurement is performed at a 10 kV busbar in the 35/10 kV substation while faults are simulated in both grid-connected and islanded mode of operation [11].

3.4.2 Data preprocesing for the Microgrid DWT-ANN algorithm

Data preprocessing is conducted in the same manner as described in section 3.3.2. However, in this application the voltages are measured directly on the 10 kV busbar of the substation, therefore the fault can be detected in any feeder of the 35/10kV substation. In order to use the proposed algorithm in a microgrid, the ANN needs to be trained to all the possible scenarios that may occur in the microgrid. First step is the creation of fault scenarios for the initial base of knowledge that ANN will learn from. The input data is prepared according to the procedure described in 3.3.2. The noise with signal to noise ratio (SNR) value of 30 dB to 50 dB is added to the signal measurements [11]. For this purpose, 89.384 simulations for three types of the fault and normal operating conditions, with various fault resistances and fault locations, are carried out [11]. The ANN takes the input set of 89.384 input vectors and 89.384 corresponding preferred outputs during a training process [11].

3.4.3 Outline of the computational procedure for the Microgrid DWT-ANN algorithm

The proposed method for fault identification and classification is based on a combination of DWT and ANN. It is based on the previous research of the author [9], [11], [39]. The computational procedure is described in section 3.3.3 However, since now the algorithm is capable to work in both grid connected and islanded mode, the procedure flowchart is further modified and shown in Figure 18.

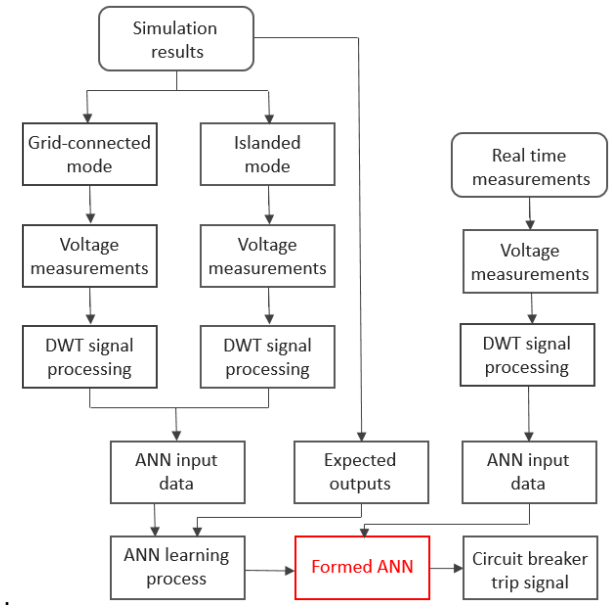

Figure 18: Proposed algorithm learning and utilization procedure [11]

With the measuring equipment installed in microgrid, the voltage waveforms can be constantly monitored with the previously defined moving time frame, while the obtained signals can be sent to the unit with a DWT-ANN algorithm software [11]. In the case of a fault identification, further actions can be undertaken.

3.5 Artificial Neural Network based Station Protection

Station protection in terms of substations feeder's protection includes following:

(a) Fault detection
(b) Fault classification
(c) Faulty feeder isolation
(d) Fault location estimation

All of the beforementioned functionalities need to have a satisfactory result in both grid-connected and islanded mode, in case the substation has a capability to become a part of the microgrid. Within these functions, the method that will be presented in the following chapter can be used to send a direct trip sequence in case of the fault, as well as provide the backup tripping function due to its high sensitivity.

3.5.1 Experimental setup for the Artificial Neural Network based Station Protection

The test system that will be used for this part of research relies on the test system from the section 3.4.1. However, in this case, the feeder 1 is modelled more in detail, and current measurements are added to every 10 kV feeder. These measurements are common in the real distribution network substations, where every feeder is equipped with both voltage and current measurements. For the purpose of ANN input preparation, the following scenarios were simulated:

(a) The single-phase-earth faults (AE), phase-phase-earth faults (ABE) and three-phase faults (ABCE) on feeder 1, on lines L1, L2 and L3,
(b) The single-phase-earth faults (AE), phase-phase-earth faults (ABE) and three-phase faults (ABCE) on feeder 2, on line L4,
(c) The single-phase-earth faults (AE), phase-phase-earth faults (ABE) and three-phase faults (ABCE) on feeder 3, on line L5.
(d) Normal operation scenarios

Faults were simulated over the fault resistances in range of 0 – 100 Ω, on various locations from 0 to 100% of line length. The loads and DG power outputs are changed in each simulation scenario. These values were randomized, but in the defined range, in order to simulate the dynamic behaviour of the system components. In this setup, every simulation has different loads and DG power outputs. Additionally, during the simulations, different levels of noise in the measured signals were added in the range of 30 to 50 signal to noise ratio (SNR).

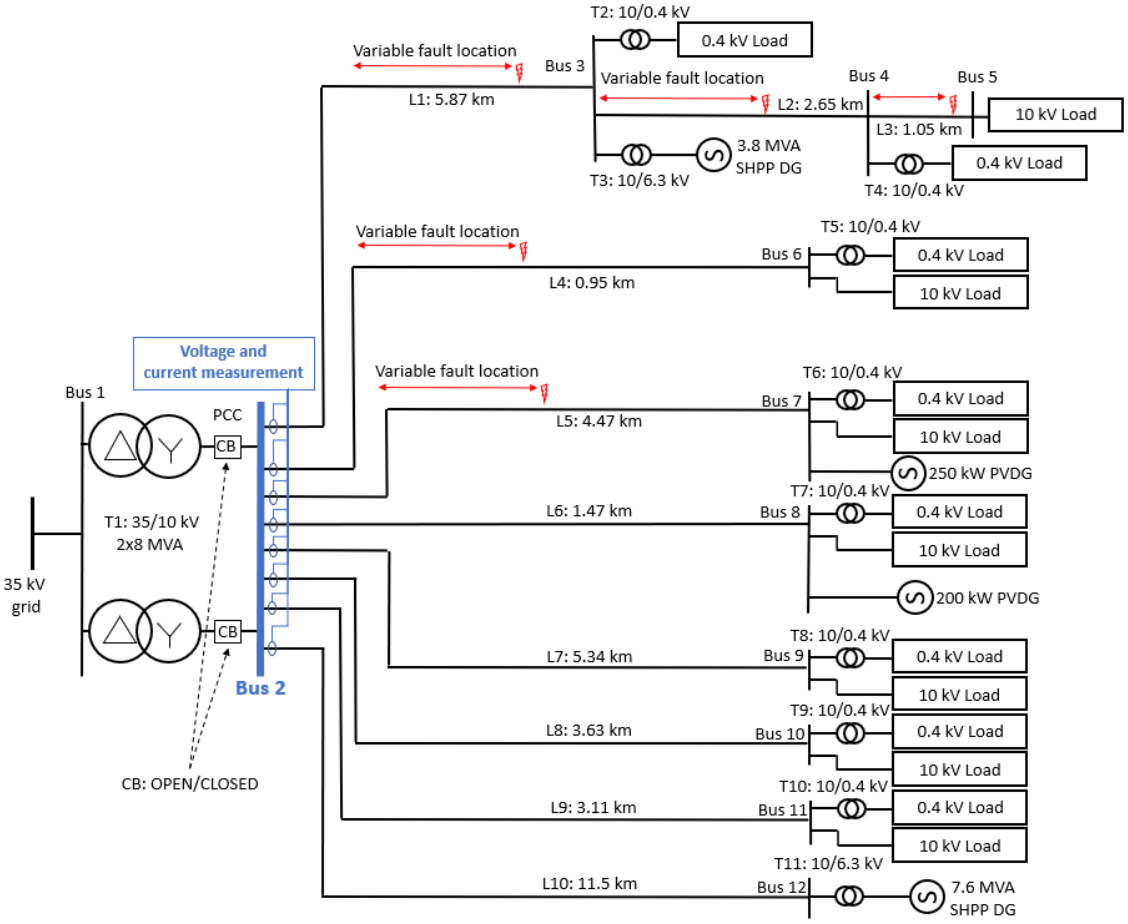

Figure 19: The developed 12-bus test system for station protection algorithm testing

The measurement of voltages and currents is performed during the 100 ms time frame, on the 10 kV feeders of the system. The test system is shown in Figure 19. Obtained voltage and current measurements from these feeders are sent to the DWT preprocessing algorithm in order to create the inputs for ANNs.

3.5.2 Data preprocessing for the Artificial Neural Network based Station Protection

Since the algorithm for station protection has more functionalities, the more data will need to be prepared. Here, multiple neural networks are developed, where each one of them provides a certain function. Hence, the data are prepared in two stages. First stage of data preprocessing is carried out in the same manner as described in section 3.3.2., where the measured busbar voltages are used. This data will be used for the training process of the ANN that will detect and classify the fault in the system.

The second stage of data preprocessing is the part where data for feeder selection and fault location algorithm are prepared. In this stage, the feeder currents are measured and pre-processed in the same manner as described in section 3.3.2. The example of current signature signal for feeder selection is shown in Figure 20.

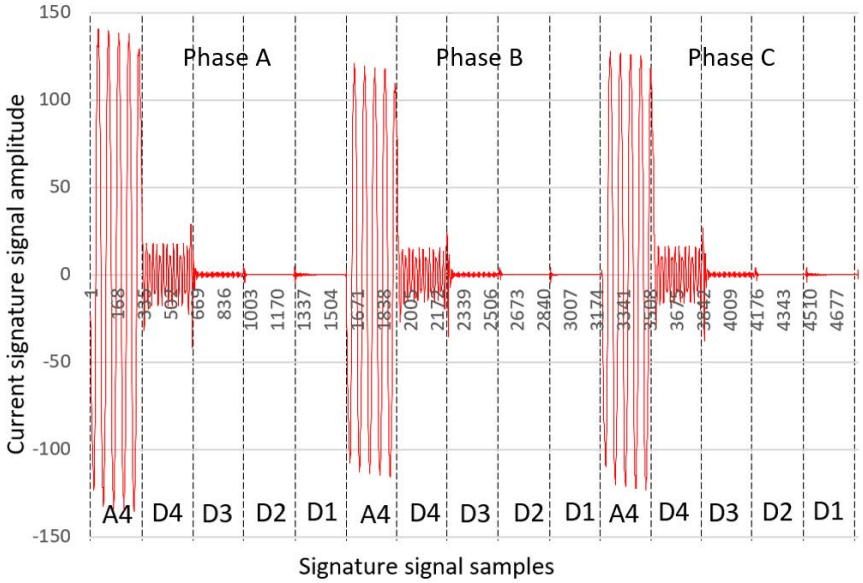

Figure 20: Example of current based signature signal for feeder selection and fault location estimation algorithms in case of single-phase-earth fault (A-E)

3.5.3 Outline of the computational procedure for the Artificial Neural Network based Station Protection

The signature signal construction is done in the same manner as described in section 3.3.3. Generally, the computational procedure for fault identification and classification is same as the procedure described in section 3.4.3. However, this output is used as a starting point for the next part of the algorithm – the faulty feeder selection. If the fault is detected (AE, ABE or ABCE) the procedure continues according to the flowchart shown in Figure 21. For this purpose, a separate neural network is developed that takes the current based signature signals as inputs.

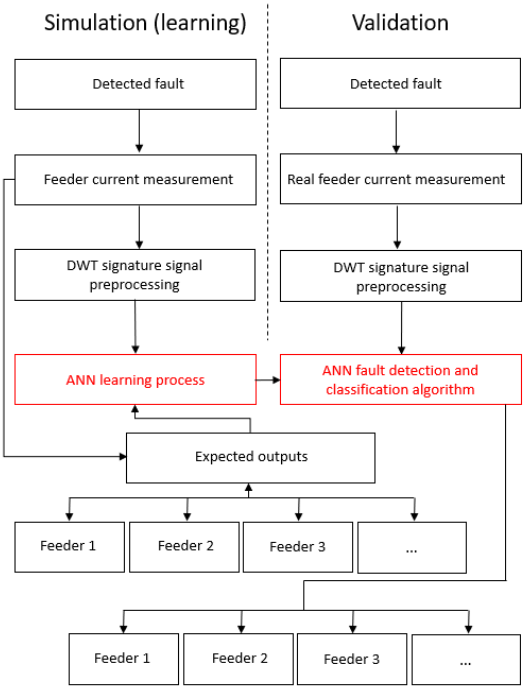

Figure 21: Algorithm for the feeder DWT-ANN feeder isolation

The developed ANN for feeder selection algorithm takes the reprocessed feeder current as input and has two possible outputs – fault has occurred in feeder or fault has not occurred in that feeder. For this purpose, 3 feeders were selected and tested in order to prove the algorithm accuracy, as shown in Figure 19. After a successfully isolated feeder, the fault location estimation algorithm takes place. Since in this stage the fault type and the faulty feeder are known, the separate ANNs for each feeder is trained in order to achieve better accuracy. The computational procedure is shown in Figure 22.

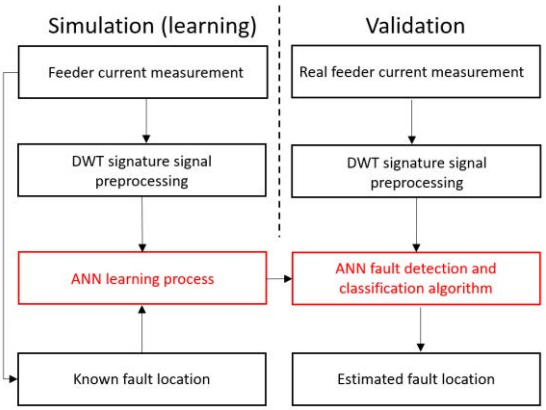

Figure 22: The DWT-ANN based fault location estimation algorithm

The ANN developed for the purpose of fault location takes current based signature signals and has outputs in the range of 0 to 1, which denote the place where the fault occurred (for example: 0.55 means fault at 55% of feeder length). After all these steps, the algorithm should be able to detect the fault, classify the fault type, isolate the faulty feeder and finally estimate the fault location.

4 Evaluation and Comparison

This section will give the results of each methodology presented in section 3. These results will show advantages and disadvantages of the methodologies, and therefore clearly define the path of the total research that led to the ANN based station protection.

4.1 Fault location estimation based on artificial neural networks and Fast Fourier transform – The FFT-ANN algorithm

As a result of the methodology and simulation scenarios presented in section 3.1, the results are obtained. As shown in Figure 6, the power quality meters are not present in every busbar in the 8-bus test system, which is realistic scenario in the real power system from the economical point of view. Since the power quality meters are installed in 4 places in the system, the ANN input vector will contain 240 values, that represent the voltage and current harmonics measured by the 4 devices [13]. The output vector has two values that represent the fault location and fault resistance value.

The mean squared error (MSE) of the proposed ANN locator is 2.4196 m in the case of fault location, and 0.47913 Ω in the case of resistance estimation [13]. In order to demonstrate the proposed locator accuracy, new 5 fault scenarios are simulated, in completely different locations, and different fault resistance values [13]. These values present the new data that ANN is not trained to [13]. The results of the proposed ANN fault locator in the 8-bus system are presented in Table 3.

Test case number	**Desired output**		**Actual output**	
	Fault location (% length)	**Fault resistance (Ω)**	**Fault location (% length)**	**Fault resistance (Ω)**
Test case 1	16	20	16,0169	19,6297
Test case 2	31	35	30,9853	35,1864
Test case 3	46	50	45,9688	49,9218
Test case 4	76	80	75,9458	80,1732
Test case 5	91	95	91,1041	94,8026
Mean squared error (MSE)			< 0.1	0,479

Table 3: Output of the FFT-ANN fault locator for different fault resistances and fault locations in an 8 – bus test system

The locator could be installed in the power system with appropriate communication infrastructure [13]. When the fault occurs, the data can be sent to the one single unit with a proposed ANN algorithm. Following the procedure showed in Figure 8, the algorithm can estimate the fault location and fault resistance. This approach showed the applicability of the fault location estimation in a power system line with satisfactory results, and it contributes to the operation of the power system, by providing the more accurate fault location, and finally reducing the outage time and improving the power quality.

Since the measurement period is at least 200 ms, and the power quality meters need to be connected with the appropriate communication infrastructure, the algorithm is intended to be used for post processing. However, the obtained results demonstrated the approach to be promising tool for data anylsis. On the other hand, in order to detect fault, the total detection time needs to be considerably lower.

4.2 Fault classification based on artificial neural networks and Hilbert-Huang transform – The HHT-ANN algorithm

The results presented in the previous section demonstrated appropriate accuracy for the fault location and fault resistance evaluation in the HV test system. Motivated by these results, the next challenge was to deal with the detection and classification of the faults in the distribution systems, especially the high impedance ones. After the procedure described in section 3.2, the ANN is trained and ready for new scenarios. In order to demonstrate the accuracy of the created ANN, five new fault scenarios are simulated, and the proposed classifier is tested. Results of these tests are shown in Table 4. The accuracy in the resistance range from 20 to 600 Ω, for classifying the faults in one MV feeder with is more than 99%.

Test case number	**Fault resistance (Ω)**	**Desired output (fault type)**	**Actual output (fault type)**
Test case 1	**20**	Single-phase-earth fault (AE)	Single-phase-earth fault (AE)
Test case 2	**110**	No fault	No fault
Test case 3	**290**	Three-phase fault (ABCE)	Three-phase fault (ABCE)
Test case 4	**380**	Single-phase-earth fault (AE)	Single-phase-earth fault (AE)
Test case 5	**470**	Phase-phase-earth fault (ABE)	Phase-phase-earth fault (ABE)
Mean squared error (MSE)			< 1%

Table 4: Output of the HHT-ANN classifier

Even though the HHT-ANN approach gave great results from the point of fault classification, the number of IMFs that occur in the signal can vary, and thus hide the important information in the higher order IMFs, which affects the robustness of the method. This imposed the necessity for different, more appropriate preprocessing method. The tests did not include the changes in system like load changes, noise, switching of the large consumers and faults in different feeders.

4.3 Faults identification and classification using artificial neural networks and discrete wavelet transform – The DWT-ANN algorithm

Since the number of IMSs can occur, and therefore hide the important fault information in the higher order IMFs, a different preprocessing method is chosen. By preprocessing the signal with the DWT, all the important signal information can be kept in the fixed numbers of details and approximations regardless of the signal complexity. Again, the results are presented in the same manner. Table 5 shows classifier results for 5 fault scenarios, where column *Desired output* presents a simulated-fault type and column *Actual output* an evaluated fault type [9], [39]. Column *Actual output* presents the ANN output for each fault scenario [9], [39]. The proposed DWT – ANN algorithm has an accuracy over 99% in the range of 20 – 600 Ω for all fault locations in one MV feeder of the system.

Test case number	**Fault resistance (Ω)**	**Fault location (% length)**	**Desired output (fault type)**	**Actual output (fault type)**
Test case 1	**20**	0.01	Single-phase-earth fault (AE)	Single-phase-earth fault (AE)
Test case 2	**110**	0.16	No fault	No fault
Test case 3	**290**	0.46	Three-phase fault (ABCE)	Three-phase fault (ABCE)
Test case 4	**380**	0.61	Single-phase-earth fault (AE)	Single-phase-earth fault (AE)
Test case 5	**470**	0.76	Phase-phase-earth fault (ABE)	Phase-phase-earth fault (ABE)
Mean squared error (MSE)				< 1%

Table 5: Output of the DWT-ANN classifier for different fault resistances, fault locations and fault types

The proposed algorithm is designed to be used in the online mode [9], [39]. The storage method is important since the grouped DWT components take a lot of storage [9], [39]. Few minutes old data can be deleted if no disturbances are recorded, while the voltage waveforms can be saved for a later analysis [9], [39]. The approach demonstrated its applicability to fault detection and classification, especially when it comes to high impedance faults. However, this approach can detect and classify faults in just one feeder, i.e. where the measurement is present. On the other hand, these faults have low fault currents, which is exactly what is happening in the case of the fault in the islanded microgrid. The tests did not include the changes in system like load changes, noise, switching of the large consumers and faults in different feeders.

4.4 Faults identification and classification in microgrids based on artificial neural networks and discrete wavelet transform – The Microgrid DWT-ANN algorithm

Since the DWT-ANN algorithm showed its accuracy in the detection and classification of the high impedance faults in the distributions system, the next step in the research was to test the algorithm on the microgrid that can work both in grid connected and islanded mode, and detect faults in all microgrid feeders. As a result of the process described in section 3.4, the proposed DWT - ANN algorithm is capable to accurately identify the fault and distinguish between the three possible categories of faults for both modes of microgrid operation, regardless of the fault-resistance value and fault location, with the 85.74% accuracy in the 0-300 Ω fault resistance range, with the SNR value of 30 dB [11]. Of course, the accuracy improves with the noise reduction, thus having the accuracy of 96.92% with SNR value of 40 dB (which is a common value in most 10 or 20 kV power networks), and having the accuracy over 99% with SNR values over 50 dB [11]. The algorithm error for various SNR values is shown in Figure 23.

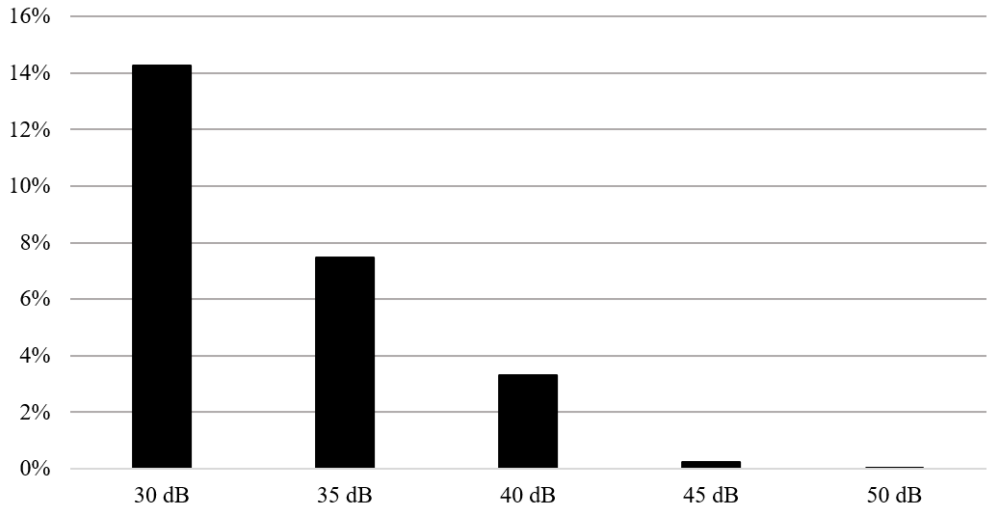

Figure 23: Algorithm error for various signal to noise (SNR) values

After the training and testing process, the created ANN is perfectly capable to identify and classify faults in the both modes of microgrid operation [11]. Table 6 shows classifier results to this fault scenarios, where column Desired output presents a simulated-fault type and column Actual output an evaluated fault type [11].

Test case number	Fault resistance (Ω)	Fault location (% length)	Desired output (fault type)	Actual output (fault type)
Grid-connected operation				
Test case 1	**20**	16	Single-phase-earth fault (AE)	Single-phase-earth fault (AE)
Test case 2	**110**	31	No fault	No fault
Test case 3	**200**	46	Phase-phase-earth fault (ABE)	Phase-phase-earth fault (ABE)
Test case 4	**290**	78	Three-phase fault (ABCE)	Three-phase fault (ABCE)
Islanded operation				
Test case 5	**20**	16	Single-phase-earth fault (AE)	Single-phase-earth fault (AE)
Test case 6	**110**	31	No fault	No fault
Test case 7	**200**	46	Phase-phase-earth fault (ABE)	Phase-phase-earth fault (ABE)
Test case 8	**290**	78	Three-phase fault (ABCE)	Three-phase fault (ABCE)
Mean squared error (MSE)				< 1 % (50 dB noise)

Table 6: Example of the DWT-ANN classifier output for different fault resistances, fault locations and fault types in both modes of microgrid operation

Generally, DWT is widely used for the noise-removal applications [40], [41], which is one of the main reasons that it performs very well in this application. Moreover, since the proposed algorithm is paired with ANNs, which are known to have a high accuracy in the pattern classification and noise removal ability [9], this issue is addressed even more effectively. This method with measurement in the 10 kV busbar of the primary substation ensures fault detection on all microgrid feeders, but does not detect the faulty feeder, i.e. the feeder that fault occurred on. However, these tests did not include the changes in system like load changes, switching of the large consumers and faults in different feeders. The lack of the faulty feeder detection and robustness of the method due to the dynamic nature of the microgrid led to the final research: The ANN based station protection.

4.5 Artificial Neural Network based Station Protection

As the natural research question after the previous research, dynamic behaviour of the microgrid should be taken into consideration. Therefore, the test system is set up according to the section 3.5. The results obtained from the methodology and test scenarios presented in section 3.5. show the practicality and accuracy of the proposed algorithm. In this part of research, the moving window measurement frame is set to 100 ms, in order to record at least 5 full periods of voltage and current. This approach proved to be an improvement since there are more information about the fault (and post fault) behaviour recorded and sent to the learning algorithm. On the other hand, 100 ms fault detection time still presents a

satisfactory result. The other important consideration is that the fault resistance values in this setup were in range from 0 to 100 Ω, which is a common fault resistance range.

The loads and DG power outputs are changed in each simulation scenario. These values were randomized, but in the defined range, in order to simulate the dynamic behaviour of the system components. In this setup, every simulation scenario has different loads and DG power outputs, in order to achieve the robustness of the proposed method. Additionally, during the simulations, different levels of noise are added to the measured signals, in the range from 21.94 dB to 50 dB of signal to noise ratio (SNR). The noise level of 21.94 dB presents the noise level that would occur in the case of THD (Total Harmonic Distortion) of 8%, which is the limit for the THD in MV networks according to the EN50160 standard [42]. The measurement of voltages and currents is performed on the 10 kV feeders of the system. Obtained voltage and current measurements from these feeders are sent to the DWT preprocessing algorithm in order to create the inputs for ANNs

Following the procedure described in previous sections, a very large number of simulation scenarios is provided, more precisely 570.000 scenarios for the fault detection and classification ANN, 1.728.000 scenarios for the faulty feeder selection ANN and 144.000 scenarios for the fault location estimation. Totally, 2.442.000 scenarios were simulated and prepared for the ANN learning process. Following figures show the accuracy for various functionalities of the station protection algorithm in both grid connected and islanded mode of operation.

The algorithm error for the SNR of 21.94 dB is 17.73 % and it drops down to zero in for the SNR value of 50 dB, in the case of grid connected mode of operation, as shown in Figure 24. However, in the islanded mode of operation of the microgrid, the algorithm error for the SNR of 21.94 dB is 7.63 % and it drops down to 0.0604 % in case of the SNR of 50 dB.

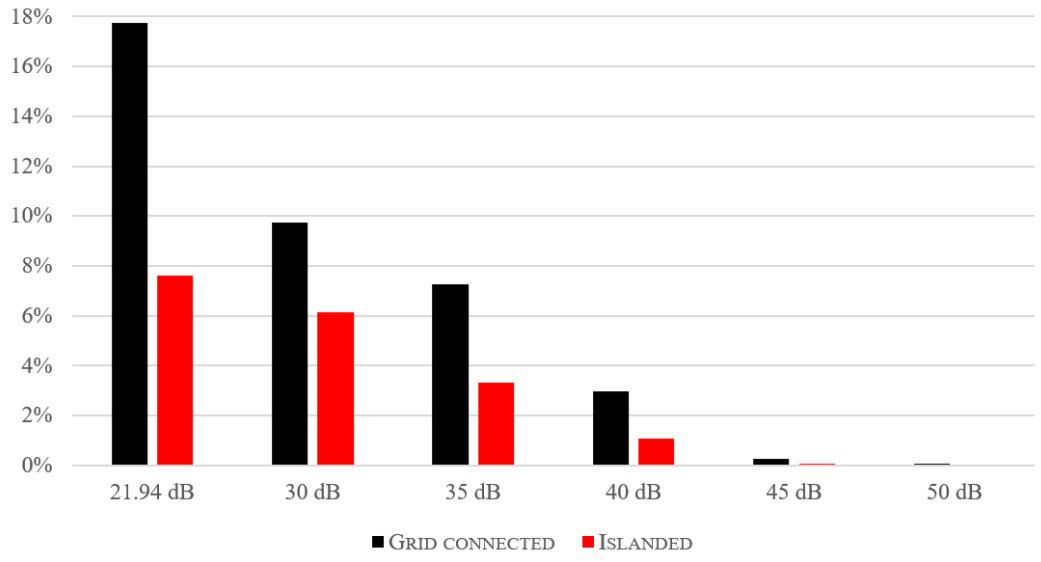

Figure 24. Fault detection and classification algorithm error (%) for various signal to noise (SNR) values in both modes of operation

Figure 24 shows the algorithm error for various SNR values for grid connected and island mode of operation. In grid connected mode the detection error is 8.05 % for the SNR value of 21.94 dB and it drops to 0.882 % for the SNR value of 50 dB. On the other hand, in the islanded mode of operation, the error is in range from 5.006 % to 3.47e-3 % for SNR values from 21.94 to 50 dB.

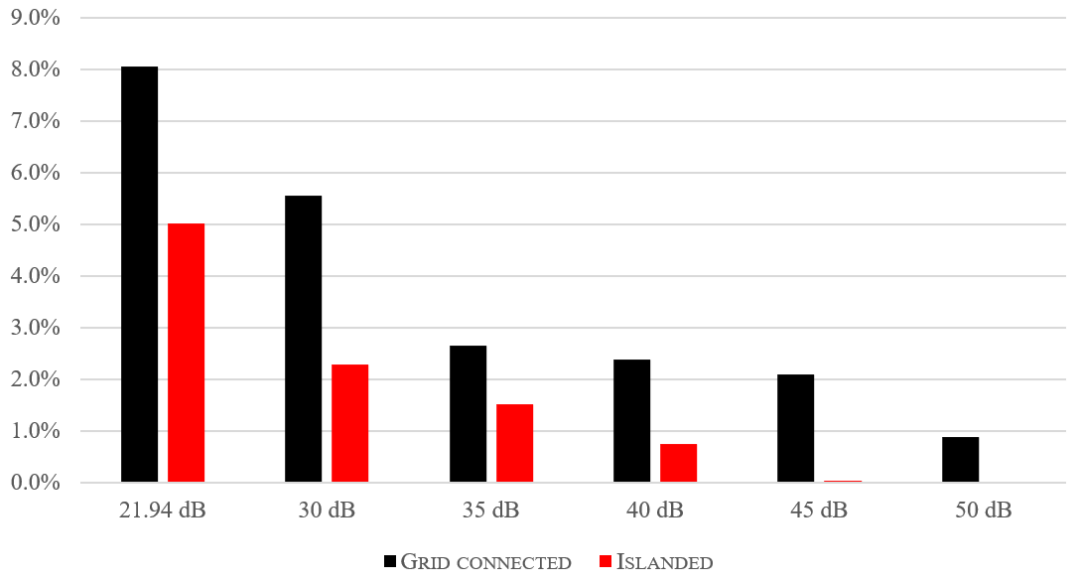

Figure 25. Faulty feeder detection algorithm error (%) for various signal to noise (SNR) values in both modes mode of operation

Since previously presented problems are a pattern recognition problem, the ANN could successfully classify the inputs into the set of target categories. However, the fault location algorithm is a fitting problem, where an ANN needs to map between set a dataset of numerical inputs and set of numerical targets, in this case the location of the fault in the faulty feeder.

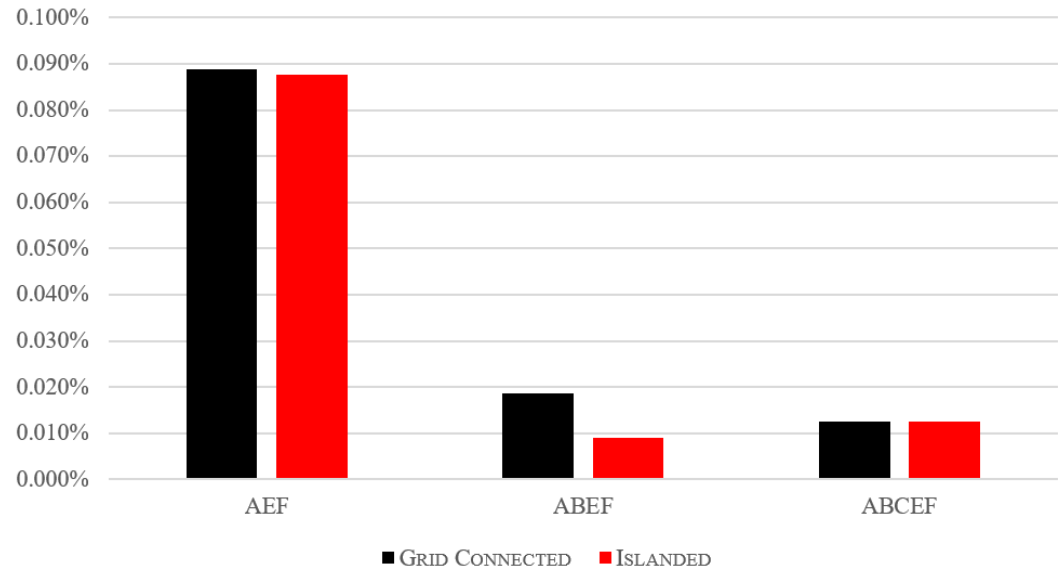

Figure 26: Fault location algorithm error (%) for both modes of microgrid operation

The Feeder 1 presents a most challenging one for fault location, and because of that, the algorithm is tested in the Feeder 1. Figure 26 shows the fault location algorithm error for both modes of the microgrid

operation. The obtained results show that the mode of microgrid operation does not significantly affect the fault location algorithm accuracy. The same stands for the noise level, since the different levels of noise in signal (SNR value from 21.94 to 50 dB) did not significantly affect the accuracy. More precisely, the difference in accuracy for SNR value of 21.94 dB and SNR value of 50 dB was less than 0.01% for all types of faults in both modes of operation.

In order to demonstrate the importance of the moving time frame that is used for capturing the voltages and currents, the results for two levels of SNR in islanded mode of operation are shown in Figure 27. The results show that the algorithm can successfully work even with the 30 ms moving time frame, but with increased error. By increasing the time frame size, the error decreases since capturing more data helps to reflect the fault scenario better.

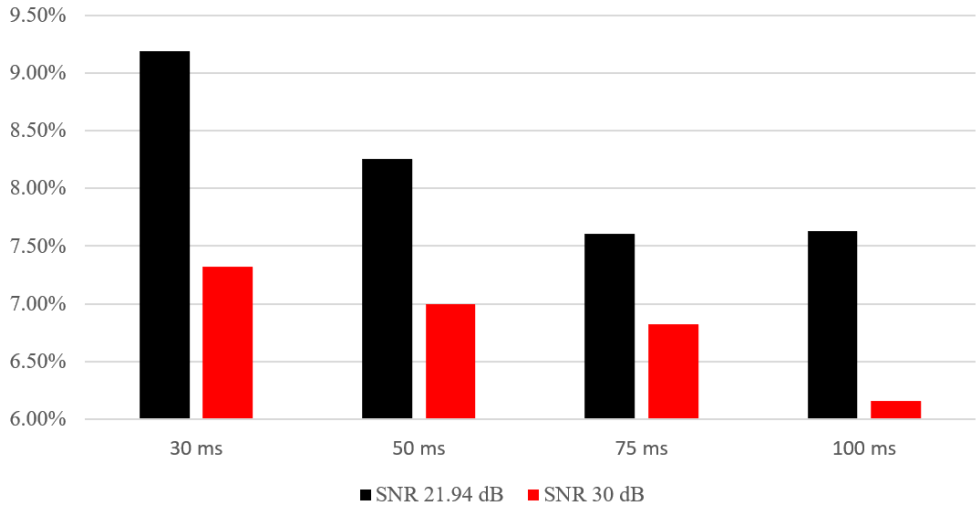

Figure 27: Fault detection and classification algorithm error (%) for two signal to noise (SNR) values in islanded mode of operation depending on moving time frame size

The presented results showed the accuracy of the algorithm for different noise levels, however, the SNR value of 21.94 dB is an extreme case. The measurements in the Bosnia and Herzegovina MV network show that the THD levels rise to 2%, which is around 35 dB of the SNR value. These THD levels usually occur in the remote parts of long feeders, where system impedance is high. Since the algorithm proposed in this paper is intended to be used at the substation, where system impedance is usually low, the noise levels are not expected to be this high. Therefore, the accuracy is expected to be at least 93% for the fault detection and classification, 97% for faulty feeder detection and 99.91% for fault location in worst scenarios.

5 Conclusions and Future Research Directions

The appropriate microgrid protection system still presents a challenge for the DSOs and an open research area for the researchers, due to the complex nature of the microgrids. Therefore, this thesis proposes a method to improve the existing protection strategies by using the artificial intelligence-based algorithm.

The presented work demonstrated the applicability of the ANN-based algorithm for distribution system protection functionalities. This research evolved from the pure fault location estimation in HV power systems to the multiple station protection functionalities in distribution microgrids. Over the years, the results of research and new findings led to the DWT pre-processed data coupled with ANNs.

When it comes to the research questions that defined the research, each one of these questions is answered through this thesis. However, the summary answers will be given here. The fourth research question was: How the proposed methods deal with changes in the short-circuit levels, dynamic changes of the other distribution system parameters and different network topologies? The results presented in this thesis demonstrated the accuracy and practicality of the station protection algorithm in terms of fault detection, fault type classification, faulty feeder detection and fault location estimation. Numerous operating scenarios of the test system based on the real distribution network were used for algorithm testing. These scenarios include variable loads, DG power outputs, fault locations, faulty feeders, fault resistances, fault types, noise levels, system load curve points and microgrid operation modes. All these dynamic changes that include the changes in the short-circuit levels and change of distribution system parameters have been included in the process of simulation and testing of the proposed methods.

First research question was: How can advanced protection algorithms based on artificial intelligence improve current protection schemes? Considering the robustness of the algorithm to all variations that are mentioned in the answer to the fourth research question, it is believed to be a promising concept for the upgrade of the existing microgrid protection strategies.

The second research question was: How is microgrid protection seen in terms of sustainability? Microgrids can be improve power quality and increase reliability and. Since microgrid mainly rely on the utilization of the renewable DG, there are direct environmental benefits that come with the increased use of microgrids. The continuous environmental pollution, intensive climate change, and new sustainable technologies have led to rationalization of the energy usage through the renewable energy. Thus, in terms of sustainability, a microgrid reduces both pollution and global warming because it consequently produces less pollutants.

The third research question was: What socioeconomic, technical and financial factors justify the usage of the advanced protection schemes in microgrids? Electricity supply interruptions are less and less accepted by both consumers and regulators, making the requirements for the reliability of supply higher than ever. Meanwhile, distribution system operators struggle to achieve these requirements, mainly because of the infeasibility of the investments. However, if the consumers were willing to pay for the increased reliability of supply, these requirements can be achieved. The research results showed that

consumers are willing to pay for better service. The obtained information can be used to analyse the investments in distribution systems and future microgrids in order to target exactly those investments that will improve the reliability of that part of the distribution system. In that way, consumers that are willing to pay more for more reliable electricity could have a special designed pricing tariff that would justify the additional investments in the reliability.

The fifth research question was: How does the noise level in measured signals affect the accuracy of the protection system? Different levels of noise were included in the measured signals during the testing of the protection methodologies. Generally, the higher the noise level is, the higher the error of the protection functionalities is. However, the levels of noise that are common in real distribution networks are usually below the noise levels that were used in this research. Since both DWT and ANN are knows as great tools when it comes to dealing with noisy signals, this issue is well addressed.

The sixth and the final research question was: How does the size of the moving time frame affects the accuracy of the protection system? The moving time frame size changed in different methodologies that are presented in this thesis. It ranges from 200ms in the case of FFT-ANN algorithm to 30ms in the microgrid DWT-ANN algorithm. Since all the proposed methodologies use ANNs, larger input vector means more data that describe the fault scenario better. Because of that, the accuracy decreases as the moving time frame size decreases. However, since all analysed moving time frame sizes are in milliseconds, it can still be considered as appropriate time for fault detection and classification.

Even though the ANN based algorithms presented in this thesis demonstrated their applicability, there are still some limitations of the analysed methods. As in every machine learning methodology, corner cases that may occur during the system operation may lead to false estimation. These cases can be solved by additional ANN training. Another limitation is the larger change of the system topology. Significant changes in the network topology can also lead to false estimation due to the significant change in the system parameters. This issue can also be solved by training the ANN to all possible network topologies, or to have multiple trained ANNs that will be operational depending on the network topology.

Future research directions should include the robustness improvements and validation of the algorithm on multiple real microgrids. This should include designing and testing of functionalities that can overcome the previously mentioned limitations.

In summary, this thesis contributes to the existing body of knowledge by developing, testing and comparing new methods in terms of power system protection whose application presents an improvement when compared to the functionalities of the existing protection devices.

6 References

[1] M. Ding, Y. Zhang, and M. Mao, “Key technologies for microgrids-a review,” in *1st International Conference on Sustainable Power Generation and Supply, SUPERGEN ’09*, 2009.

[2] J. Kennedy, P. Ciufo, and A. Agalgaonkar, “A review of protection systems for distribution networks embedded with renewable generation,” *Renewable and Sustainable Energy Reviews*. 2016.

[3] S. A. Hosseini, H. A. Abyaneh, S. H. H. Sadeghi, F. Razavi, and A. Nasiri, “An overview of microgrid protection methods and the factors involved,” *Renewable and Sustainable Energy Reviews*. 2016.

[4] B. J. Brearley and R. R. Prabu, “A review on issues and approaches for microgrid protection,” *Renewable and Sustainable Energy Reviews*. 2017.

[5] M. Sedighizadeh, A. Rezazadeh, and N. I. Elkalashy, “Approaches in high impedance fault detection a Chronological review,” *Adv. Electr. Comput. Eng.*, 2010.

[6] T. Hubana, “Artificial Intelligence based Station Protection Concept for Medium Voltage Microgrids,” in *2020 19th International Symposium INFOTEH-JAHORINA (INFOTEH)*, 2020, pp. 1–6.

[7] T. Hubana, M. Šarić, and S. Avdaković, *Classification of Distribution Network Faults Using Hilbert-Huang Transform and Artificial Neural Network*, vol. 59. 2019.

[8] M. Šarić, T. Hubana, and E. Begić, *Fuzzy Logic Based Approach for Faults Identification and Classification in Medium Voltage Isolated Distribution Network*, vol. 28. 2018.

[9] T. Hubana, M. Šaric, and S. Avdakovic, “High-impedance fault identification and classification using a discrete wavelet transform and artificial neural networks,” *Elektroteh. Vestnik/Electrotechnical Rev.*, vol. 85, no. 3, 2018.

[10] E. Šemić, M. Šarić, and T. Hubana, *Influence of Solar PVDG on Electrical Energy Losses in Low Voltage Distribution Network*, vol. 28. 2018.

[11] T. Hubana, M. Šarić, and S. Avdaković, *New Approach for Fault Identification and Classification in Microgrids*, vol. 83. 2020.

[12] T. Hubana, S. Hodzic, E. Alihodzic, and A. Mulaosmanovic, *The Valuation of Kron Reduction Application in Load Flow Methods*, vol. 59. 2019.

[13] T. Hubana, “Transmission lines fault location estimation based on artificial neural networks and power quality monitoring data,” in *Proceedings - 2018 IEEE PES Innovative Smart Grid Technologies Conference Europe, ISGT-Europe 2018*, 2018.

[14] T. Hubana, E. Begić, and M. Šarić, “Voltage Sag Propagation Caused by Faults in Medium Voltage Distribution Network,” in *Lecture Notes in Networks and Systems*, 2018.

[15] T. Hubana and N. Ljevo, *Willingness to Pay for Reliable Electricity: A Contingent Valuation Study in Bosnia and Herzegovina*, vol. 83. 2020.

[16] D. Kriesel, *A brief Introduction on Neural Networks*. 2007.

[17] M. Jamil, S. K. Sharma, and R. Singh, “Fault detection and classification in electrical power transmission system using artificial neural network,” *Springerplus*, 2015.

[18] Z. Zhang, “Learning algorithm of wavelet network based on sampling theory,” *Neurocomputing*, 2007.

[19] S. Mallat, *A Wavelet Tour of Signal Processing*. 2009.

[20] P. Ma, Y. Chang, and G. Jiang, “Frequency characterizations of epoxy/CNTs composites under com-pression at different strain rates,” *Adv. Compos. Lett.*, 2016.

[21] T. Pfajfar, J. Meyer, P. Schegner, and I. Papic, “Influence of instrument transformers on harmonic distortion assessment,” in *IEEE Power and Energy Society General Meeting*, 2012.

[22] J. Meyer, R. Stiegler, M. Klatt, M. Elst, and E. Sperling, “Accuracy of harmonic voltage measurements in the frequency range up to 5 kHz using conventional Instrument Transformers,” *21st Conf. Electr. Distrib. CIRED*, 2011.

[23] M. H. J. Bollen, J. V. Milanovic, and N. Cukalevski, “CIGRE/CIRED JWG C4.112 - Power Quality Monitoring,” *Renew. Energy Power Qual. J.*, 2014.

[24] F. A. A. Aziz, M. I. Shapiai, A. F. A. Aziz, F. Ali, A. Maliha, and Z. Ibrahim, “EEG brain symmetry index using hilbert huang transform,” in *Communications in Computer and Information Science*, 2017.

[25] Y. Guo, C. Li, Y. Li, and S. Gao, “Research on the Power System Fault Classification Based on HHT and SVM Using Wide-area Information,” *Energy Power Eng.*, 2013.

[26] B. L. Barnhart, “The Hilbert-Huang Transform : theory , applications , development by,” *Theiss, Univ. Iowa*, 2011.
[27] H. Leng, X. Li, J. Zhu, H. Tang, Z. Zhang, and N. Ghadimi, “A new wind power prediction method based on ridgelet transforms, hybrid feature selection and closed-loop forecasting,” *Adv. Eng. Informatics*, 2018.
[28] F. M. Villalobos-Castaldi, J. Ruiz-Pinales, N. C. K. Valverde, and M. Flores, “Time-frequency analysis of spontaneous pupillary oscillation signals using the Hilbert-Huang transform,” *Biomed. Signal Process. Control*, 2016.
[29] N. E. Huang and Z. Wu, “A review on Hilbert-Huang transform: Method and its applications to geophysical studies,” *Reviews of Geophysics*. 2008.
[30] M. Choudhury and A. Ganguly, “Transmission line fault classification using discrete wavelet transform,” in *2015 International Conference on Energy, Power and Environment: Towards Sustainable Growth, ICEPE 2015*, 2016.
[31] K. M. Jagtap and D. K. Khatod, “Novel approach for loss allocation of distribution networks with DGs,” *Electr. Power Syst. Res.*, 2017.
[32] S. Daud, A. F. A. Kadir, and C. K. Gan, “The impacts of distributed Photovoltaic generation on power distribution networks losses,” in *2015 IEEE Student Conference on Research and Development, SCOReD 2015*, 2015.
[33] A. F. A. Kadir, T. Khatib, and W. Elmenreich, “Integrating photovoltaic systems in power system: Power quality impacts and optimal planning challenges,” *International Journal of Photoenergy*. 2014.
[34] P. Gakhar, T. Manglani, and D. K. Doda, “Advancement & Role of DG Technology in Distribution System,” *Int. J. Recent Res. Rev.*, 2013.
[35] D. T. Ton and M. A. Smith, “The U.S. Department of Energy’s Microgrid Initiative,” *Electr. J.*, 2012.
[36] A. Hirsch, Y. Parag, and J. Guerrero, “Microgrids: A review of technologies, key drivers, and outstanding issues,” *Renewable and Sustainable Energy Reviews*. 2018.
[37] N. K. Choudhary, S. R. Mohanty, and R. K. Singh, “A review on Microgrid protection,” in *2014 International Electrical Engineering Congress, iEECON 2014*, 2014.
[38] IEC, “IEC 61000-4-7 : Electromagnetic Compatibility, General Guide on Harmonics and Inter-harmonics Measurements and Instrumentation,” 1991.
[39] T. Hubana, M. Saric, and S. Avdakovic, “Approach for identification and classification of HIFs in medium voltage distribution networks,” *IET Gener. Transm. Distrib.*, vol. 12, no. 5, 2018.
[40] R. K. Sarawale and S. R. Chougule, “Noise removal using double-density dual-tree complex DWT,” in *2013 IEEE 2nd International Conference on Image Information Processing, IEEE ICIIP 2013*, 2013.
[41] A. R. Haider Mohomad, C. P. Diduch, Y. Biletskiy, R. Shao, and L. Chang, “Removal of measurement noise spikes in grid-connected power converters,” in *2013 4th IEEE International Symposium on Power Electronics for Distributed Generation Systems, PEDG 2013 - Conference Proceedings*, 2013.
[42] DKE, “DIN EN 50160 - Merkmale der Spannung in öffentlichen Elektrizitätsversorgungsnetzen,” 2011.

7 Appendix

7.1 Published papers related to the PhD thesis

The following list gives the published papers that are directly related to the PhD thesis, where parts of the PhD thesis are analyzed in detail in each paper:

1. **T. Hubana**, "Artificial Intelligence based Station Protection Concept for Medium Voltage Microgrids," 2020 19th International Symposium INFOTEH-JAHORINA (INFOTEH), East Sarajevo, Bosnia and Herzegovina, 2020, pp. 1-6.

2. **T. Hubana**, M. Šarić, S. Avdaković, „New Approach for Fault Identification and Classification in Microgrids" In: Avdaković S., Mujčić A., Mujezinović A., Uzunović T., Volić I. (eds) Advanced Technologies, Systems, and Applications IV. IAT 2019. Lecture Notes in Networks and Systems, vol 83. Springer, Cham 2020

3. **T. Hubana,** N. Ljevo, „Willingness to Pay for Reliable Electricity: A Contingent Valuation Study in Bosnia and Herzegovina" In: Avdaković S., Mujčić A., Mujezinović A., Uzunović T., Volić I. (eds) Advanced Technologies, Systems, and Applications IV. IAT 2019. Lecture Notes in Networks and Systems, vol 83. Springer, Cham 2020

4. **T. Hubana**, M. Šarić, S. Avdaković, "Classification of Distribution Network Faults Using Hilbert-Huang Transform and Artificial Neural Network", In: Avdaković S. (eds) Advanced Technologies, Systems, and Applications III. IAT 2018. Lecture Notes in Networks and Systems, vol 59. Springer, Cham 2019

5. **T. Hubana**, "Transmission lines fault location estimation based on artificial neural networks and power quality monitoring data", 2018 IEEE PES Innovative Smart Grid Technologies Conference Europe (ISGT-Europe), Sarajevo, 2018, pp. 1-6.

6. **T. Hubana**, M. Šarić, S. Avdaković, "High-impedance fault identification and classification using a discrete wavelet transform and artificial neural networks", Elektrotehniški Vestnik 85(3): 109-114, 2018

7. **T. Hubana**, M. Saric, S. Avdakovic, "Approach for Identification and Classification of HIFs in Medium Voltage Distribution Networks", IET Generation, Transmission & Distribution Journal, ISSN 1751-8687, DOI: 10.1049/iet-gtd.2017.0883, November, 2017

The papers are attached in the section 8.

7.2 Non-thesis related scientific and practical published papers

The following list gives the published and/or presented papers that are not directly related to the PhD thesis:

1. **T. Hubana**, E. Šemić, N. Laković, “Machine Learning based Electrical Load Forecasting using Decision Tree Algorithms“, In: Avdaković S. (eds) Advanced Technologies, Systems, and Applications III. IAT 2020. Lecture Notes in Networks and Systems, Springer, Cham 2 – In Press
2. M. Saric, **T. Hubana**, E. Begic, “Fuzzy Logic Based Approach for Faults Identification and Classification in Medium Voltage Isolated Distribution Network”, In: Hadžikadić M., Avdaković S. (eds) Advanced Technologies, Systems, and Applications II. IAT 2017. Lecture Notes in Networks and Systems, vol 28. Springer, Cham, 2018
3. **T. Hubana**, S. Hodzic, E. Alihodzic, A. Mulaosmanovic “The Valuation of Kron Reduction Application in Load Flow Methods“, In: Avdaković S. (eds) Advanced Technologies, Systems, and Applications III. IAT 2018. Lecture Notes in Networks and Systems, vol 59. Springer, Cham 2019
4. **T. Hubana**, E. Begic, M. Saric, “Voltage Sag Propagation Caused by Faults in Medium Voltage Distribution Network”, In: Hadžikadić M., Avdaković S. (eds) Advanced Technologies, Systems, and Applications II. IAT 2017. Lecture Notes in Networks and Systems, vol 28. Springer, Cham, 2018
5. E. Šemić, M. Saric, **T. Hubana**, “Influence of Solar PVDG on Electrical Energy Losses in Low Voltage Distribution Network” In: Hadžikadić M., Avdaković S. (eds) Advanced Technologies, Systems, and Applications II. IAT 2017. Lecture Notes in Networks and Systems, vol 28. Springer, Cham, 2018
6. E. Šemić**, T. Hubana** and M. Šarić, "Distributed Generation Allocation in Low Voltage Distribution Network Using Artificial Neural Network," IEEE EUROCON 2019 -18th International Conference on Smart Technologies, Novi Sad, Serbia, 2019, pp. 1-6.
7. **T. Hubana**, N. Ljevo, “Willingness to Pay for Reliable Supply from Renewable Energy Sources: A Contingent Valuation Study in Bosnia And Herzegovina” CIGRE - Bosnia and Herzegovina Committee, 14th Session, Neum, Bosnia and Herzegovina, October 2019
8. N. Lakovic, **T. Hubana**, J. Karadza-Komic, “Estimation of Missing Smart Meter Data Using Artificial Neural Networks”, CIGRE - Bosnia and Herzegovina Committee, 14th Session, Neum, Bosnia and Herzegovina, October 2019
9. J. Karadza-Komic, **T. Hubana**, N. Lakovic, “Voltage Unbalance Analysis in Low Voltage Distribution Networks Using Smart Meters”, CIGRE - Bosnia and Herzegovina Committee, 14th Session, Neum, Bosnia and Herzegovina, October 2019

10. E. Begic, **T. Hubana**, “Automated Data Acquisition Based Transformer Parameters Estimation” In: Avdaković S. (eds) Advanced Technologies, Systems, and Applications III. IAT 2018. Lecture Notes in Networks and Systems, vol 60. Springer, Cham, 2019

11. **T. Hubana**, “Coordination of the Low Voltage Microgrid Protection Considering Investment Cost“, 1. Conference BH K/O CIRED, Mostar, Bosnia and Herzegovina, October 2018

12. **T. Hubana**, E. Begic, M. Saric, “Voltage Control in Distribution Network Using Variable Power Factor Operated Distributed Generation” IEEE Student and Young Professional Congress Sarajevo 2016, Sarajevo, BiH, 2016

13. A. Kavaz, S. Hodzic, **T. Hubana**, A. Bevrnja, E. Alihodzic, A. Mulaosmanovic, S. Curevac, N. Đozić, H. Merzićet al. “Stand-alone Photovoltaic System Solar-Tree”, BH K CIGRE Session 2015, Neum, BiH, 2015

14. **T. Hubana**, A. Mulaosmanovic, E. Alihodzic, S. Hodzic, “The Impact of Air Temperature Change on Active and Reactive Power Demand on Wide Area of The City of Mostar”, Advancement of Arts and Sciences in Bosnia and Herzegovina Conference, Brcko, BiH, 2015.

15. **T. Hubana**, S. Hodzic, Dz. Klepo, “Discrete Wavelet Transformation (DWT) Application for Low Frequency Electromechanical Oscillations Identification and Analysis in Electric Power Systems”, International University of Sarajevo Graduate Conference 2015, Sarajevo, BiH, 2015

16. A. Kavaz, S. Hodžić, **T. Hubana**, S. Ćurevac, N. Đozić, H. Merzić, H. Tanković, K. Dervišević, E. Alihodžić, E. Sikira, D. Rahić, N. Kavazović, F. Tanković, B. Šestan, "Solar Tree Poject", Proceedings of the IEEESTEC 6th Student Project Conference, Niš, Serbia, 2013, pp. 25-28,

7.3 Thesis outline

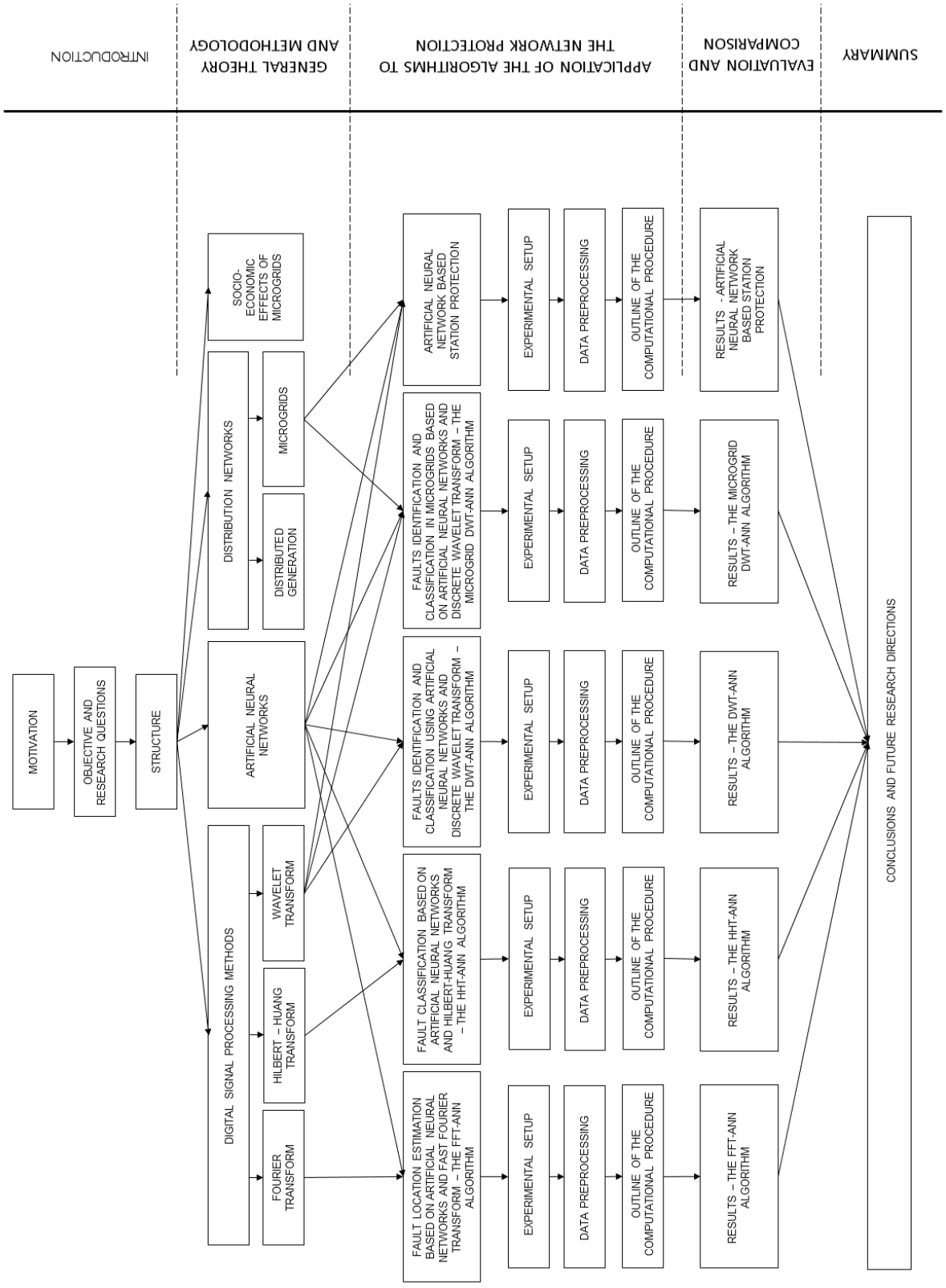

8 Included papers

8.1 Artificial Intelligence based Station Protection Concept for Medium Voltage Microgrids

8.2 New Approach for Fault Identification and Classification in Microgrids

8.3 Willingness to Pay for Reliable Electricity: A Contingent Valuation Study in Bosnia and Herzegovina

8.4 Classification of Distribution Network Faults Using Hilbert-Huang Transform and Artificial Neural Network

8.5 Transmission lines fault location estimation based on artificial neural networks and power quality monitoring data

8.6 High-impedance fault identification and classification using a discrete wavelet transform and artificial neural networks

8.7 Approach for Identification and Classification of HIFs in Medium Voltage Distribution Networks

Artificial Intelligence based Station Protection Concept for Medium Voltage Microgrids

Tarik Hubana
Institute of Electrical Power Systems
Graz University of Technology
Graz, Austria
t.hubana@student.tugraz.at

Abstract— **Despite the rapid improvements in the field of microgrid protection, it continues to be one of the most important challenges faced by the distribution system operators. With the introduction of this new operation concept, the existing protection devices are not able to successfully identify, classify and localize different types of faults that occur in the microgrids due to their dynamic behaviour, especially in the islanded mode of operation. This paper presents a methodology that provides the station protection functionalities that include detection and classification of faults, isolation of the faulty feeder and fault location estimation. The proposed method is based on discrete wavelet transform and artificial neural networks. The test system based on the real data, completely developed in MATLAB Simulink, is used to demonstrate the accuracy of all functionalities of the station protection algorithm that can be easily applied in microgrids. The presented results demonstrated the method accuracy and showed that it can be used as an upgrade of the existing protection equipment for the future implementation of the advanced microgrid station protection system.**

Keywords—Microgrids, Power system protection, Artificial neural networks, Discrete wavelet transforms

I. INTRODUCTION

The distribution systems are facing large changes. The advances in technology have enabled the usage of new technologies such as smart meters, distribution management systems, distributed generation and storage, and finally the smart grids as a concept that includes all the above. The usage of these technologies, with enough generation from the distributed resources in a part of the distribution system, meets the prerequisites for an islanded operation of that part of the distribution system. This is a point where a new concept needs to be introduced to the traditional distribution systems, i.e. the microgrids. The microgrid is usually a part of a system fed from one substation that during the fault in the main grid, can disconnect from the main grid and continue to operate in islanded mode. However, the protection of such a dynamic system is not an easy task. The detection and clearance of the faults remains to be one of the main challenges. With the significant improvements in the field of the advanced protection techniques, mainly owned to the advancement of signal processing and computational methods, this problem presents an important area of research.

There are many challenges in the research area of the microgrid protection mainly because of the dynamic behaviour of the microgrid [1]–[4]. Generally, the microgrid protection schemes depend on some key factors as: microgrid type, microgrid topology, type of DG resources, communication type, data preprocessing, relay model, fault details and method of grounding [2], [4]–[6]. Thus, by following the recent progress in the area of the advanced distribution system protection [7]–[12] and constant upgrades of the distribution grid, the power quality and reliability levels arrived at a point in which additional investments are just not feasible [13]. This creates a need for an affordable and intelligent protection system that can be easily incorporated with the exiting protection equipment. Since most of the current protection schemes use embedded systems or microprocessor-based computers, an implementation of an advanced station protection scheme that uses the existing measuring equipment for inputs and provides a comprehensive station protection appears to be a promising direction for existing methods upgrades.

Hence, researchers started to investigate this area using many methods, where the artificial neural networks (ANNs) emerged as a promising tool for fault detection [14]–[16]. Usually, ANNs are paired with appropriate data processing, in order to prepare the inputs for the ANN, where the discrete wavelet transform (DWT) is found to be an appropriate pre-processing tool [17]–[21]. However, very few researchers have implemented the full station protection of the microgrid with functionalities that include detection and classification of faults, isolation of the faulty feeder and fault location estimation. Therefore, it is justified to further explore the area of an affordable, reliable and intelligent microgrid station protection system that remains one of the highest priorities in this field.

Because of the all the above, in this paper a new method for microgrid station protection is proposed. This method is developed and tested in MATLAB Simulink environment. The following sections will give the theoretical background of the proposed method, followed by the insight to the methodology

978-1-7281-4775-8/20/$31.00

and testing results. Finally, future research directions and conclusions will be given.

II. THEORETICAL BACKGROUND

The method proposed in this paper uses DWT as a tool for data preprocessing, in order to create inputs for the ANN. Therefore, the following subsections will give a brief theoretical background of these tools.

A. Discrete Wavelet Transform

In numerical functional analysis, a discrete wavelet transform (DWT) is any wavelet transform for which the wavelets are discretely sampled. As with other wavelet transforms, a key advantage it has over Fourier transform is temporal resolution since it captures both frequency and location infomation.

Wavelet transform of a signal $f(t) \in L^2(R)$, where L^2 is the Lebesgue vector space, is defined by the inner product between $\Psi_{ab}(t)$ and $f(t)$ as [22]:

$$WT(f,a,b) = \frac{1}{\sqrt{a}} \int_{-\infty}^{+\infty} f(t)\, \Psi\left(\frac{t-b}{a}\right) dt$$

The wavelet transform of the sampled waveforms is obtained by implementing DWT given by [22]:

$$DWT(f,m,n) = \frac{1}{\sqrt{a_0^m}} \sum_k f(t)\, \Psi\left(\frac{n - k a_0^m}{a_0^m}\right)$$

here a and b from the previous equation are replaced by a_0^m and ka_0^m, k and m being integer variables. In a standard DWT, the coefficients are sampled from a continuous WT on a dyadic grid, $a_0 = 2$ and $b_0 = 1$, yielding $a_0^0 = 1$, $a_0^{-1} = 2^{-1}$, etc. [22].

B. Artificial Neural Networks

The study of artificial neural networks is motivated by their similarity to successfully working biological systems, which consist of very simple but numerous nerve cells that work massively in parallel and have the capability to learn [23].

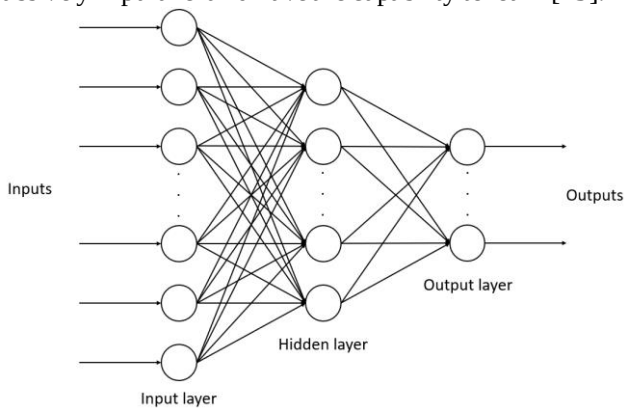

Figure 1. Structure of the ANN

The neural network does not require any programming, since it can learn from training samples, with an outcome to generalize and associate data. After successful training, a neural network can find reasonable solutions for similar problems of the same class that were not explicitly trained, which in turn results in a high degree of fault tolerance against noisy input data [23]. In this paper, two types of ANNs are used, the ANN for neural pattern recognition and the ANN for neural fitting. The pattern recognition ANNs are using a scaled conjugate gradient backpropagation training function, and the fitting ANN a Levenberg-Marquardt training method. The hyperbolic tangent sigmoid transfer function and linear transfer function is used as activation function in hidden and output layer respectively.

III. METHODOLOGY

Station protection in terms of substations feeder's protection includes fault detection, fault classification, faulty feeder isolation and fault location estimation. All the beforementioned functionalities need to have a satisfactory result in both grid connected and islanded mode, in case the substation has a capability to become a part of the microgrid. Within these functions, the method that will be presented in the following chapter can be used to send a direct trip sequence in case of the fault, as well as provide the backup tripping function due to its high sensitivity.

A. Experimental setup for the Artificial Neural Network based Station Protection

The test system presents a part of a real isolated medium voltage distribution network from the Bosnia and Herzegovina distribution system. The system presents a substation with eight feeders and 12 buses, as shown in figure 2.

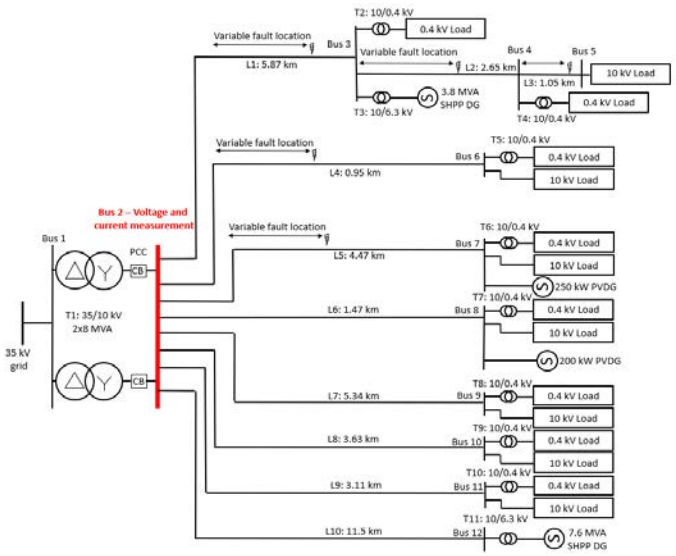

Figure 2. The modified 12-bus microgrid test system

Current and voltage measurements are present in every 10-kV feeder. These measurements are common in the real distribution network substations, where every feeder is equipped with both voltage and current measurements. For the

purpose of ANN input preparation, the following scenarios were simulated:

- The single-phase-earth faults (AE), phase-phase-earth faults (ABE) and three-phase faults (ABCE) on feeder 1, on lines L1, L2 and L3,
- The single-phase-earth faults (AE), phase-phase-earth faults (ABE) and three-phase faults (ABCE) on feeder 2, on line L4,
- The single-phase-earth faults (AE), phase-phase-earth faults (ABE) and three-phase faults (ABCE) on feeder 3, on line L5.
- Normal operation scenarios

Faults were simulated over the fault resistances in the range of 0 – 100 Ω, on various locations from 0 to 100% of line length. The moving window measurement frame is set to 100 ms, in order to record at least 5 full periods of voltage and current. The loads and DG power outputs are changed in each simulation scenario. These values were randomized, but in the defined range, in order to simulate the dynamic behaviour of the system components. In this setup, every simulation scenario has different loads and DG power outputs, in order to achieve the robustness of the proposed method.

Additionally, during the simulations, different levels of noise are added to the measured signals, in the range from 21.94 dB to 50 dB of signal to noise ratio (SNR). The noise level of 21.94 dB presents the noise level that would occur in the case of THD (Total Harmonic Distortion) of 8%, which is the limit for the THD in MV networks according to the EN50160 standard [24]. The measurement of voltages and currents is performed on the 10 kV feeders of the system. Obtained voltage and current measurements from these feeders are sent to the DWT preprocessing algorithm in order to create the inputs for ANNs.

B. *Data preprocessing for the Artificial Neural Network based Station Protection*

Since the algorithm for station protection has more functionalities, multiple neural networks are developed, where each one of them provides a certain function. After simulating the fault, for each fault scenario, the voltage and current waveforms are measured. Afterwards, the DWT is applied to these signals, and as a result, details and approximation components are obtained. Four levels of decomposition are used in order to get the frequency bands shown in Table *1*.

Table 1: Frequency bands used for the multi scale analysis

Detail 1	Detail 2	Detail 3	Detail 4	Approximation 4
800 - 1600 Hz	400 - 800 Hz	200 - 400 Hz	100 - 200 Hz	50 - 100 Hz

Since these frequency bands have important information about the fault in the system, a signature signal for each fault scenario is created by composing all these signals into one, as shown in fig. 3.

This signature signal gives a good insight into system behaviour during the fault conditions. This data will be used for the training process of the ANN that will provide all functionalities of the microgrid station protection. This signature signals present the input to the ANN.

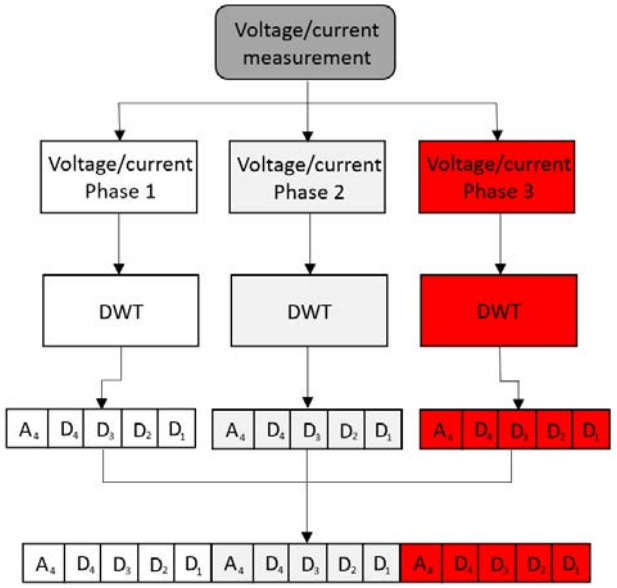

Figure 3. The DWT preprocessing flowchart

After simulating many possible operating and fault scenarios a unique signal for each scenario is created. Figure 4 shows an example of the created voltage signature signal.

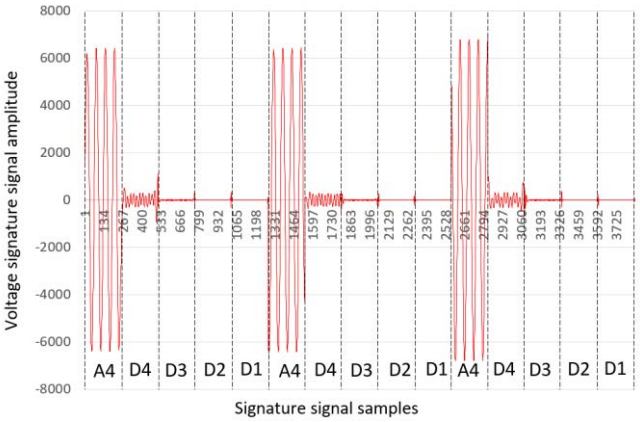

Figure 4: Voltage based DWT signature signal for AE fault

This voltage signature signal will be used for the functionality of fault detection and fault type classification. For feeder selection and fault location algorithm, current based signature signals are used. The feeder currents are measured and pre-processed in the same manner as voltage measurements.

C. *Outline of the computational procedure for the Artificial Neural Network based Station Protection*

The algorithm proposed in this research is based on DWT signal preprocessing, as shown in Figure 3. The proposed DWT - ANN algorithm needs training in order to accurately detect the

fault and distinguish between the possible types of faults, regardless of the fault-resistance value and fault location. After the training and testing process, the created ANN can be used to classify faults in the distribution system. The flowchart of the working principle of this method is shown in Figure 5. This ANN takes a voltage-based signature signal (4815 values) as input, and has 4 possible outputs (AE, ABE or ABCE faults or no fault).

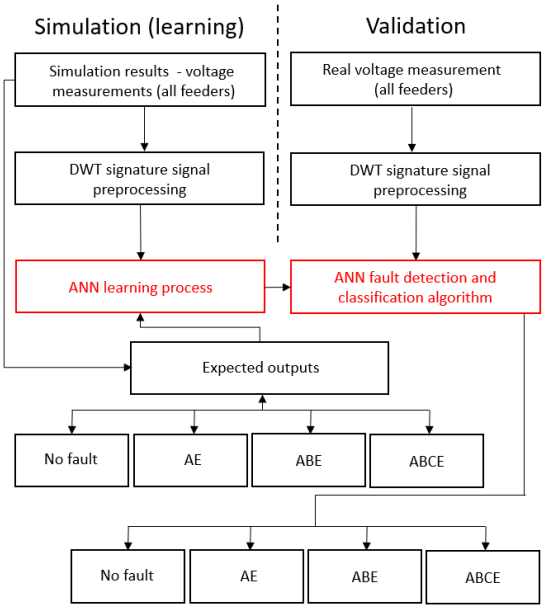

Figure 5. The DWT-ANN algorithm utilization flowchart

This output is used as a starting point for the next part of the algorithm – the faulty feeder selection. If the fault is detected (AE, ABE or ABCE) the procedure continues according to the flowchart shown in Figure 6.

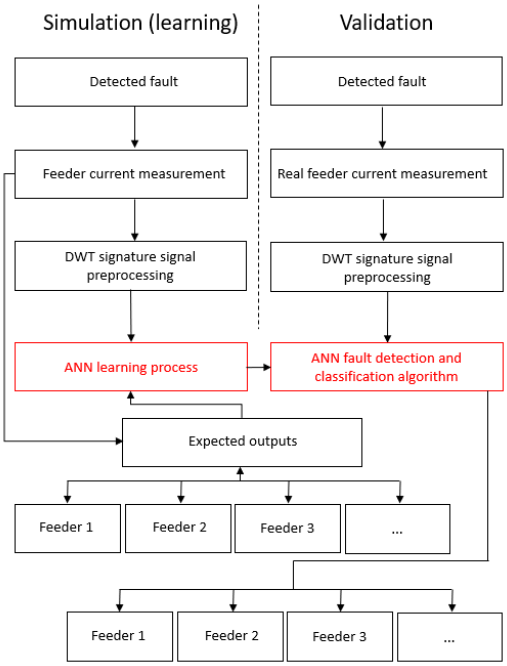

Figure 6. Algorithm for the feeder DWT-ANN feeder isolation

The developed ANN for feeder selection algorithm takes the pre-processed feeder current signals as inputs (4815 values) and has two possible outputs – fault has occurred in feeder or fault has not occurred in that feeder. For this purpose, 3 feeders were selected and tested in order to prove the algorithm accuracy. After a successfully isolated feeder, it is important to estimate the fault location. Since in this stage the fault type and the faulty feeder are known, the separate ANN for each feeder is engaged, in order to estimate the fault location. The computational procedure is shown in Figure 7.

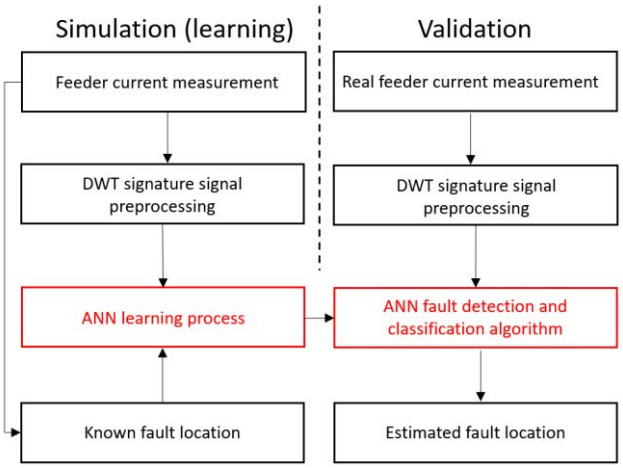

Figure 7. The DWT-ANN based fault location estimation algorithm

For this purpose, a separate neural network that takes the current based signature signals as inputs is used. The ANN developed for the purpose of fault location again uses the current-based signature signals as inputs (4815 values) and has outputs in the range of 0 to 1, which denote the place where the fault occurred (for example: 0.55 means fault at 55% of feeder length). After all these steps, the algorithm should be able to detect the fault, classify the fault type, isolate the faulty feeder and finally estimate the fault location.

IV. Results and Discussion

Following the procedure described in previous sections, a very large number of simulation scenarios is provided, more precisely 570.000 scenarios for the fault detection and classification ANN, 1.728.000 scenarios for the faulty feeder selection ANN and 144.000 scenarios for the fault location estimation. Totally, 2.442.000 scenarios were simulated and prepared for the ANN learning process, where 75% of the data was used for training, 15% for validation and 10% for testing.

Different values of noise are added to the measured signals in the range of 21.94 to 50 dB of the SNR. The 21.94 dB value corresponds to the 8% of the THD that is the maximum harmonics level allowed in MV distribution networks. Following figures show the accuracy for various functionalities of the station protection algorithm in both grid connected and islanded mode of operation.

The algorithm error for the SNR of 21.94 dB is 17.73 % and it drops down to zero in for the SNR value of 50 dB, in the case of grid connected mode of operation, as shown in Figure 8.

However, in the islanded mode of operation of the microgrid, the algorithm error for the SNR of 21.94 dB is 7.63 % and it drops down to 0.0604% in case of the SNR of 50 dB.

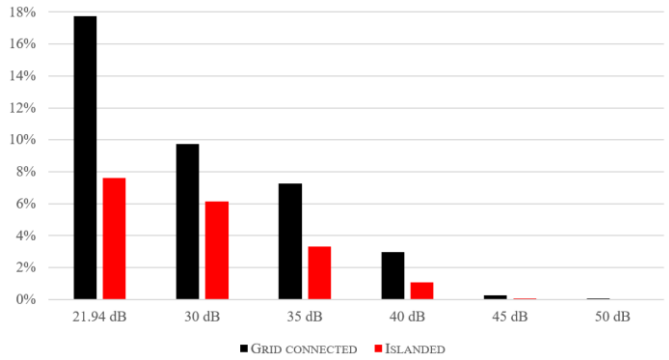

Figure 8. Fault detection and classification algorithm error (%) for various signal to noise (SNR) values in both modes mode of operation

Figure 8 shows the algorithm error for various SNR values for grid connected and island mode of operation. In grid connected mode the detection error is 8.05 % for the SNR value of 21.94 dB and it drops to 0.882 % for the SNR value of 50 db. On the other hand, in the islanded mode of operation, the error is in range from 5.006 % to 3.47e-3 % for SNR values from 21.94 to 50 db.

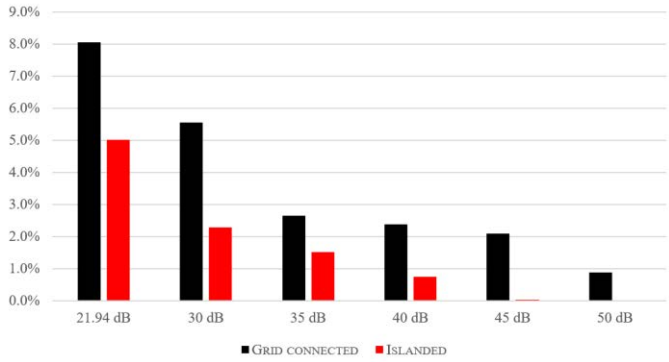

Figure 9. Faulty feeder detection algorithm error (%) for various signal to noise (SNR) values in both modes of operation

Since previously presented problems are a pattern recognition problem, the ANN could successfully classify the inputs into the set of target categories. However, the fault location algorithm is a fitting problem, where an ANN needs to map between set a dataset of numerical inputs and set of numerical targets, in this case the location of the fault in the faulty feeder.

The Feeder 1 presents a most challenging one for fault location, and because of that, the algorithm is tested in the Feeder 1. Figure 10 shows the fault location algorithm error for both modes of the microgrid operation. The obtained results show that the mode of microgrid operation does not significantly affect the fault location algorithm accuracy. The same stands for the noise level, since the different levels of noise in signal (SNR value from 21.94 to 50 dBs) did not significantly affect the accuracy. More precisely, the difference in accuracy for SNR value of 21.94 dB and SNR value of 50 dB was less than 0.01% for all types of faults in both modes of operation.

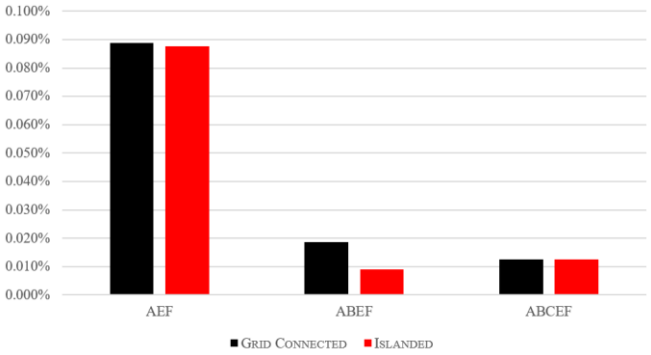

Figure 10: Fault location algorithm error (%) for both modes of microgrid operation

The presented results showed the accuracy of the algorithm for different noise levels, however, the SNR value of 21.94 dB is an extreme case. The measurements in the Bosnia and Herzegovina MV network show that the THD levels rise to 2%, which is around 35 dB of the SNR value. These THD levels usually occur in the remote parts of long feeders, system impedance is high. Since the algorithm proposed in this paper is intended to be used at the substation, where system impedance is usually low, the noise levels are not expected to be this high. Therefore, the accuracy is expected to be at least 93% for the fault detection and classification, 97% for faulty feeder detection and 99.91% for fault location in worst scenarios.

V. CONCLUSION

Appropriate microgrid protection system still presents a challenge for the DSOs and an open research area for the researchers, due to the complex nature of the microgrids. Therefore, this paper proposes a method to improve the existing protection strategies by using the artificial intelligence-based algorithm.

The results presented in this paper demonstrated the accuracy and practicality of the station protection algorithm in terms of fault detection, fault type classification, faulty feeder detection and fault location estimation. Numerous operating scenarios of the test system based on real distribution network were used for algorithm testing. These scenarios include variable loads, distributed generation power outputs, fault locations, faulty feeders, fault resistances, faults types, noise levels, system load curve points and microgrid operation modes.

Considering the robustness of the algorithm to all beforementioned variations that may occur in the microgrid, it is believed to be a promising concept for the upgrade of the existing microgrid protection strategies.

Future research directions should include more possible scenarios that can lead to the false tripping. This study is a part of a larger research project whose objective is to contribute to the development of an artificial intelligence-based microgrid

protection system that presents an easy upgrade to the existing protection systems.

REFERENCES

[1] J. Kennedy, P. Ciufo, and A. Agalgaonkar, "A review of protection systems for distribution networks embedded with renewable generation," *Renewable and Sustainable Energy Reviews*. 2016.

[2] B. J. Brearley and R. R. Prabu, "A review on issues and approaches for microgrid protection," *Renewable and Sustainable Energy Reviews*. 2017.

[3] N. K. Choudhary, S. R. Mohanty, and R. K. Singh, "A review on Microgrid protection," in *2014 International Electrical Engineering Congress, iEECON 2014*, 2014.

[4] S. A. Hosseini, H. A. Abyaneh, S. H. H. Sadeghi, F. Razavi, and A. Nasiri, "An overview of microgrid protection methods and the factors involved," *Renewable and Sustainable Energy Reviews*. 2016.

[5] H. Laaksonen and P. Hovila, "Enhanced MV microgrid protection scheme for detecting high-impedance faults," in *2017 IEEE Manchester PowerTech, Powertech 2017*, 2017.

[6] T. S. Ustun, C. Ozansoy, and A. Zayegh, "Recent developments in microgrids and example cases around the world - A review," *Renewable and Sustainable Energy Reviews*. 2011.

[7] T. Hubana, M. Saric, and S. Avdakovic, "Approach for identification and classification of HIFs in medium voltage distribution networks," *IET Gener. Transm. Distrib.*, vol. 12, no. 5, 2018.

[8] T. Hubana, "Transmission lines fault location estimation based on artificial neural networks and power quality monitoring data," in *Proceedings - 2018 IEEE PES Innovative Smart Grid Technologies Conference Europe, ISGT-Europe 2018*, 2018.

[9] T. Hubana, M. Šarić, and S. Avdaković, *Classification of Distribution Network Faults Using Hilbert-Huang Transform and Artificial Neural Network*, vol. 59. 2019.

[10] T. Hubana, M. Šaric, and S. Avdakovic, "High-impedance fault identification and classification using a discrete wavelet transform and artificial neural networks," *Elektroteh. Vestnik/Electrotechnical Rev.*, vol. 85, no. 3, 2018.

[11] M. Šarić, T. Hubana, and E. Begić, *Fuzzy Logic Based Approach for Faults Identification and Classification in Medium Voltage Isolated Distribution Network*, vol. 28. 2018.

[12] T. Hubana, M. Šarić, and S. Avdaković, *New Approach for Fault Identification and Classification in Microgrids*, vol. 83. 2020.

[13] T. Hubana and N. Ljevo, *Willingness to Pay for Reliable Electricity: A Contingent Valuation Study in Bosnia and Herzegovina*, vol. 83. 2020.

[14] H. Lin, J. M. Guerrero, C. Jia, Z. H. Tan, J. C. Vasquez, and C. Liu, "Adaptive overcurrent protection for microgrids in extensive distribution systems," in *IECON Proceedings (Industrial Electronics Conference)*, 2016.

[15] S. Zarrabian, R. Belkacemi, and A. A. Babalola, "Intelligent mitigation of blackout in real-time microgrids: Neural network approach," in *2016 IEEE Power and Energy Conference at Illinois, PECI 2016*, 2016.

[16] H. Lin, K. Sun, Z. H. Tan, C. Liu, J. M. Guerrero, and J. C. Vasquez, "Adaptive protection combined with machine learning for microgrids," *IET Gener. Transm. Distrib.*, 2019.

[17] Y. Y. Hong, Y. H. Wei, Y. R. Chang, Y. Der Lee, and P. W. Liu, "Fault detection and location by static switches in microgrids using wavelet transform and adaptive network-based fuzzy inference system," *Energies*, 2014.

[18] B. K. Panigrahi, P. K. Ray, P. K. Rout, and A. Kiran, "Fault Detection and Classification Using Wavelet Transform and Neuro Fuzzy System," in *Proceedings of the 2018 International Conference on Current Trends towards Converging Technologies, ICCTCT 2018*, 2018.

[19] M. Manohar, E. Koley, and S. Ghosh, "A reliable fault detection and classification scheme based on wavelet transform and ensemble of SVM for microgrid protection," in *Proceedings of the 2017 3rd International Conference on Applied and Theoretical Computing and Communication Technology, iCATccT 2017*, 2018.

[20] S. P. Puthenpurakel and P. R. Subadhra, "Identification and classification of microgrid disturbances in a hybrid distributed generation system using wavelet transform," in *2016 International Conference on Next Generation Intelligent Systems, ICNGIS 2016*, 2017.

[21] J. J. Q. Yu, Y. Hou, A. Y. S. Lam, and V. O. K. Li, "Intelligent fault detection scheme for microgrids with wavelet-based deep neural networks," *IEEE Trans. Smart Grid*, 2019.

[22] M. Choudhury and A. Ganguly, "Transmission line fault classification using discrete wavelet transform," in *2015 International Conference on Energy, Power and Environment: Towards Sustainable Growth, ICEPE 2015*, 2016.

[23] D. Kriesel, *A brief Introduction on Neural Networks*. 2007.

[24] DKE, "DIN EN 50160 - Merkmale der Spannung in öffentlichen Elektrizitätsversorgungsnetzen," 2011.

New Approach for Fault Identification and Classification in Microgrids

Tarik Hubana[1(✉)], Mirza Šarić[2], and Samir Avdaković[3]

[1] Technical University Graz, Graz, Austria
t.hubana@student.tugraz.at
[2] Public Enterprise Elektroprivreda of Bosnia and Herzegovina, Mostar, Bosnia and Herzegovina
m.saric@epbih.ba
[3] Faculty of Electrical Engineering, University of Sarajevo, Sarajevo, Bosnia and Herzegovina
s.avdakovic@epbih.ba

Abstract. Power system fault identification and classification continues to be one of the most important challenges faced by the power system operators. In spite of the dramatic improvements in this field, the existing protection devices are not able to successfully identify and classify all types of faults which occur power system. The situation in even more the complex in the case of microgrids due to their dynamic behavior and inherent peculiarities. This paper presents a novel method for identification and classification of faults in the microgrid. The proposed method is based on Descrete Wavelet Transform (DWT) and Artificial Neural Networks (ANN). The model is completely developed in MATLAB Simulink and is significant because it can be applied for practical identification and classification of faults in microgrids. The obtained results indicate that the proposed algorithm can be used as a promising foundation for the future implementation of the microgrid protection devices.

1 Introduction

The management and operation of modern power systems present numerous challenges for Distribution System Operators (DSO) throughout the world. One of the main challenges remains the detection and clearance of the power system faults. New energy paradigm stimulates development and operation of microgrids, which adds complexity to the existing protection schemes. There have been some significant improvements in this field, mainly owned to the advancement of signal processing, information and communication technologies, computational methods but also regulatory requirements. However, this remains and important area of research, especially when microgrids are considered.

This paper presents a new method for identification and classification of faults with particular attention to microgrid faults. This method is developed and tested in MATLAB Simulink and is based on Descrete Wavelet Transform (DWT) and Artificial Neural Networks (ANN). The contributions of this a papers are as follows:

S. Avdaković et al. (Eds.): IAT 2019, LNNS 83, pp. 27–39, 2020.
https://doi.org/10.1007/978-3-030-24986-1_3

(1) Design, test and validate a new method for identification and classification of the faults which can be applied in the realistic microgrid systems
(2) Provide a robust and flexible foundation for the future implementation of the microgrid protection devices.

There are numerous challenges in the area of microgrid protection, such as changes in the short-circuit level, false tripping signals, blindness of protection, prohibition of automatic reclosing, are unsynchronized reclosing. Microgrid protection depends on some key factors as: microgrid type, microgrid topology, type of DG resources, communication type, the time delay of communication links, a method of analysing data and detecting faults, relay type, fault type and method of grounding [1–4]. Existing methods of microgrid protection can be grouped in three categories: placement of special limitations on DGs, using external devices and protection system modification [5]. Protection system modification is the most promising method, especially the adaptive protection scheme.

Requirements for appropriate microgrid protection method, which can adapt dynamic changes of these networks and guarantee speed and selectivity of protection system, lead us to adaptive protection. Nowadays, with the advent of new technologies and digital relays and communication links, adaptive protection can play a pivotal role in protection of future networks [6]. Thus, researchers investigate this area using many methods, among them the artificial neural networks too [7–9]. However, the investments in the microgrid protection should be feasible, considering the fact that microgrids are usually set up on MV or LV networks [10].

Following the recent progress in the area of the advanced distribution system protection [11–13] and constant upgrades of the distribution grid, the power quality and reliability levels arrived at a point in which additional investments are just not feasible. This creates a need for an affordable and yet intelligent protection system. Since the currently available adaptive protection schemes most commonly use microprocessor based relays or industrial computers, an implementation of an advanced protection scheme that takes more parameters as input and provides better protection appears to be a promising direction for upgrades and future development. The use of signal processing and machine learning algorithms is a promising approach for global decision making which that lead to the successful fault isolation. Therefore, it is justified to further explore the area of a cost-effective, reliable and intelligent microgrid protection system that remains one of the highest priorities in this field.

2 Theoretical Background

2.1 Discrete Wavelet Transform

The wavelet transform is used in numerous engineering applications. It is regarded as a mathematical tool that has numerous advantages when compared with traditional methods in a stochastic signal-processing application, mainly because waveform

analysis is performed in a time scale region [14]. WT of a signal $f(t) \in L^2(R)$, where L^2 is the Lebesgue vector space, is defined by the inner product between $\Psi_{ab}(t)$ and $f(t)$ as [14]:

$$WT(f,a,b) = \frac{1}{\sqrt{a}} \int_{-\infty}^{+\infty} f(t) \Psi \left(\frac{t-b}{a} \right) dt \tag{1}$$

where a and b are the scaling (dilation) and translation (time shift) constants, respectively, and Ψ is the wavelet function which may not be real as assumed in the above equation for simplicity [14]. The Wavelet transform of the sampled waveforms is obtained by implementing DWT given by [14]:

$$DWT(f,m,n) = \frac{1}{\sqrt{a_0^m}} \sum_k f(t) \Psi \left(\frac{n - k a_0^m}{a_0^m} \right) \tag{2}$$

here a and b from Eq. (1) are replaced by a_0^m and ka_0^m, k and m being integer variables. In a standard DWT, the coefficients are sampled from a continuous WT on a dyadic grid, $a_0 = 2$ and $b_0 = 1$, yielding $a_0^0 = 1$, $a_0^{-1} = 2^{-1}$, etc. [14].

2.2 Artificial Neural Networks

When it comes to artificial neural networks, the output is a feedback to the input to calculate the change in the values of the weights [15]. The weights of the back-error-propagation algorithm for the neural network are chosen randomly to prevent a bias toward any particular output. The first step in the algorithm is a forward propagation [15]:

$$a_j = \sum_i^m w_{ji}^{(1)} x_i \tag{3}$$

$$z_j = f(a_j) \tag{4}$$

$$y_j = \sum_i^M w_{kj}^{(2)} z_j \tag{5}$$

where a_j represents the weighted sum of the inputs, w_{ij} is the weight associated with the connection, x_i are the inputs, z_j is the activation unit of (input) that sends a connection to unit j and y_i is the i-th output.

The second step is a calculation of the output difference [15]:

$$\delta_k = y_k - t_k \tag{6}$$

where δ_k represents the derivative of the error at a k-th neuron, y_k is the activation output of unit k and t_k is the corresponding target of the input.

The next step is back propagation for hidden layers [15]:

$$\delta_j = (1 - z_j^2) \sum_{k=1}^{K} w_{kj} \delta_k \tag{7}$$

where δ_j is the derivative of error w_{kj} to a_j.

Afterwards, the gradient of the error with respect to the first- and the second-layer weights is calculated, and the previous weights are updated. The mean square error for each output in each iteration is calculated by [15]:

$$MSE = \frac{1}{N} \sum_{1}^{N} (E_i - E_o)^2 \tag{8}$$

where N is the number of iterations, E_i is the actual output and E_o is the output of the model.

After each step, the weights are updated with the new ones and the process is repeated for the entire set of input-output combinations available in the training-data set, and this process is repeated until the network converges for the given values of the targets for a predefined value of the error tolerance [15].

2.3 Microgrids

A microgrid is a group of interconnected loads and distributed energy resources within clearly defined electrical boundaries that acts as a single controllable entity with respect to the grid. Microgrid presents an active distribution network, which consists of distributed generation (DG) resources, different loads at the voltage level of distribution, and energy storage elements. A microgrid can connect and disconnect from the grid to enable it to operate in both grid-connected or island mode [16].

From a network perspective, a microgrid is advantageous because it is a controlled unit and can be exploited as a concentrated load. From the point of view of customers, a microgrid can be designed to meet their special needs such as higher local reliability, fewer feeder losses, better local voltages, increased efficiency, voltage sag correction, and uninterruptible power supply [10]. From an environmental standpoint, a microgrid reduces environmental pollution and global warming because it produces less pollutants [1].

The main components of the microgrid are DGs, distributed energy storage devices and critical/non-critical loads. Microgrid is connected to the public distribution network through Point of Common Coupling (PCC) and there is a separation device in the bus section, which can switch smoothly between the grid- connected mode and the islanded mode. The capacity of a microgrid is generally between kilowatts and megawatts, and it is interconnected to low or middle level distribution networks [17].

3 Test System

The 11-bus test system developed for the purpose of algorithm testing presents a part of a real medium voltage distribution system operating in the area of the City of Mostar (Bosnia and Herzegovina) which is similar to typical distribution systems used throughout Europe. However, this real power system is modified by adding the renewable resources that can generate enough power for the system to work in islanded mode. The DGs rated powers are the common rated powers of small hydro power plants (SHPP) and photovoltaic (PV) DGs that occur in the Bosnia and Herzegovina distribution network.

The microgrid is supplied from a 35/10 kV two parallel transformers (which presents a place of common coupling – PCC) via 10 kV feeders. In case of the fault in the main grid, the microgrid can be disconnected from the main grid via 10 kV circuit breakers (CBs) that are placed in the 35/10 kV substation. In that case, the DGs supply the 10 kV microgrid. The LV customers are supplied via 10/0.4 kV substations. The 11-bus test system supplies electricity in an urban/suburban area and mostly consists of underground cables. The simulation model is developed in MATLAB/Simulink software and presents a three-phase model of the previously described microgrid. A single line diagram of the test system is shown in Fig. 1.

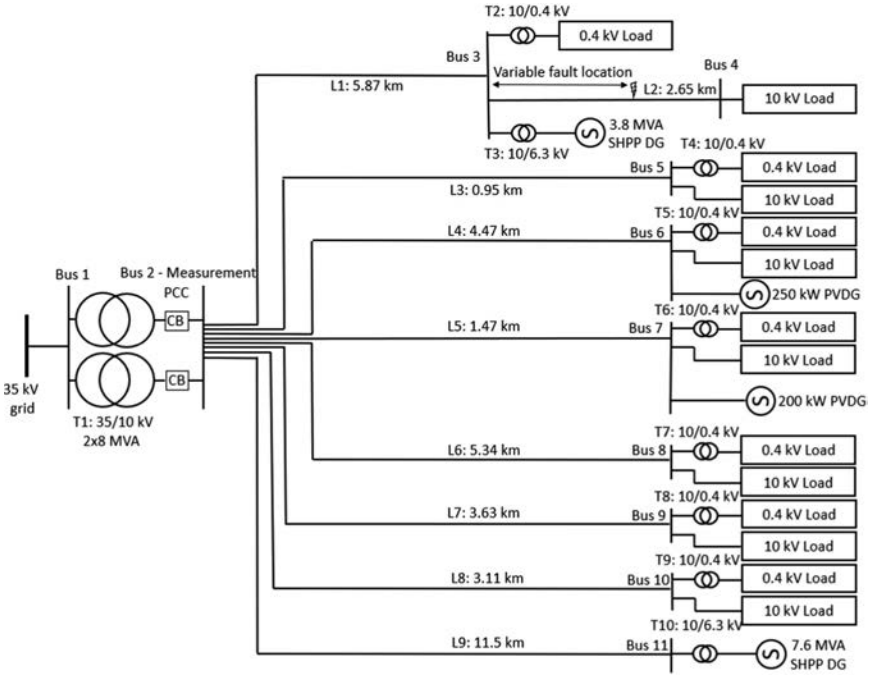

Fig. 1. 11-bus test system single line diagram

The faults are simulated on a 10 kV underground cable that feeds the entire consumption area. In order to test the algorithm behaviour in the challenging microgrid scenarios such as changes in the short-circuit level, false tripping signals, blindness of protection, the fault is simulated in the line between a SHPP and the rest of the consumers. Faults are simulated for different fault resistances (in the range from 0 Ω to 300 Ω) and at different fault locations. The simulated faults are phase A to the ground fault (AG), phase A to phase B to the ground fault (ABG) and phase A to phase B to phase C to the ground fault (ABCG). The measurement is performed at a 10 kV busbar in the 35/10 kV substation. The faults are simulated in both grid-connected and islanded mode of operation.

The sampling frequency of the current protection relays and measuring equipment in the Bosnia and Herzegovina EPDS is 3.2 kHz. Since the existing equipment already operates with this sampling frequency, a logical upgrade would be to use this equipment coupled with the proposed algorithm.

This fact is the reason for using the chosen sampling frequency in the measurement process. For the proposed DWT-ANN algorithm, the condition with no fault and the conditions with three types of the fault are simulated for various resistance values and fault locations, for both modes of microgrid operation giving a total of 89.384 fault scenarios.

4 Outline of the Computational Procedure

The proposed method for fault identification and classification is based on a combination of DWT and ANN. It is based on the previous research of the authors [12, 18]. It performs with details and approximation waveforms rather than with calculated coefficients. After simulating all the possible fault scenarios, for each fault and different values of the fault location and resistance, the voltage waveforms are generated. The fault is simulated during the entire simulation time, i.e. (0–0.08 s). When the voltage waveforms are generated, DWT is applied to these waveforms. The procedure of signature signal generation is shown in Fig. 2.

A Daubechies 4 wavelet is used at a 3.2 kHz voltage signal, therefore one approximation and four details are obtained for each voltage. Four levels of decomposition are used in this paper in order to get the following frequency bands [12]:

- First detail level - frequency band: [800, 1600] Hz,
- Second detail level - frequency band: [400, 800] Hz,
- Third detail level - frequency band: [200, 400] Hz,
- Fourth detail level - frequency band: [100, 200] Hz,
- Fourth approximation level - frequency band: [50, 100] Hz

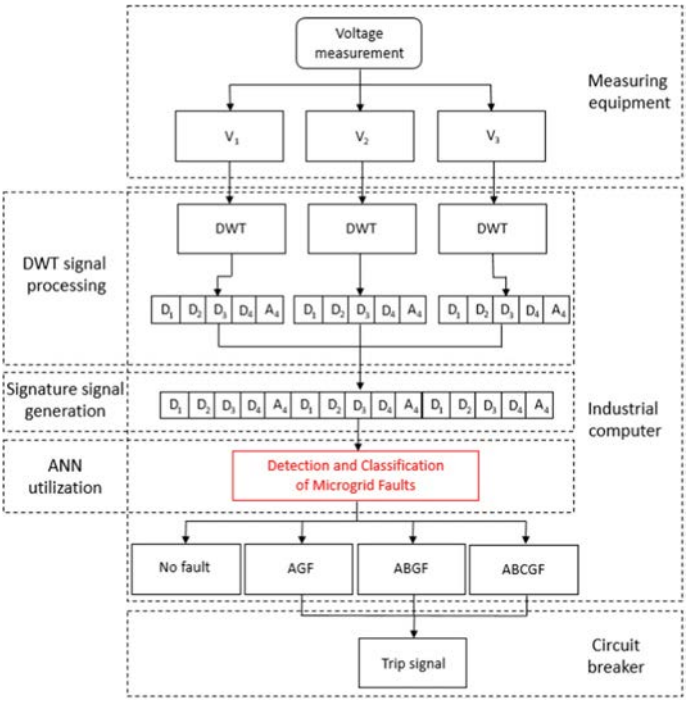

Fig. 2. Proposed method algorithm (signature signal generation)

The A4 waveform is a base sinusoidal wave and reflects the signal behavior during each fault. The rest of the DWT waveforms are higher harmonic components of the voltage signal, and therefore they reflect a distinctive voltage behavior during each fault type. The algorithm is also tested by the Symlet 4 and Biorthogonal 4.4 wavelet families, and the total algorithm output results do not differ from the Daubechies 4 wavelet family. Therefore, it is not necessary to be particularly cautious regarding the choice of the wavelet family. The DWT signal components give a good insight into the system behavior during fault conditions. For this reason, they are used as representative signals for each fault type. Afterwards, these DWT signals are combined and grouped and represent a unique "signature" for each fault, which represents the input to ANN. After that, ANN is trained with a large set of this data, becoming capable to detect and identify the EPDS faults.

Once trained, the ANN is capable of fault identification and classification, according to the algorithm shown in Fig. 3. With the measuring equipment installed in microgrid, the voltage waveforms can constantly monitored with the previously defined moving time frame, while the obtained signals are sent to an installed industrial computer with a DWT-ANN algorithm software. In the case of a fault identification, an appropriate trip signal can be sent to the circuit breaker.

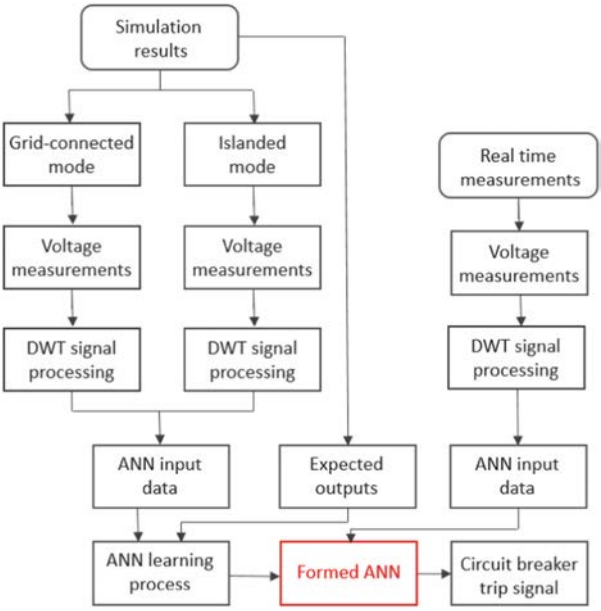

Fig. 3. Proposed algorithm learning and utilization procedure

5 Results and Discussion

In order to use the proposed algorithm in a real microgrid, the ANN needs to be trained to all the possible scenarios that may occur in the microgrid. Since the algorithm is planned to be used in the online mode to constantly monitor the system voltages, it can constantly improve and learn new possible microgrid operating scenarios, making the algorithm even better over time.

The algorithm consists of two phases. First one is the creation of fault scenario for the initial base of knowledge that ANN will learn from. Firstly, the input data for ANN needs to be created. In order to get a unique signature signal for every fault type, a signal that reflects each possible state needs to be created. For this purpose, 89.384 simulations for three types of the fault and normal operating conditions, with various fault resistances and fault locations, are carried out. For each fault scenario, each phase voltage is measured and preprocessed with the help of DWT. By combining the DWT signals of all phase voltages for each fault scenario, a signature signal that reflects the system behavior during each fault is created. This signature signal is a signal that is built simply by adding the start of the next signal to the end of the previous signal using the details and approximation waveforms for each fault scenario in the system, i.e. this signal is composed from the DWT waveforms of the currently measured voltage signal. A signature signal example for single line to ground fault is shown in Fig. 4.

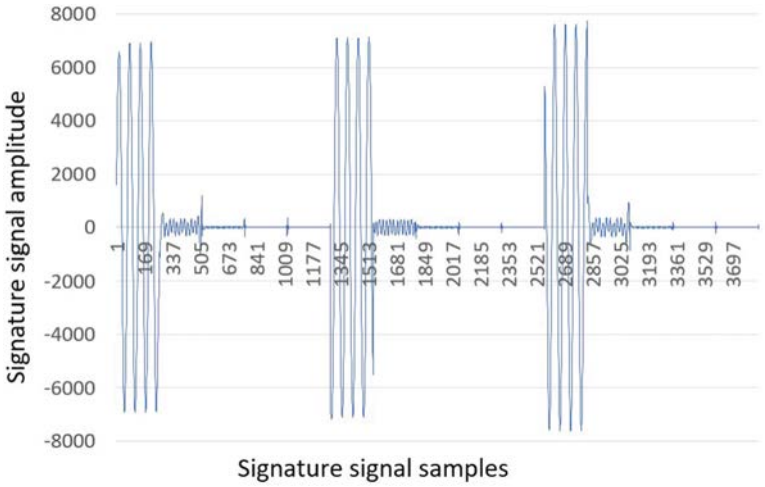

Fig. 4. Examples of signature signals for AG fault

The differences between the created signals for a particular fault type are apparently negligible, but ANN is capable to classify them correctly. Higher harmonic components, which are important in the identification process, can be efficiently identified in the DWT filters of the corresponding frequency range. Generally, DWT is widely used for the noise-removal applications [19, 20], which is one of the main reasons that it performs very well in this application. The noise with signal to noise ratio (SNR) value of 30 db is added to the signal measurements [21]. Moreover, since the proposed algorithm is paired with ANNs, which are known to have a high accuracy in the pattern classification and noise removal ability [18], this issue is addressed even more effectively.

After this unique signal for each fault scenario is created, the input set of data for ANN training is ready. The ANN takes the input set of 89.384 input vectors and 89.384 corresponding preferred outputs during a training process. After that, trained ANN has four possible outputs, where each output notes the normal operating condition and three types of microgrid faults.

As a result of the training process, the proposed DWT - ANN algorithm is capable to accurately identify the fault and distinguish between the three possible categories of faults for both modes of microgrid operation, regardless of the fault-resistance value and fault location, with the 85.74% accuracy in the 0–300 Ω fault resistance range, with the SNR value of 30 db. Of course, the accuracy improves with the noise reduction, thus having the accuracy of 96.92% with SNR value of 40 db (which is a common value in most 10 or 20 kV power networks), and having the 100% accuracy with SNR values over 50 db. The algorithm error for various SNR values is shown in Fig. 5.

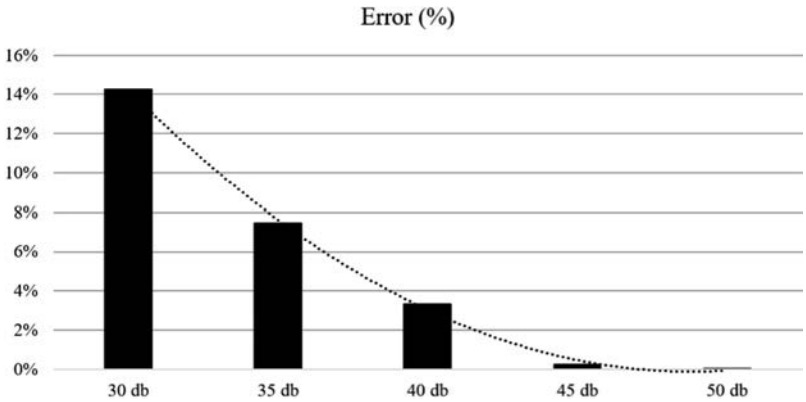

Fig. 5. Algorithm error for various signal to noise (SNR) values

After the training and testing process, the created ANN is perfectly capable to identify and classify faults in the both modes of microgrid operation. In order to get provide an insigtht into the algorithm efficiency, it is necessary to test it with new fault scenarios with new resistance values and different fault locations, i.e. fault scenarios that ANN is not trained to.

For this purpose, new simulations with new parameters are carried out. Table 1 shows classifier results to this fault scenarios, where column *Desired output* presents a simulated-fault type and column *Actual output* an evaluated fault type. The percentage values present the absence or presence of a specific fault. Column Actual output presents the ANN output for each fault scenario.

Table 1. Example of the DWT-ANN classifier output for different fault resistances, fault locations and fault types

Resistance (Ω)	Fault location (% line length)	Desired output				Actual output (ANN output)			
		AGF	ABGF	ABCGF	No fault	AGF	ABGF	ABCGF	No fault
Grid-connected operation									
20	16	1	0	0	0	0.9944	0.0022	0.0002	0.0031
110	31	0	0	0	1	0.0109	0.0001	0.0003	0.9885
200	46	0	1	0	0	0.0018	0.9952	0.0025	0.0003
290	78	0	0	1	0	0.0007	0.0022	0.9965	0.0004
Islanded operation									
20	16	1	0	0	0	0.9944	0.0022	0.0002	0.0031
110	31	0	0	0	1	0.0494	0.0005	0.0008	0.9491
200	46	0	1	0	0	0.0066	0.9925	0.0007	3.3e-06
290	78	0	0	1	0	0.0003	0.0021	0.9885	0.0089

The proposed algorithm is planned to be used in the online mode. The storage method is important since the grouped DWT components take a lot of storage. However, a present-day industrial computer will be enough for online monitoring. Few minutes old data can be deleted if no disturbances are recorded. However, voltage waveforms can be saved for a later analysis.

6 Future Research Directions

The list of the microgrid fault types is not exhausted by the faults included in this paper. The high level of noise can also lead to misclassificaiton. However, this algorithm is applicable to new scenarios since it can be easily extended by an additional training of the ANN. The proposed algorithm has a potential practical application in terms of its implementation in the microgrid protection system devices. In order to achieve this, it is necessary to improve the robustness of the proposed algorithm, which remains an important future research direction. Finally, an extension in the number of the system components and scenarios that can lead to a false tripping signal is proposed for future consideration.

7 Conclusion

Identification and classification of the power system faults, especially in the microgrid remains an important challenge faced by the DSO, because the existing protection devices are unable to detect nor classify such failures due to the complex and dynamic behavior of the microgrid. For these reasons, this topic presents an open research area. The paper proposes a method to improve the existing algorithms for identification and classification of microgrid faults based on DWT and ANN.

For algorithm testing, a test system based on a part of the real distribution network from Bosnia and Herzegovina is developed in MATLAB Simulink. The proposed method has a practical significance since it can be applied to a real microgrid and it accurately identifies and classifies faults in the 0–300 Ω range of the fault resistance for various fault locations. The proposed algorithm is believed to be a promising approach to the future implementation of the microgrid protection devices.

It is important to point out that the proposed algorithm is not immune to the large load and switching state changes, and in order to overcome this, further training with more operating scenarios is required. The possible upgrades of the existing algorithm are pointed out in the future research directions section. This study is a part of an ongoing research into advanced power system protection algorithms, whose ultimate goal is to develop a system that has satisfactory accuracy for detection and classification of the power distribution network faults.

References

1. Hosseini, S.A., Abyaneh, H.A., Sadeghi, S.H.H., Razavi, F., Nasiri, A.: An overview of microgrid protection methods and the factors involved. Renew. Sustain. Energy Rev. **64**, 174–186 (2016)
2. Brearley, B.J., Prabu, R.R.: A review on issues and approaches for microgrid protection. Renew. Sustain. Energy Rev. **67**, 988–997 (2017)
3. Laaksonen, H., Hovila, P.: Enhanced MV microgrid protection scheme for detecting high-impedance faults. In: 2017 IEEE Manchester PowerTech, Manchester (2017)
4. Ustun, T.S., Ozansoy, C., Zayegh, A.: Recent developments in microgrids and example cases around the world—A review. Renew. Sustain. Energy Rev. **15**, 4030–4041 (2011)
5. Mohamed, N.A., Salama, M.M.A.: A review on the proposed solutions to microgrid protection problems. In: 2016 IEEE Canadian Conference on Electrical and Computer Engineering (CCECE), Vancouver (2016)
6. Memon, A.A., Kauhaniemi, K.: A critical review of AC Microgrid protection issues and available solutions. Electr. Power Syst. Res. **129**, 23–31 (2015)
7. Lin, H., Guerrero, J.M., Jia, C., Tan, Z.-h., Vasquez, J.C., Liu, C.: Adaptive overcurrent protection for microgrids in extensive distribution systems. In: IECON 2016 - 42nd Annual Conference of the IEEE Industrial Electronics Society, Florence (2016)
8. Yu, J.J.Q., Hou, Y., Lam, A.Y.S., Li, V.O.K.: Intelligent fault detection scheme for microgrids with wavelet-based deep neural networks. IEEE Trans. Smart Grid **10**(2), 1694–1703 (2019)
9. Zarrabian, S., Belkacemi, R., Babalola, A.A.: Intelligent mitigation of blackout in real-time microgrids: neural network approach. In: 2016 IEEE Power and Energy Conference at Illinois (PECI), Urbana (2016)
10. Hubana, T.: Coordination of the low voltage microgrid protection considering investment cost. In: 1. Conference BH BH K/O CIRED, Mostar (2018)
11. Hubana, T.: Transmission lines fault location estimation based on artificial neural networks and power quality monitoring data. In: 2018 IEEE PES Innovative Smart Grid Technologies Conference Europe (ISGT-Europe), Sarajevo (2018)
12. Hubana, T., Saric, M., Avdakovic, S.: Approach for identification and classification of HIFs in medium voltage distribution networks. IET Gener. Transm. Distrib. J. **12**(5), 1145–1152 (2018)
13. Hubana, T., Saric, M., Avdakovic, S.: Classification of distribution network faults using Hilbert-Huang transform and artificial neural network. In: IAT 2018: Advanced Technologies, Systems, and Applications III, pp. 114–131. Cham, Springer (2019)
14. Choudhury, M., Ganguly, A.: Transmission line fault classification using discrete wavelet transform. In: International Conference on Energy, Power and Environment: Towards Sustainable Growth (ICEPE), Shillong (2015)
15. Jamil, M., Sharma, S.K., Singh, R.: Fault detection and classification in electrical power transmission system using artificial neural network. SpringerPlus **4**, 334 (2015)
16. Hirsch, A., Parag, Y., Guerrero, J.: Microgrids: A review of technologies, key drivers, and outstanding issues. Renew. Sustain. Energy Rev. **90**, 402–411 (2018)
17. Chaudhary, N.K., Mohanty, S.R., Singh, R.K.: A review on microgrid protection. In: Proceedings of the International Electrical Engineering Congress 2014, Pattaya City, Thailand (2014)
18. Hubana, T., Saric, M., Avdakovic, S.: High-impedance fault identification and classification using a discrete wavelet transform and artificial neural networks. Elektrotehniški Vestn. **85** (3), 109–114 (2018)

19. Sarawale, R.K., Chougule, S.R.: Noise removal using double-density dual-tree complex DWT. In: 2013 IEEE Second International Conference on Image Information Processing (ICIIP-2013), Shimla (2013)
20. Haider Mohamad, A.R., Diduch, C.P., Biletskiy, Y., Shao, R., Chang, L.: Removal of measurement noise spikes in grid-connected power converters. In: 2013 4th IEEE International Symposium on Power Electronics for Distributed Generation Systems (PEDG), Shimla (2013)
21. Talebi, S.P., Mandic, D.P.: Frequency estimation in three-phase power systems with harmonic contamination: A multistage quaternion Kalman filtering approach. Imperial College London (2016)

Willingness to Pay for Reliable Electricity: A Contingent Valuation Study in Bosnia and Herzegovina

Tarik Hubana[1(✉)] and Nerman Ljevo[2]

[1] Technical University Graz, Graz, Austria
t.hubana@student.tugraz.at
[2] Faculty of Management and Business Economy, Sarajevo, Bosnia and Herzegovina
nerman.ljevo@fmpe.edu.ba

Abstract. The expectation of electricity consumers to be served by electric utilities with higher levels of power quality and reliability becomes more stringent than ever, with the growth of total energy consumption worldwide, and mostly in developed areas and countries. Electricity supply interruptions less and less accepted by both consumers and regulators, imitated by the change of the consumer behavior and increased requirements by the regulator, making the requirements for the reliability of supply higher than ever. Meanwhile, distribution system operators struggle to achieve these requirements, mainly because of the infeasibility of the investments. However, if the consumers were willing to pay for the increased reliability of supply, these requirements can be achieved. Using a sample of 436 residential and business consumers in Sarajevo, Bosnia and Herzegovina, in this paper a willingness to pay (WTP) for an improved electricity service for both residential and business consumers is estimated by using the contingent valuation method (CVM). The average WTP of domestic consumers for avoiding one-hour interruption is estimated to be 3.02 BAM, while the average WTP of business consumers is 105.4 BAM. Information on the value of reliable service can be used to assess the economic efficiency of investments in distribution systems in order to strategically target investments to consumers segments that receive the most benefit from system improvements, and to numerically quantify the risk associated with different operating, planning and investment strategies.

1 Introduction

Electric power systems are subject to constant change in the last decade. New technologies, standards, and requirements from both consumers and regulators impose large investments in electric power system, in order to improve the power quality and reliability levels. In general, very severe outages and blackouts that occurred in the past decade in the in Europe clearly showed that, besides the price of electricity, continuity of service (in terms of reliability/continuity of supply) is also a very important issue for consumers and society as a whole. Hence, the power system faults are particularly unwelcome events because, apart from causing the system interruption, they create

S. Avdaković et al. (Eds.): IAT 2019, LNNS 83, pp. 107–116, 2020.
https://doi.org/10.1007/978-3-030-24986-1_8

numerous technical issues such as voltage sags [1]. Consequently, the management and operation of the electric-power distribution systems have also changed [2]. One of the guiding principles in evaluating investments designed to improve the reliability of electricity systems is that these investments should be economically efficient. That is, the cost of improving the reliability and power quality supplied by an electric system should not exceed the value of the economic loss to consumers that the system improvement is intended to prevent [3]. With the advances in the area of the advanced distribution system protection [4–6], and constant upgrades of the distribution grid, the power quality and reliability levels are brought to the margin where additional investments are just not feasible. On the other hand, to the distribution system operator the investments may be related to benefits related to rewards or penalties in accordance to the total non-delivered energy when individual standards of quality of service are not met [7]. This is a point where consumers need to take part in the process. In order to have a more reliable supply of energy, consumers can pay for an improved service. This paper estimates this value that presents a key parameter that can be used to assess the economic efficiency of investments in distribution systems in order to strategically target investments that will improve the reliability of that part of the distribution system.

There is a growing number of researchers that have focused on identifying the financial attributes that define the quality of service provided by an electricity supplier. In an attempt to provide guidance to regulators, and to assist distribution companies in designing service packages, Goett et al. [8] undertook a study on consumers' willingness to pay for various service attributes. Beenstock et al. [9] used a revealed preference approach (on business consumers and not domestic consumers) in which the cost of an outage may be inferred from the actions taken by consumers to mitigate losses induced by unsupplied electricity. They exploit data on investment in back-up generators that mitigate losses in the event of an outage [10].

Mansouri et al. [13] undertook a survey to identify environmental attitudes and beliefs, energy-use behavior and ownership levels for certain appliances and their utilization patterns, among household residents in the southeast of England. The results indicate that consumers are interested in receiving information concerning household energy use and the associated environmental impact, and are willing to modify their behavior in order to reduce household energy consumption and environmental damage [10].

Due to various economic, technical, and political problems, a low quality of electricity supplied by the grid can be expected in some developing countries. This issue can be characterized by the intermittent and unreliable supply of electricity to the consumers commonly through supply interruptions, either planned or unplanned [11]. A low reliability of electricity supply affects individuals and family life as well as being interrelated with the development and economic condition of a country. For instance, according to Murphy et al. [12], a reduction in the number of outages from 100 days per year to 10 days per year corresponds to more than a two-fold increase in GDP per person. Thus, an investment in the power system reliability, supported by the consumer's participation can present a driver for the development of certain societies.

2 Contingent Valuation Method

The contingent valuation method (CVM) is a widely used method for estimating economic values for all kinds of ecosystem services and environmental goods which are not traded in the market and hence have no market price. CVM is typically used to estimate the benefits (or costs) of a change in the level of provision (or in the level of quality) of a public good. The contingent valuation method is applied through conducting a survey in which people are directly asked how much they would be willing to pay (WTP) for a (change in) specific environmental service. It is also possible to ask people the amount of compensation that they would be willing to accept (WTA) to give up an environmental service. The first approach is called 'contingent' valuation, because people are asked to state their willingness to pay, contingent on a particular scenario and the environmental service described to the respondent [14].

The willingness to pay (WTP) is defined as the amount of money a household is willing to pay for a specific level of service, for example, in order to reduce the number and duration of outages from a base level to another level for the same duration. A willingness-to-pay study can provide evidence that the service provider can put before a regulator to support expenditure plans, by highlighting which aspects of service quality are important to consumers and, importantly, estimating the value consumers place on various service attributes. The estimated willingness to pay can then be compared with the incremental costs of achieving such improvements, as part of the service provider's business planning and the regulator's decision-making process. Consumers' willingness to pay provides an 'upper-bound' on the financial incentive or reimbursement that should be associated with service improvements. The 'lower-bound' is represented by the incremental cost to the business of improving that aspect of service quality [10].

The consumers' added value of service reliability can be quantified by the willingness of consumers to pay for service reliability, taking into account the resources (e.g., income) by the residential consumer or by a firm's expected net revenues associated with the added reliability. A system improvement is considered economically efficient if its marginal societal benefits (the economic value of the improvement in reliability) exceed the marginal societal costs (the cost of the investment, including direct as well as indirect (e.g., environmental costs). The cost of system improvements is usually estimated using engineering cost analysis. The economic value of the benefit to consumers is estimated as the avoided economic loss that would have occurred if the investment had not occurred [3].

Therefore, regulators and institutions are strongly promoting the improvement of continuity of service in the electricity sector. Then reliability of supply and its value are the key factors for the decision-making process underlying expansion plans not only of electricity generation systems but also of transmission and distribution networks. It is evident that low levels of investment can result in unreliable supply (unacceptable low continuity), while excessive investments can result in unnecessary expenditures with a resulting increase of the cost of electricity to consumers. The literature does not agree on whether or in which situations CA-based WTP measures outperform direct WTP

measurements in terms of their accuracy in predicting actual buying/payment behaviors [15].

It is inconvenient to ask residential consumers to estimate the interruption costs because household respondents are unable to accurately estimate the costs. Even though business consumers can more accurately determine the interruption cost, both consumer groups are generally asked two questions: how much would you be willing to pay for electric service to avoid the power interruption in the case of this interruption (WTP)? and how much would you accept as a credit for a particular interruption scenario (willingness to accept or WTA)? In both cases they should be asked to assess these values in the real-life scenarios in order to make the estimation more accurate.

3 Reliability of Supply

Reliability of supply is defined as the ability of a unit (component or system) to perform a demanded function for an appointed time interval under preset conditions. To give a preliminary impression of the reliability of the electricity supply as a whole a calculation of the actual availability of the utility grid or the "mean time between failure (MTBF)" is usually conducted. Availability is defined as the percentage of time that a system is functional, or the time the system is up, divided by the total time at risk [12]. Also, MTBF can easily be calculated, since availability is MTBF divided by the total of MTBF + MTTR (mean time to repair) [12].

However, the almost universal measure of reliability is the average loss of supply (in minutes) per consumer over a year, or SAIDI (System Average Interruption Duration Index). SAIDI/SAIFI = CAIDI, where SAIFI (System Average Interruption Frequency Index) is the average number of interruptions to supply per consumer over a year; and CAIDI (Customer Average Interruption Duration Index) is the average duration of each supply interruption within a particular year. SAIDI may not be the best measure of reliability for the purposes of creating financial incentives for performance because it is a measure of the per consumer loss of supply, which implies that the distributor receives extra revenue by reducing minutes lost per consumer [10]. However, the self-reported reliability indices by the distribution system operators do not always represent the actual situation accurately. In this sense, knowledge about the experience of the grid users can be useful to evaluate the reality of the reliability indices of electricity service [11].

4 Methodology

The research is based on two samples: domestic and business consumers of electricity. A regression model is established based on the multiple regression for each of the samples. Using the inferential statistical method, it was shown which predictor has the most influence on the criterion variable (for both samples) and with the help of the descriptive statistics methods, it was possible to display and understand the sample characteristics. In the survey, in the sample of domestic consumers 364 respondents gave their views on the consumption of electricity, their properties, and personal life

and consumer habits. Multiple linear regression represents the basic regression model and with it the corresponding transformation reduces the number of non-linear models. The model for willingness of paying domestic consumer for the reliability of electricity has eight variables:

$$Y = \alpha + \beta_1 X_1 + \beta_2 X_2 + \beta_3 X_3 + \varepsilon \quad (1)$$

Where:

Y - dependent variable (for willingness of paying for the reliability of electricity – domestic consumers);

α - section on Y - axis (constant);

β1, β2, β3 - slope coefficients;

X1 - electric heating;

X2 - employment;

X3 - time spent at home;

ε - statistical member (standard error).

Within the research, in the sample of business consumers, the sample size was N = 72 electricity consumers - legal entities. In this part, WTP of the consumers for more reliability of electricity supply is considered a priori. The multi-regression equation for business users has four variables, according to Eq. (2).

$$Y = \alpha + \beta_1 X_1 + \beta_2 X_2 + \beta_3 X_3 + \beta_4 X_4 + \varepsilon \quad (2)$$

Where:

Y - dependent variable (for willingness of paying for the reliability of electricity – business consumers);

α –section on Y – axis (constant);

β1, β2, β3, β4 - slope coefficients;

X1 - size of the enterprise;

X2 - sector of activity;

X3 - backup system;

X4 - monthly bill for electricity;

ε - statistical member (standard error).

Both models should anticipate the behavior of the criterion variable under the influence of the predictor, and it must be established which predictor has the greatest impact on the criterion variable in both samples.

5 Results and Discussion

Of the total number of respondents, 43% of men (156 respondents) and 57% of women (206 respondents) are in the sample of domestic consumers. The main goal of the research process in this part was to investigate the willingness of the users of electricity to pay for the improved reliability of electricity supply. The following table shows the willingness of respondents to pay for the improved reliability of electricity supply (Table 1).

Table 1. WTP for improved reliability: domestic consumers

		Frequency	Percent	Valid percent	Cumulative percent
Valid	NO	91	25.0	25.6	25.6
	YES	265	72.8	74.4	100.0
Missing	Total	356	97.8	100.0	
	System	8	2.2		
Total		364	100.0		

Of the total number of respondents, 74.4% are willing to pay more for the reliability of electricity supply, while 25.6% of them answered negatively on this issue (Table 2).

Table 2. Model summary – domestic consumers

Model	R	R square	Adjusted R square	Std. error of the estimate	Change statistics				
					R square change	F change	df1	df2	Sig. F change
1	.642[a]	.412	.410	.653	.412	222.710	1	318	.000
2	.821[b]	.673	.671	.488	.261	253.590	1	317	.000
3	.821[c]	.674	.671	.488	.001	.789	1	316	.375

where:

a. Predictors: (Constant), Electric heating

b. Predictors: (Constant), Electric heating, Employment

c. Predictors: (Constant), Electric heating, Employment, Time spent in the house

In the previous table the sum of the multiple regression model is presented, which refers to domestic consumers. The R mark indicates the multi-correlation coefficient, while R Square is the multi-determination coefficient. What is significant in this analysis is that the adjusted R square coefficient, which represents the corrected multiple-determination coefficient, and a less biased score than the multi-determination coefficient. If taken as an example of variable one (electric heating), it can be concluded that there are 41% of individual differences in terms of the attitude towards increasing the payment for the reliability of electricity that we can explain in the population based on individual differences on the predictors taken together, i.e. based on their linear combination. The standard model error indicates that the model is not very accurate. In the context of testing hypotheses related to multiple regression, it can be set in two ways, i.e., to use ANOVA analysis, where the hypothesis of the multi-determination coefficient could be tested (which is also the general multi-regression hypothesis) and testing the hypothesis for each predictor variable. In addition, the statistical significance for each of the variables in the model can be determined, and this data can be obtained by inspecting the confidence interval. However, in this part of the research, two key questions are posed. First, it relates to the appearance of the model for the "WTP for improved reliability of electricity supply", and the second is: "Which predictor is the most important?" The model is constructed according to the Eq. 3.

$$WTP_{Domesticconsumers} = 110,9 + 31,2X_1 + 31,9X_2 - 2,18X_3 \quad (3)$$

The second question is which predictor is the most important, and in this part, it is important to note that it is necessary, in order to give an answer to this question, each new predictor to introduce gradually into the model, and see the contribution of each predictor to a criterion variable. The best approach is through the semi partial correlation of the predictor.

In this section, the R Square Change, or the F Change is considered in the order of the highest to the minimum: 222,71 (var 1) > 253,590 (var 2) > 0,789 (var 3).

According to the results, socio-economic parameters can be ranked in the following way (according to the effect of increased payment of reliability of electricity - from the highest to the least important parameter): electric heating, employment and time spent in the house. When it comes to business consumers, research has shown that even 97.2% of surveyed companies are willing to pay more for improved reliability of electricity supply, while only 2.8% companies have responded negatively to this issue. The conceptual multi-regression model that should explain the WTP for the reliability of electricity supply for business consumers has 4 predictors, which are: size of enterprise (micro, small, medium and large enterprises), business sector (agricultural, commercial, educational, health, service sector, other sector), back-up system possession (yes/no) and the electricity bills value. Within the research, 20.8% of micro enterprises, 37.5% of small companies, 30.6% of medium and 11.1% of large enterprises are included. When analyzing the sectors, the survey covered most of the enterprises from the commercial (37.5%) and service sector (30.6%), and the least from the education sector (6.9%). It is important to emphasize, in the context of considering back up the power supply system that 55% of enterprises use backup power, while 45% do not use this option. The large number of the analyzed companies have a monthly allocation for electricity over 1000 BAM, which is quite understandable (Table 3).

Table 3. Model summary – business consumers

Model	R	R square	Adjusted R square	Std. error of the estimate	Change statistics				
					R square change	F change	df1	df2	Sig. F change
1	.501[a]	.251	.240	.527	.251	22.815	1	68	.000
2	.502[b]	.252	.229	.531	.001	.046	1	67	.830
3	.502[c]	.252	.218	.535	.001	.057	1	66	.812
4	.917[d]	.841	.831	.248	.588	240.33	1	65	.000

where:

a. Predictors: (Constant), Type of enterprise:

b. Predictors: (Constant), Type of enterprise: Activity sector;

c. Predictors: (Constant), Type of enterprise: Activity sector; Back – up system;

d. Predictors: (Constant), Type of enterprise: Activity sector; Back – up system; Electricity bill

The equation describing the behavior of the criterion variable is shown in Eq. 4.

$$\mathrm{WTP}_{\mathrm{Businessconsumers}} = 53,2 + 33,3X_1 + 2,4X_2 + 0,3X_3 + 29,7X_4 \quad (4)$$

When it comes to the statistical significance of each of the variables in its impact on the criterion variable, then we can conclude it by considering F Change statistics as follows: 240,330 (var 4) > 22,815 (var 1) > 0,057 (var 3) > 0,046 (var 2). It is shown that electricity bill is the most important predictor in the model. It is followed by the type of enterprise. The remaining two predictors in the model are much less significant, i.e. the backup system and sector which the company belongs.

In the comparative analysis, a comparison of two samples, domestic and business consumers, and their responses in terms of WTP will be made in addition to paying for the reliability of electricity. It is important to note that in the case of domestic users, several predictors have been considered that have an impact on the criterion variable (8) in relation to business users (4). In addition, the number of respondents within the "Domestic consumers" sample is significantly higher than the "Business consumers" sample. This is understandable because harder to approach and come to the process of research by the owners of companies/managers who are relevant to find themselves in the "Business Consumers" sample of those in the first mentioned sample. However, within these circumstances certain indications of the behavior of the population I (Domestic consumers) and population II (Business consumers) can be given. Thus, it can be concluded that business consumers are much more willing to additionally pay for higher returns (97.2% of analyzed companies), compared to domestic consumers (74.4%). The most important determinant of the readiness for additional payment for the reliability of electricity supply for business consumers is the size of the enterprise (type of enterprise, type of company: micro, small, medium, large enterprise), as well as the current amount of electricity bills. The most important determinant of WTP for the reliability of electricity delivery is electric heating, monthly income and employment.

Business consumers are those who are affected more by loss of electricity supply. This is primarily seen in their responses to the question of "fair compensation for electricity distribution" for the unannounced shutdown of electricity supply. In this segment, the largest number of respondents, 26.3% would accept 5 BAM for any unannounced interruption in electricity delivery (WTA) (Table 4).

Table 4. WTP and WTA values for domestic and business consumers

Parameter	WTP		WTA	
	Domestic	Business	Domestic	Business
Mean	3.01	105.4	5.55	77.52
Median	2	20	5	10
Standard deviation	3.26	172.89	8.67	155.40
Lower limit of confidence interval	2.68	65.73	4.66	41.87
Upper limit of confidence interval	3.35	145.06	6.44	113.17
Length of confidence interval	0.67	79.32	1.78	71.29

Furthermore, 19.4% of them think that such an interruption should be refunded with 10 BAM, and 9.7% of them consider that such an interruption should be refunded with 20 BAM for every hour in which there will be no electricity deliveries. Domestic consumers are less sensitive to the cutoff of electricity supply, but of course, this problem affects them. However, this is considerably less than the business consumers are, which is seen through the answer to the same question, which was previously posted to business users. Thus, 27.5% of domestic consumers believe that every electricity cut per hour should be refunded from the distribution system operator (DSO) with a value of 3 BAM, 16.9% of them believe that this value should be 2 BAM, and 12.4% think that this should be only 1 BAM. This section shows significant differences in the importance of electricity supply to domestic and business consumers. Table 4 summarizes the WTA and WTP values for both domestic and business consumers.

In case of the WTP analysis, 18.1% of business consumers are willing to pay 10 BAM for the improved reliability of the electricity supply, 16.7% of them are willing to pay 5 BAM; 13.9% are willing to pay 50 BAM, and 12.5% are willing to pay 20 BAM. As stated in the previous paragraph, the importance of electricity for domestic and business consumers is confirmed here again, where 25.6% of domestic consumers don't want to pay for improved reliability of electricity at all. Significant data in this category is that 23% of respondents are willing to pay 5 BAM for increased reliability of electricity, while 12,9% are willing to pay 1 BAM. The average WTP of domestic consumers for avoiding one-hour interruption is estimated to be 3.02 BAM, while the average WTP of business consumers is 105.4 BAM.

6 Conclusions

In this paper, a research carried out in Bosnia and Herzegovina is presented. The results show that both residential and business consumers value reliability of the electricity service provided by DSOs. Residential consumers expressed an average willingness to pay of 3.02 BAM to avoid a one-hour outage. On the other hand, business consumers expressed an average willingness to pay of 105.4 BAM.

If an outage must occur, residential consumers did not express the difference between workdays and weekends. They are affected by the disappearance of electricity, and this disadvantage is most disturbed in the period between 18:00 h and 23:00 h. An important aspect of CVM is that there are biases that may affect the reliability and validity of the results. Some of these biases include respondents hypothetical WTP, while the real situation values are lower, different estimated amounts depending on the form of payment and non-response bias since individuals who do not participate in the survey are likely to have different values than individuals who do take part in it.

Information on the value of reliable electricity service can be used to assess the economic efficiency of investments in generation, transmission and distribution systems, to strategically target investments to consumer segments that receive the most benefit from system improvements, and to numerically quantify the risk associated with different operating, planning and investment strategies.

References

1. Hubana, T., Begic, E., Saric, M.: Voltage sag propagation caused by faults in medium voltage distribution network. In: IAT 2017: Advanced Technologies, Systems, and Applications II, pp. 409–419. Springer International Publishing AG, Cham (2018)
2. Hubana, T., Saric, M., Avdakovic, S.: High-impedance fault identification and classification using a discrete wavelet transform and artificial neural networks. Elektrotehniški Vestnik **85** (3), 109–114 (2018)
3. Sullivan, M.J., Mercurio, M.G., Schellenberg, J.A.: Estimated Value of Service Reliability for Electric Utility Consumers in the United States. Ernest Orlando Lawrence Berkeley National Laboratory, Berkeley (2009)
4. Hubana, T.: Transmission lines fault location estimation based on artificial neural networks and power quality monitoring data. In: 2018 IEEE PES Innovative Smart Grid Technologies Conference Europe (ISGT-Europe), Sarajevo (2018)
5. Hubana, T., Saric, M., Avdakovic, S.: Approach for identification and classification of HIFs in medium voltage distribution networks. IET Gener. Transm. Distrib. J. **12**(5), 1145–1152 (2018)
6. Hubana, T., Saric, M., Avdakovic, S.: Classification of distribution network faults using Hilbert-Huang transform and artificial neural network. In: IAT 2018: Advanced Technologies, Systems, and Applications III, pp. 114–131. Springer, Cham (2019)
7. Hubana, T.: Coordination of the low voltage microgrid protection considering investment cost. In: 1. Conference BH BH K/O CIRED, Mostar (2018)
8. Goett, A., Hudson, K., Train, K.: Consumers' choice among retail energy suppliers: the willingness-to-pay for service attributes. Energy J **21**(4), 1–28 (2000)
9. Beenstock, M., Goldin, G., Haitovsky, Y.: The cost of power outages in the business and public sectors in Israel: revealed preference vs. subjective valuation. Energy J. **18**(2), 39–61 (1997)
10. Hensher, D.A., Shore, N., Train, K.: Willingness to pay for residential electricity supply quality and reliability. Appl. Energy **115**, 280–292 (2014)
11. Reinders, K., Reinders, A.: Perceived and reported reliability of the electricity supply at three urban locations in Indonesia. Energies **11**, 1–27 (2018)
12. Murphy, P., Twaha, S., Murphy, I.: Analysis of the cost of reliable electricity: a new method for analyzing grid connected solar, diesel and hybrid distributed electricity systems considering an unreliable electric grid with examples in Uganda. Energy **66**, 523–534 (2014)
13. Mansouri, I., Newborough, M., Probert, D.: Energy consumption in UK households: impact of domestic electrical appliances. Appl. Energy **54**(3), 211–285 (1996)
14. Sagoff, M.: The Economy of the Earth: Philosophy, Law, and the Environment. Cambridge University Press, Cambridge (1988)
15. Gerpott, T.J., Paukert, M.: Determinants of willingness to pay for smart meters: an empirical analysis of household consumers in Germany. Energy Policy **61**, 483–495 (2013)

Classification of Distribution Network Faults Using Hilbert-Huang Transform and Artificial Neural Network

Tarik Hubana[1(✉)], Mirza Šarić[1], and Samir Avdaković[2]

[1] Public Enterprise Elektroprivreda of Bosnia and Herzegovina Mostar, Mostar, Bosnia and Herzegovina
{t.hubana,m.saric}@epbih.ba
[2] Public Enterprise Elektroprivreda of Bosnia and Herzegovina Sarajevo, Sarajevo, Bosnia and Herzegovina
s.avdakovic@epbih.ba

Abstract. Identification and classification of faults in the electrical power system remain one of the most important tasks for the system operators and managers. In particular, high impedance faults (HIF) identification and classification is an especially challenging task due to the physical properties of the waveforms and low neutral voltage. In recent years, there have been significant technology driven advances in this field of research, owned to the introduction and progress of smart grid technologies. However, this topic still remains an open area of research. This paper presents a method for classification of HIF in a medium voltage distribution network, based on the Hilbert-Huang Transform and Artificial Neural Networks. This method was tested on generated signals based on the model of a realistic distribution system. The results indicated that the proposed algorithm is capable to accurately classify HIF in the distribution system. This paper contributes to the existing research by developing and testing, on a model of realistic distribution system, a HIF classification method which offers very efficient and accurate performance.

1 Introduction

The Electrical Power System (EPS) is undoubtedly one of the most complex systems created by humans. The main purpose of the EPS is to generate, transmit and distribute electrical energy to industrial, commercial and household customers. The EPS complexity is owned to the fact that it consists of numerous complex dynamic and interacting elements, which are prone to failures, disturbances and faults. Recent years mark the period of remarkable advancement in the field of planning, operation and management of the EPS. These advancements are mainly owned to the proliferation of advanced information and telecommunication technologies in EPS, but also to the changes of regulatory framework and commitment to a new energy paradigm which comprises of energy transition from conventional to renewable generation technologies and electricity market liberalization. In particular, the introduction of smart grid technologies is regarded to be the main postulate for technology driven advancements of EPS operation and obliteration of outdated technologies and planning principles.

S. Avdaković (Ed.): IAT 2018, LNNS 59, pp. 114–131, 2019.
https://doi.org/10.1007/978-3-030-02574-8_10

However, numerous challenges still lay ahead of the visionary EPS which is smart, renewable, resilient and self-healing. One such challenge is the identification and classification of EPS faults. Even in the very early stages of EPS development, the use of high capacity electrical generating power plants and concept of the grid, i.e. synchronized electrical power plants and geographical displaced grids, required fault detection and operation of protection equipment in minimum possible time so that the power system can remain in a stable operating conditions. In modern EPS, fault identification, classification and clearance gains in importance due to the increasing regulatory and customer pressure for improvement of reliability indices, but also due to the system interconnection related issues. The faults on electrical power system lines are required to be detected, classified correctly and cleared by protective systems as soon as possible. The protection system used for line protection can also be used to initiate the other relays to protect the power system from unwelcome events which can not only cause the outages, but also numerous power quality problems such as voltage sag propagation throughout the network [1].

There are various types of power system faults. One possible classification of power system faults groups the faults according to the value of fault resistances. According to this classification scheme, there are two major categories of earth faults. The first group consists of the faults with resistances mostly below a few hundred ohms. In order to clear this type of faults, the circuit breaker tripping is usually required. These faults are most often flash-overs to the grounded parts of the network and it is possible to perform the distance computation for them. The second group of faults are the high impedance faults (HIF) which have the fault resistances in the order of thousands of ohms. In this case, the neutral potentials are very low and difficult to detect so it is not unusual that continued network operation with a sustained fault is possible [2]. Generally, HIFs are regarded as faults with current values in the range from 0 to 75 A in an effectively grounded system [3]. Their detection and classification is one of the major challenges faced by the system operators. Even if numerous contributions have been provided [4], this topic still remains an important and entirely open area of research [5].

Generally, a suitable fault detection system provides an effective, reliable, fast and secure input signal for relaying operations. The application of a pattern recognition technique could be useful in discriminating the faulty and healthy electrical power system. It also enables the user to differentiate among the phases and determine which phase of a three phase power system is experiencing a fault. This paper presents the results of the research conducted in the area of HIF classification. In particular, this paper presents a HIF in a distribution network classifier, based on Hilbert-Huang Transform (HHT) and Artificial Neural Network (ANN). The ANNs are very powerful in identifying the faulty pattern and classification of fault by pattern recognition [6]. Also, ANN have been applied to various engineering applications and can be generally considered as a fast and accurate method for classification. It is proposed that the combination of ANN with HHT, which is applied to the signal at the pre-processing stage, could be a promising approach for the classification of the HIF in the distribution network.

The rest of the paper is organized as follows. First the basic theoretical concepts relevant for the development of the proposed algorithm are presented, followed by the

outline of the algorithm structure and computational procedure. Then, then the results of the proposed algorithm application on a model of realistic distribution network are presented and discussed, together with the proposition of future research directions. Finally, the main conclusions resulting from this research are presented.

2 Theoretical Background

The following section will present the basic theoretical concepts that are relevant for the development of the proposed method.

2.1 Hilbert-Huang Transform

HHT is made up of two parts: one part is to get IMF by handling signals with EMD, and another one is to get the time-frequency spectrum by handling IMF with Hilbert transform, called Hilbert Spectral Analysis. Any signal can be broken down into some IMFs and a residue function through handling it with EMD [7].

2.1.1 Hilbert Spectral Analysis

The purpose of HHT is to demonstrate an alternative method to present spectral analysis tools for providing the time-frequency-energy description of time series data. Also, the method attempts to describe nonstationary data locally. Rather than a Fourier or wavelet based transform, the Hilbert transform was used, in order to compute instantaneous frequencies and amplitudes and describe the signal more locally [8].

The PV denotes Cauchy's principle value integral [8]:

$$H[x(t)] \equiv \hat{y}(t) = \frac{1}{\pi} PV \int_{-\infty}^{\infty} \frac{x(t)}{t-\tau} d\tau \tag{1}$$

An analytic function can be formed with the Hilbert transform pair as shown in Eq. (2) [8]:

$$z(t) = x(t) + i\hat{y}(t) = A(t)e^{i\theta(t)} \tag{2}$$

Where:

$$A(t) = \sqrt{x^2 + \hat{y}^2} \tag{3}$$

$$\theta(t) = \text{arctg}\left(\frac{\hat{y}}{x}\right), \text{ and} \tag{4}$$

$$i = \sqrt{-1} \tag{5}$$

A(t) and θ(t) are the instantaneous amplitudes and phase functions, respectively. The instantaneous frequency can then be written as the time derivative of the phase, as shown in Eq. (6) [8]:

$$\omega = \frac{d\theta(t)}{dt} \tag{6}$$

After transforming all IMFs with Hilbert transform, a series of analytic functions and instantaneous frequencies can be obtained.

2.1.2 Empirical Mode Decomposition

The EMD algorithm is one component of the HHT method. The algorithm attempts to decompose nearly any signal into a finite set of functions, whose Hilbert transforms give physical instantaneous frequency values [8]. These functions are called intrinsic mode functions (IMFs). The algorithm utilizes an iterative sifting process which successively subtracts the local mean from a signal. The sifting process is repeated until the signal meets the definition of an IMF, which will be explained shortly. Then, the IMF is subtracted from the original signal, and the sifting process is repeated on the rest. This is repeated until the final residue is a monotonic function. The last extracted IMF is the lowest frequency component of the signal, better known as the trend. Previously, the sifting process was said to stop when the signal met the criteria of an IMF [8].

The definition of an IMF, is a signal which has a zero-mean, and whose number of extrema and zero-crossings differ by at most one [9]. IMFs are considered mono-component functions which do not contain riding waves [9]. Once a signal has been fully decomposed, the signal D(t) can be written as the finite sum of the IMFs and a final residue as shown in Eq. (7).

$$D(t) = R_n(t) + \sum_{j=1}^{n} IMF_j(t) \tag{7}$$

Using previous equations, the analytic function can be formed as shown in Eq. (8) [8].

$$D(t) - R_n(t) = Re\left[\sum_{j=1}^{n} A_j(t) e^{i \int \omega_j(t) dt}\right] \tag{8}$$

Also, for reference, Eq. (9) shows the Fourier decomposition of a signal, x(t) [8].

$$D(t) = Re\left[\sum\nolimits_{j=1}^{n} A_j e^{i\omega j t}\right] \tag{9}$$

Notice that the EMD decomposition can be considered a generalized Fourier decomposition, because it describes a signal in terms of amplitude and basic functions whose amplitudes and frequencies may fluctuate with time [9].

2.2 Artificial Neural Network

An Artificial Neural Network (ANN) can be described as a set of elementary neurons that are usually connected in biologically inspired architectures and organized in several layers. Simply put, an elementary neuron is like a processor that produces an output by performing a simple non-linear operation on its inputs. A weight is attached to each and every neuron and training an ANN is the process of adjusting different weights tailored to the training set. An Artificial Neural Network learns to produce a response based on the inputs given by adjusting the node weights. Hence we need a set of data referred to as the training data set, which is used to train the neural Network [10].

Artificial neural network (ANN) can be applied to fault detection and classification effectively because it is a programming technique, capable to solve the nonlinear problems easily. The problems in which the information available is and in massive form can be dealt with. The fault classification method requires a neural network that allows it to determine the type of fault from the patterns of IMF signals, which are generated from the values measured from a three phase distribution underground cable at one terminal.

2.2.1 Back Propagation Neural Network

In the Back propagation neural network (BPNN) the output is feedback to the input to calculate the change in the values of the weights. One of the major reasons for taking the back propagation algorithm is to eliminate the one of the constraints on two layers ANNs, i.e. similar inputs lead to the similar output. The error for each iteration and for each point is calculated by initiating from the last step and by sending calculated the error backwards. The weights of the back-error-propagation algorithm for the neural network are chosen randomly, feeds back in an input pair and then obtain the result. After each step, the weights are updated with the new ones and the process is repeated for the entire set of inputs-outputs combinations available in the training data set provided by the developer. This process is repeated until the network converges for the given values of the targets for a predefined value of error tolerance. The entire process of back propagation can be understood by Fig. 1. This entire process is adopted by each and every layer in the entire the network in the backward direction [11]. The proposed algorithm uses the Mean Square Error (MSE) technique for calculating the error in each iteration. The algorithm of BPNN is as follows [11]:

Forward propagation:

$$a_j = \sum_{i}^{m} w_{ji}^{(1)} x_i \tag{10}$$

$$z_j = f(a_j) \tag{11}$$

$$y_j = \sum_{i}^{M} w_{kj}^{(2)} z_j \tag{12}$$

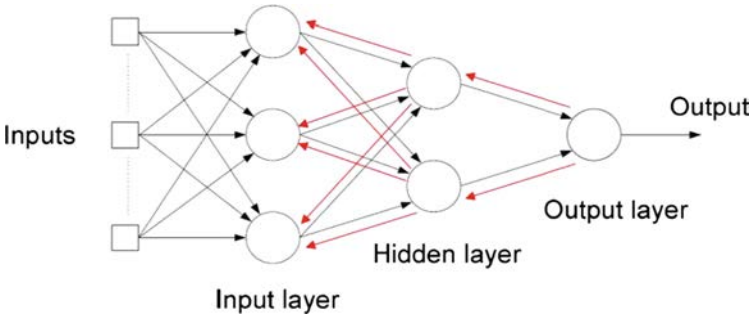

Fig. 1. Structure of back propagation ANN

Output difference:

$$\delta_k = y_k - t_k \tag{13}$$

Back propagation for hidden layers:

$$\delta_j = (1 - z_j^2) \sum_{k=1}^{K} w_{kj} \delta_k \tag{14}$$

The gradient of error with respect to first layer weights and second layer weights are calculated. In this step the previous weights are updated. In the previous equations a_j presents weighted sum of inputs, w_{ji} weight associated with the connection, x_i inputs, z_i activation unit of (input) that sends a connection to unit j, δ_k derivative of error at kth neuron, $\underline{y_i}$ ith output, y_k activation output of unit k, t_k corresponding target of input and δ_j derivative of error w_{rt} to a_j. The MSE for each output in each iteration is calculated by [11]:

$$\mathrm{MSE} = \frac{1}{N} \sum_{1}^{N} (E_i - E_o)^2 \tag{15}$$

where N is the number of iterations, Ei is actual output and Eo is out of the model [11].

Several different training algorithms for ANN are available. All these algorithms use the gradient of the performance function to determine how to adjust the weights to minimize performance. Levenberg-Marquardt optimization technique is used in the implemented ANN structure. In the proposed algorithm, IMF signals are combined and grouped and represent a unique 'signature' for each fault. After that, the ANN is trained with a large set of this data, and becomes capable to detect and identify PDN faults. It is important to note that the proposed classifier is fully customizable, very flexible and can be extended to include additional parameters and criteria.

3 Algorithm Development

This section presents an outline of the algorithm structure and computational procedure of the proposed method.

3.1 Basic Principles of the Algorithm

The proposed method algorithm is shown in Figs. 2 and 3, where Fig. 2 presents the algorithm during the ANN training process, and Fig. 3 the algorithm of the classifier in the power distribution system. The proposed classifier is completely adjustable, and by simple upgrades it is possible to implement additional parameters and criteria. The voltage in one end of the medium voltage underground cable is measured in various simulated scenarios and by applying the HHT EMD process the IMF's are obtained. This IMF's are used to create a unique system's signature during each fault scenario, and thus present a great input for ANN classifier. Finally, the ANN is trained with this data and previously known outputs.

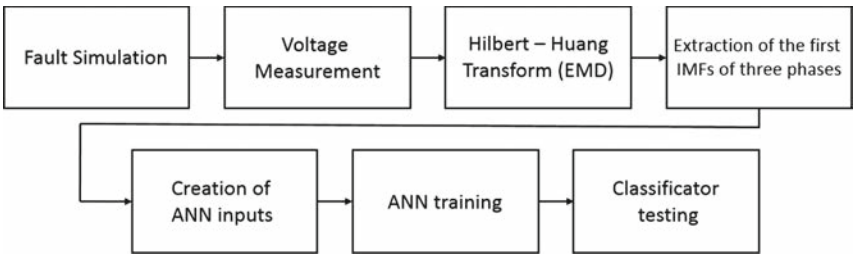

Fig. 2. Proposed method algorithm during the data preprocessing

Once created classifier is easy to use and implement in the system. One present industrial computer, paired with voltage measurements is enough for the system implementation. Measured voltages during the faulty conditions are sent to the HHT-ANN classifier, and after successful classification process, the trip signal can be sent or appropriate controls can be undertaken.

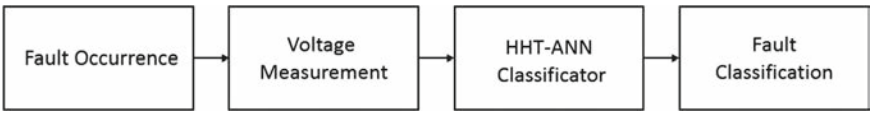

Fig. 3. Proposed classifier algorithm

3.2 Measurement Data Preprocessing

To get the characteristic quantity of the voltage signal it should be processed with Hilbert-Huang transform. High-frequency signals will be generated when a short-

circuit fault occurs which reside in IMF1. So the instantaneous frequency of IMF1 will mutate immediately the short-circuit fault takes place [7]. Through EMD decomposition, the original current signal can be changed into some IMFs. For instantaneous amplitudes of the voltage of the same line, their range and changing rate will increase sharply after short circuit happens. High-frequency signals included in short-circuit will shunt through stray capacitance between phases or earth and phases [7].

In this paper, high frequency signal IMF components are chosen to be the characteristic quantity for the further analysis. The HHT is applied to the measured voltage signals, and the first three IMF components during the single line fault with various fault resistance values are shown in Figs. 4, 5 and 6.

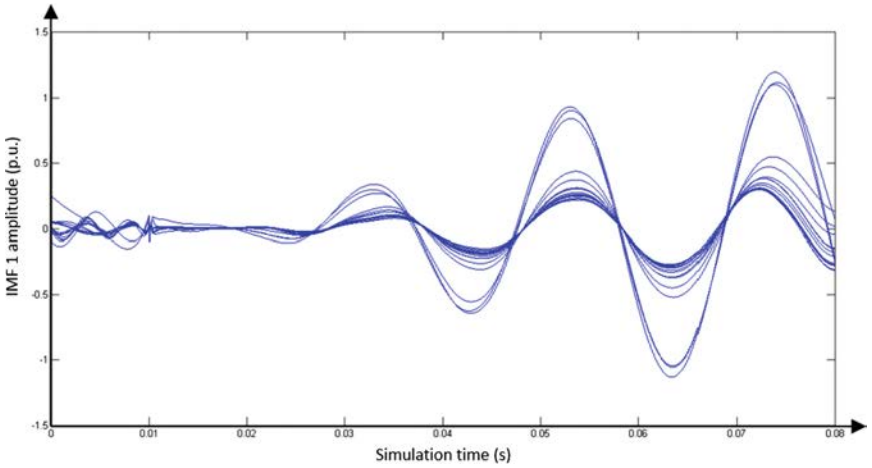

Fig. 4. IMF 1 of phase A, during the LG fault with various fault resistances

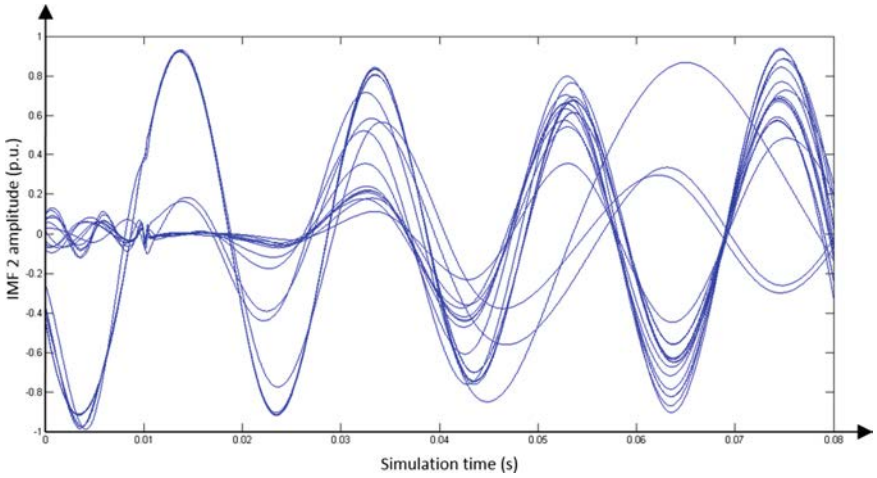

Fig. 5. IMF 2 of phase A, during the LG fault with various fault resistances

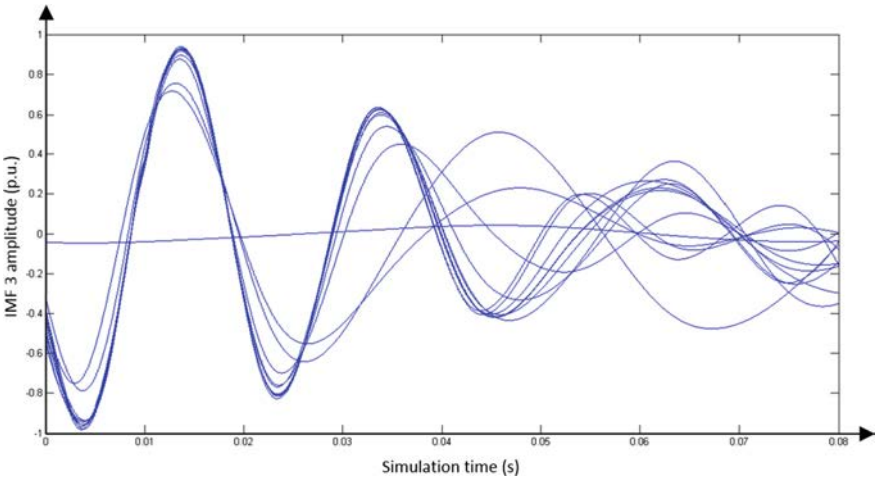

Fig. 6. IMF 3 of phase A, during the LG fault with various fault resistances

However, the number of IMF components depends of the signal complexity, and in various fault scenarios, different number of IMF components occur. Because of that, the proposed algorithm works with first IMF components, since the first IMF component is always present in every signal.

3.3 Training and Testing

Simulations are carried out in different fault scenarios for getting various fault patterns. The system model as well as ANN training is carried out using MATLAB and MATALB Simulink simulation software. Three different fault types (LG, LLG, LLLG faults) are simulated. The fault resistances ranged from 20 to 600 Ω. The number of neurons in hidden layers, is determined empirically by experimenting with various network configurations, and 11 hidden neurons are chosen since it presents a compromise between satisfying accuracy and training speed. The ANNs are fed with the sixty signals for every particular fault scenario, resulting in 180 total scenarios. The classification ANN output layer has three neurons, indicating which fault is taking place (LG, LLG or LLLG) are involved in the fault event. A total of 180 simulations were generated, and 80% of them were used for training, and the other 10% for validating and 10% for testing. Once trained, the networks performance is tested using a validation data set. The suitable network, which showed satisfactory results is finally created, and ready for use in various fault scenarios.

4 Results and Discussion

This section presets the results and discussion of the proposed algorithm application on a model of realistic distribution network, together with the proposition of future research directions.

4.1 Test System

The developed test system represents a part of a real power distribution system in the area of the City of Mostar. Consumers are fed over 35/10 kV transformer, via 10 kV underground cables, 10/0.4 kV distribution transformers and finally over 0.4 kV low voltage network. The test system is developed in MATLAB Simulink simulation software as shown in Fig. 7.

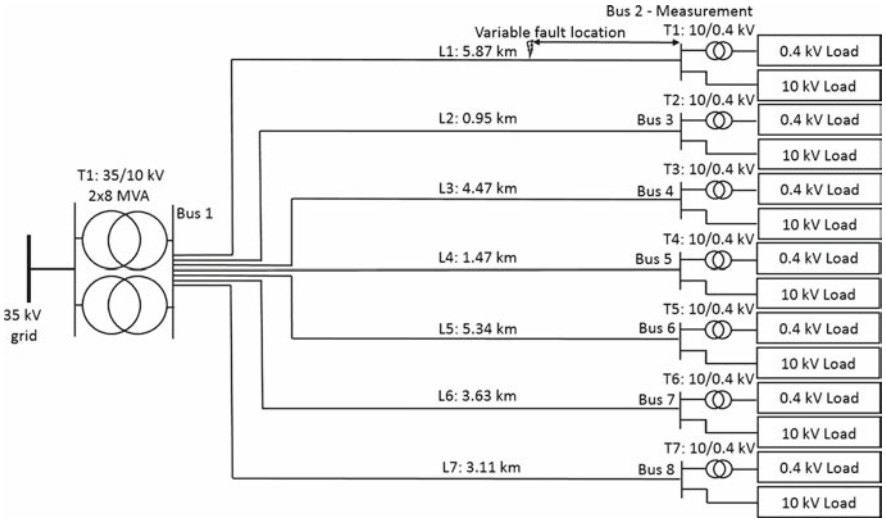

Fig. 7. The developed test system

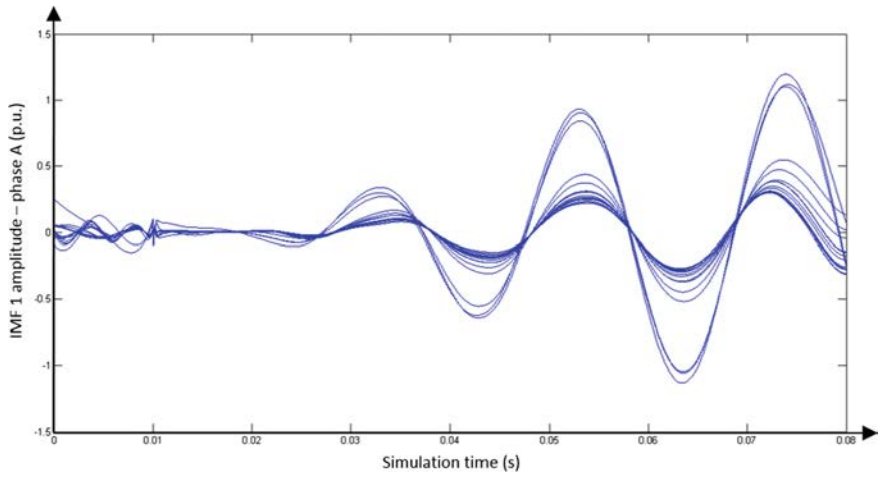

Fig. 8. IMF 1 of phase A, during the LG fault with various fault resistances

Faults are simulated on the 10 kV busbar of the 10/0.4 kV transformer, over various fault locations (in the range from 20 to 600 Ω). The LG, LLG and LLLG faults are simulated. Voltage measurements devices are connected to the 10 kV busbar of the 10/0.4 kV transformer, with the sampling frequency of 3.2 kHz, which is the sampling frequency of the present relays in the power distribution system.

4.2 Simulation Results

During the classification process in distribution network, it is necessary to monitor the IMF component's behavior in all three phases, since every voltage phase has a

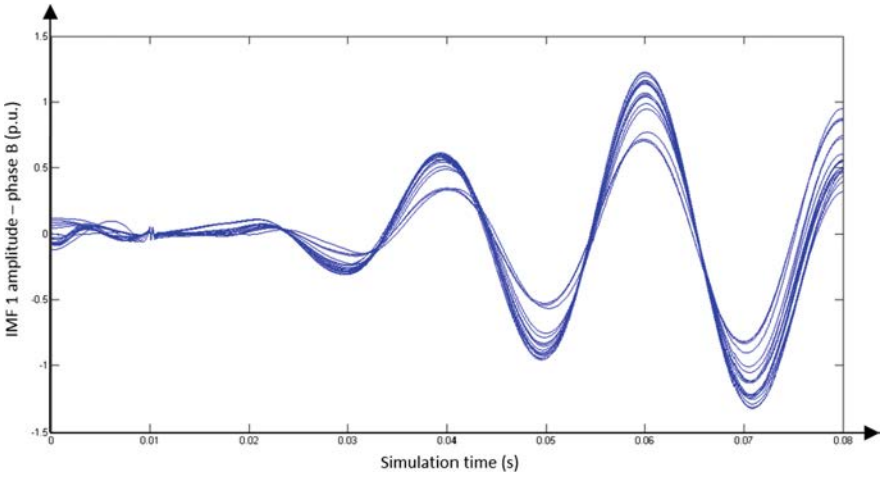

Fig. 9. IMF 1 of phase B, during the LG fault with various fault resistances

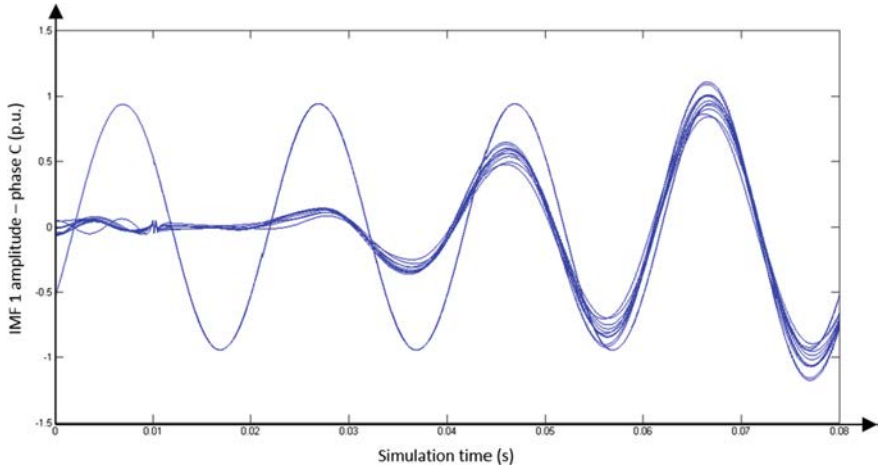

Fig. 10. IMF 1 of phase C, during the LG fault with various fault resistances

characteristic behavior during the fault. As previously mentioned, only the first IMF components will be used by the classifier. The first IMF components of every voltage phase during the LG fault are shown in Figs. 8, 9 and 10.

Figures 11, 12 and 13 show the first IMF components during the LLG fault.

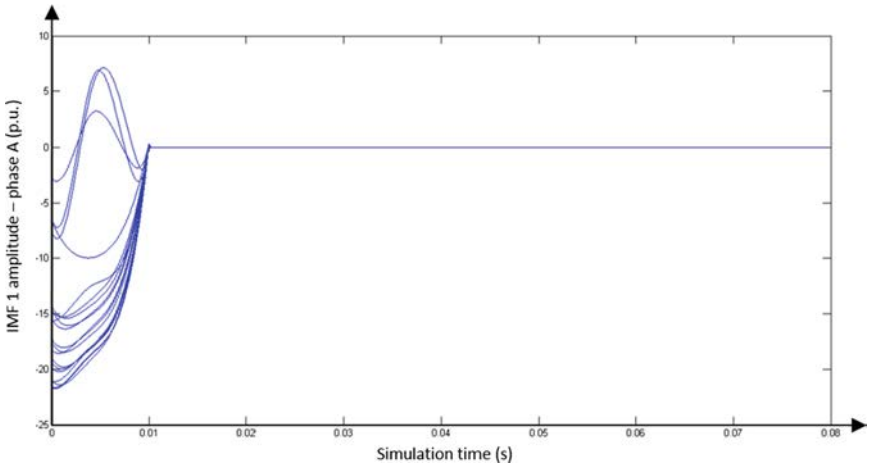

Fig. 11. IMF 1 of phase A, during the LLG fault with various fault resistances

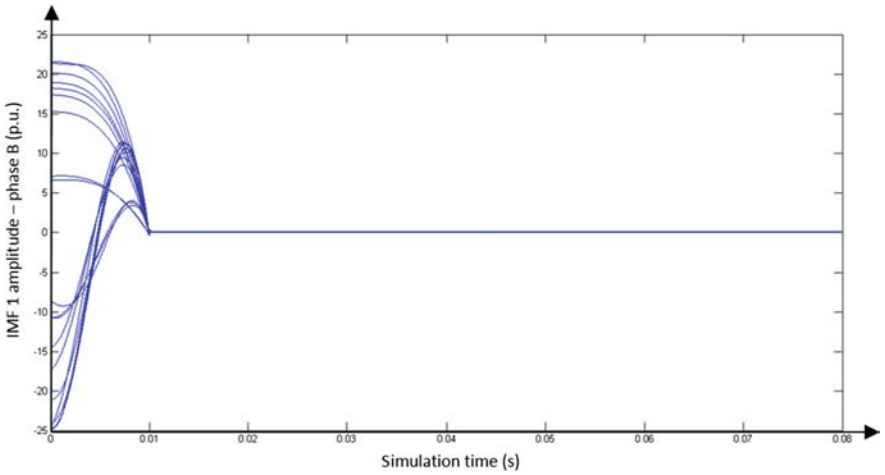

Fig. 12. IMF 1 of phase B, during the LLG fault with various fault resistances

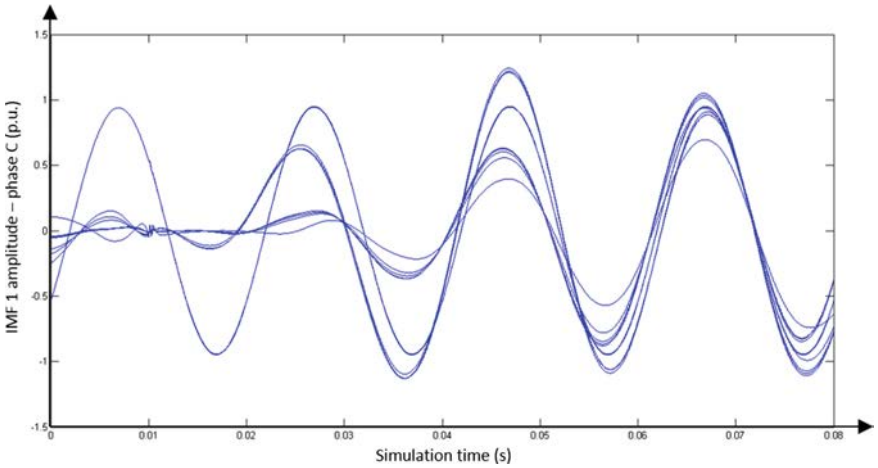

Fig. 13. IMF 1 of phase C, during the LLG fault with various fault resistances

Figures 14, 15 and 16 show the first IMF components during the LLLG fault.

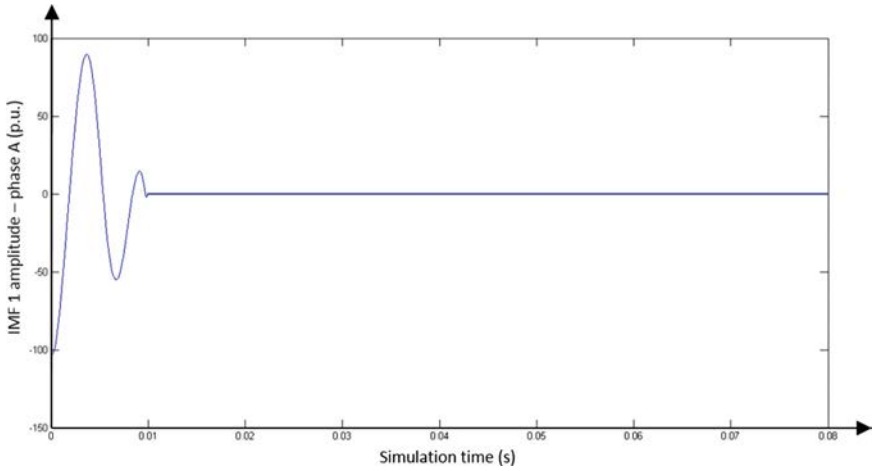

Fig. 14. IMF 1 of phase A, during the LLLG fault with various fault resistances

Figures 11, 12 and 13 show that the value of the first IMF component in the fault conditions is close to zero, but the IMF of the healthy phase has different shape for various fault resistances. Figures 14, 15 and 16 show that the fault resistance does not affect the IMF amplitude during the LLLG fault. Since the classifier is based on ANN, it is necessary to create appropriate ANN inputs. In order to reflect the system behavior in the best manner, a unique signal that contains IMF's of each phase is created. By grouping the signals into one signal, a unique system's signature that responds to

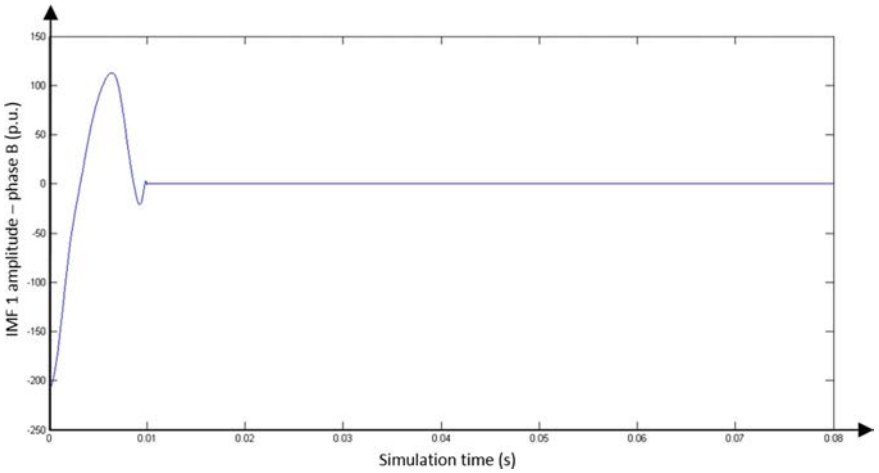

Fig. 15. IMF 1 of phase B, during the LLLG fault with various fault resistances

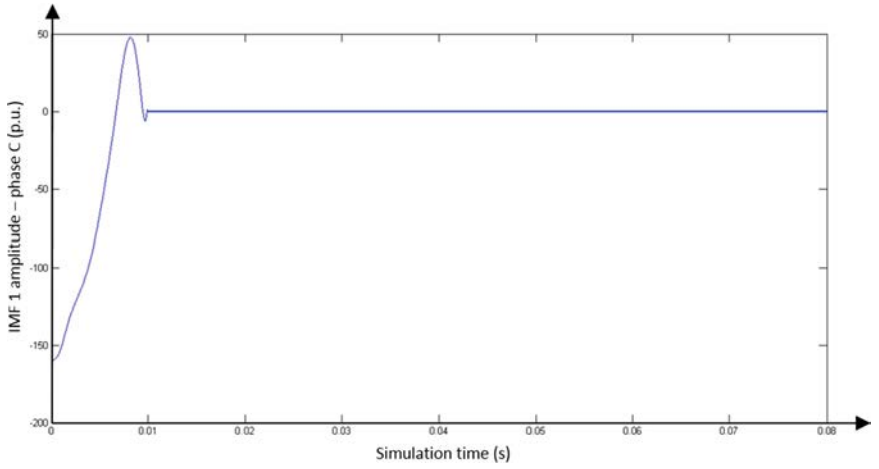

Fig. 16. IMF 1 of phase C, during the LLLG fault with various fault resistances

specific fault scenario is created. Figures 17, 18 and 19 show the grouped IMF signals for each fault type with 60 different fault resistances.

After the grouped signals are created, the ANN inputs are ready. The designed network takes in the set of total 180 inputs. The neural network has three outputs, each of them corresponding to the three fault. Hence the outputs are either 0 or 1 denoting the absence or presence of a fault, and the various possible permutations can represent each of the various faults accordingly.

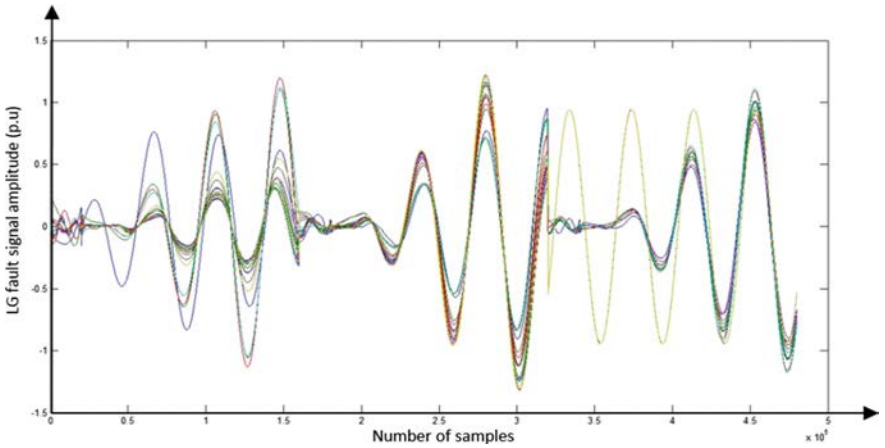

Fig. 17. Grouped IMF signal in case of LG fault for various fault resistances

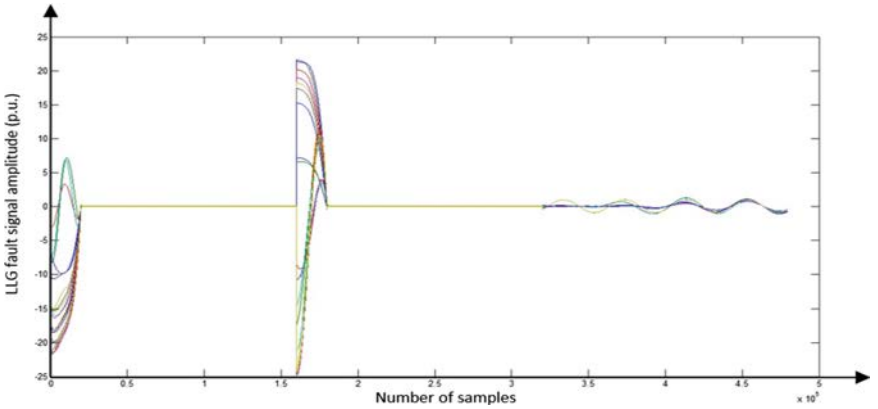

Fig. 18. Grouped IMF signal in case of LLG fault for various fault resistances

4.3 Test of the HHT-ANN Algorithm

After the training process, the ANN is created, with the MSE of 3.469e-4. However, the ANN outputs are not exactly 0 or 1, due to the classification error. This means that he outputs are not unambiguous, but one additional step where the highest value of each output is set to 1, and all other to 0, fixes this problem (Fig. 20).

In order to test the created ANN, the ANN will be tested with completely new fault scenarios, with fault resistance values that ANN is not trained to. New 15 random fault scenarios are simulated, and the proposed classifier is tested. Results of 8 tests are shown in Table 1.

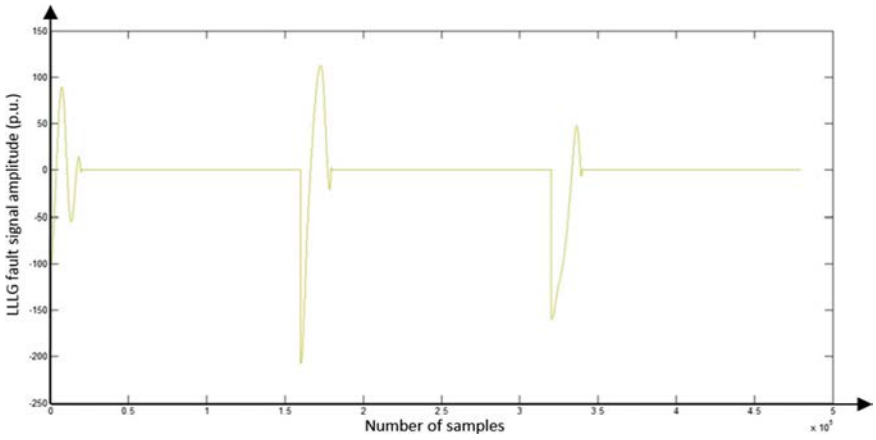

Fig. 19. Grouped IMF signal in case of LLLG fault for various fault resistances

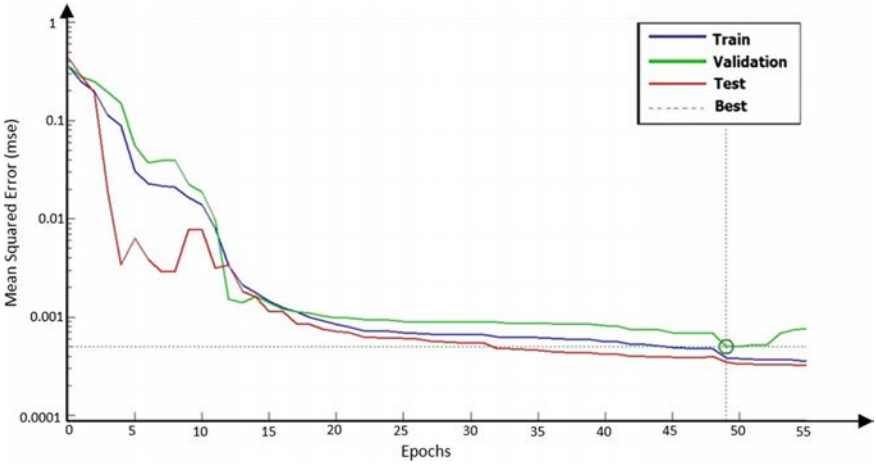

Fig. 20. The ANN training performance

Table 1 shows the efficiency of the proposed HHT-ANN classifier. The accuracy in the resistance range from 20 to 600 Ω is 100%. Future research directions will be to take the fault location and other possible fault types into consideration. This research is part of a large project, whose goal is to develop a new more accurate fault detector and classifier that overcomes the problems of the traditional protection devices.

Table 1. Output of the HHT-ANN classifier

Resistance (Ω)	Desired output (fault type)				Actual output (fault type)			
	LG	LLG	LLLG	No fault	LG	LLG	LLLG	No fault
20	1	0	0	0	1	0	0	0
110	0	0	0	1	0	0	0	1
200	0	1	0	0	0	1	0	0
290	0	0	1	0	0	0	1	0
380	1	0	0	0	1	0	0	0
470	0	1	0	0	0	1	0	0
470	0	1	0	0	0	1	0	0
560	0	0	0	1	0	0	0	1

5 Conclusion

Classification of faults, especially the HIFs in distribution networks is a serious problem, because the existing protection devices are unable to detect nor classify such failures. Thus, an unconventional approach to the problem is required, and therefore a fault classifier based on HHT and ANN is proposed as a possible solution.

For the purpose of algorithm testing, a test system based on a part of the real distribution network from Bosnia and Herzegovina is developed in MATLAB Simulink. Results obtained by applying the proposed algorithm demonstrated that the algorithm presents a good solution for classification of faults in distribution networks. Accuracy of the HHT-ANN algorithm is 100% in the 20–600 Ω range of fault resistances. It is important to point out that the developed ANN is not immune to the large load and switching state changes, and in order to overcome this, further ANN training is required. The algorithm turns out to be promising when it comes to the future heuristic power system protection devices.

This study is a part of an ongoing research whose objective is to contribute to the development of an advanced protection system that has satisfactory accuracy for detection and classification of the power distribution network faults. And important future research should extend the number of system elements and scenarios that can lead to the false fault classification.

References

1. Hubana, T., Begić, E., Šarić, M.: Voltage sag propagation caused by faults in medium voltage distribution network. In: Hadžikadić, M., Avdaković, S. (eds.) Advanced Technologies, Systems, and Applications II, IAT 2017. Lecture Notes in Networks and Systems, vol. 28. Springer, Cham (2018)
2. Hanninen, S.: Single phase earth faults in high impedance grounded networks. Technical Research Centre of Finland, VTT Publications, Espoo (2001)
3. Wang, B., Geng, J., Dong, X.: High-impedance fault detection based on non-linear voltage-current characteristic profile identification. IEEE Trans. Smart Grid **9**(4), 3783–3791 (2017)

4. Hubana, T., Šarić, M., Avdaković, S.: Approach for identification and classification of HIFs in medium voltage distribution networks. IET Gener. Transm. Distrib. **12**(5), 1145–1152 (2018)
5. Šarić, M., Hubana, T., Begić, E.: Fuzzy logic based approach for faults identification and classification in medium voltage isolated distribution network. In: Hadžikadić, M., Avdaković, S. (eds.) Advanced Technologies, Systems, and Applications II, IAT 2017. Lecture Notes in Networks and Systems, vol 28. Springer, Cham (2018)
6. Jamil, M., Sharma, S., Singh, R.: Fault detection and classification in electrical power transmission system using artificial neural network. Springer Plus **4**, 334 (2015). https://doi.org/10.1186/s40064-015-1080-x
7. Guo, Y., Li, C., Li, Y., Gao, S.: Research on the power system fault classification based on HHT and SVM using wide-area information. Energy Power Eng. **5**(4B), 138–142 (2013). https://doi.org/10.4236/epe.2013.54B026
8. Bradley, B.L.: The Hilbert-Huang Transform: theory, applications, development - PhD thesis. University of Iowa, Iowa City (2011)
9. Huang, N.E., Wu, Z.: A review on Hilbert-Huang transform: method and its applications to geophysical studies. Rev. Geophys. **46**(2), 1944:9208 (2008)
10. Ayyagari, S.B.: Artificial Neural Network Based Fault Location for Transmission Lines - Master's theses. University of Kentucky, Lexington (2011)
11. Haykin, S.: Neural Networks: A Comprehensive Foundation. Macmillan College Publishing Company, London (1994)

Transmission lines fault location estimation based on artificial neural networks and power quality monitoring data

Tarik Hubana
Distribution System Operator Mostar
PE Elektroprivreda BiH d.d. - Sarajevo
Mostar, Bosnia and Herzegovina
t.hubana@epbih.ba

***Abstract* — Fault location estimation is a very important question in electric power system, in order to isolate the fault as soon as possible, and to recover the system with minimal interruptions. In that way, electric equipment is less stressed, and buyers more satisfied. Electric power lines are exposed to environment and probability of line failure is generally higher than other system element failure. Current electric power systems are equipped with high sampling rate power quality meters that are installed in the places of common coupling with distribution systems or high voltage consumers. Data obtained by these power quality meters, especially the voltage and current harmonics present a valuable information about system behavior, even in the faulty conditions. In this paper fault location and fault resistance is estimated by using a combination of artificial neural networks and voltage and current harmonics measured by power quality meters installed only in important system busbars. Results obtained from the real 110 kV transmission system show that a proposed algorithm can be used successfully in fault location and fault resistance estimation in one part of the electric power system. This paper makes a contribution to the existing body of knowledge by developing and testing a new method whose application represents a natural and a feasible upgrade using the existing measurement and communication equipment.**

Keywords—power systems; transmission lines, faults; fault location; measurement, neural networks; power quality; harmonics.

I. INTRODUCTION

Transmission lines are main components of every power system and their protection is needed to provide the system reliability and to minimize the damage of the equipment. Transmission lines are often more prone to the failures since there are more exposed than other electric power system (EPS) components. Failures on the transmission lines cause short circuits, which cause mechanical and thermal stresses that are potentially harmful to the high-voltage equipment. Quick transmission lines fault detection enables quick isolation of the faulty lines, thus protecting it from the harmful effects of failure.

In the past few years there was a noticeable increase in the number of power quality monitors (PQMs) the EPSs. Disturbances in the systems are instant and they occur randomly, so for their analysis, it is needed more than just the detection, i.e. they need to be recorded during a specified time interval. During the monitoring time, a large number of power quality parameters are being monitored, and some of them can be especially interesting and give an appropriate insight into system behavior. Since the PQMs have a large sampling rate, they are able to record the voltage and current harmonic components (harmonics), unlike other conventional measuring equipment. A certain number of PQMs are already installed in the EPSs, and thus they present a great measuring tool for multiple implementations. However, even with all these measurements, there is a category of problems that cannot be formulated with conventional algorithms. The study of artificial neural networks (ANNs) is motivated by their similarity with biological systems that work successfully and consist of a very simple but a large number of nerve cells that work in parallel and have the ability to learn. A specific output based on input data can be obtained by adjusting the weights of the artificial neural network. ANNs are known to have high accuracy in pattern classification and generalization, fast response, noise removal ability, and prediction capability [1].

Over the years, various algorithms for fault location are proposed and developed, with the significant expand of the heuristic algorithm-based fault locators as shown in [2]. Current fault location methods often include a manual search for the fault using various sets of data collected during the fault and a short circuit program to simulate faults and derive a location which can take hours to complete if an engineer and information are available [3]. Then, patrols are requested, often from the beginning of the line to its end(s). The time-of-day, line length, line location and weather impact the duration and safety of this activity [3]. The advances in signal processing techniques, artificial intelligence and machine learning, global positioning system (GPS) and communications have enabled more and more researchers to carry out studies with high breadth and depth where the limits of traditional fault protection techniques can be stretched [4]. Papers [2], [5-9] suggest using computational intelligence for fault location, with high speed broadband communication or GPS. A fault location estimation is more challenging, and large number of authors [10-12] use phasor measurement units (PMUs) for measurement and data collecting. However, PQMs can be used as the source of these measurements as well. Papers [13] and [14] use this date for fault classification, while [15] successfully determines the fault location, but not the fault resistance. One such system is already installed by the DTE Energy Electric Company in USA EPS [3],

978-1-5386-4505-5/18/$31.00 ©2018 IEEE

and ordinarily used for fault location purposes, but the accuracy still needs to be improved.

The majority of papers that deal with PQM data usage are limited to the fault detection and classification or are being applied on a single transmission line. The algorithm proposed in this paper uses existing PQM harmonics data, measured only in few EPS busbars, combined with ANNs, and as a result, successfully estimates the fault location and fault resistance. The two test systems, the 2-bus and the 8-bus test system, developed in MATLAB Simulink for this purpose, represent a part of a real 110 kV EPS where the PQMs are located at both busbars in 2-bus system and 4 busbars in 8-bus system of interest, i.e. at the places of energy exchange.

II. METHODOLOGY

A. Harmonics monitoring in EPS

Voltage and current harmonics propagation in EPS is directly correlated with the efficient EPS operation. The harmonics propagation and voltage distortions are directly propagated from the transmission network to the medium voltage and low voltage distribution networks [16]. The power quality measurement is carried out by PQMs, whether with portable or stationary PQMs.

When using stationary PQMs, several conditions are used to select an installation location [16]:

- PQMs installation at the required locations as defined by the regulator;
- PQMs installation at numerous sites so that a statistically representative sample is achieved;
- PQMs installation on locations based on consumers complaints to the power quality;
- PQMs installation at places where important and / or sensitive consumers are or will be connected;
- PQMs installation in places where high levels of power quality disturbances are expected;
- PQMs installation at sites that are significant for EPS operation (transformers, important overhead lines, important drains);
- PQMs installation at power exchange locations (transmission to distribution network place of common coupling, transmission systems interconnections).

Stationary PQMs are connected to the substations, and they can be connected together to monitor the part of the EPS. If they happen to be a time synchronized PQMs, set to monitor, analyze, record and report the power quality synchronously, then this system presents an efficient and relevant system for power quality monitoring in the certain part of the system [16]. The system for the power quality monitoring, besides the PQMs, needs to include an internal communication network, with many incorporated devices and with the central supervision system [16]. Depending on the communication network performance and capacity, and the type of the PQMs, it is possible to implement an advanced continuous power quality monitoring system in order to operate the system more reliably, economically justified and efficiently. In the future EPS, some power quality parameters could represent the control variables of the EPS, and one of the possible implementations is a fault location system.

B. Errors in the HV measurements

The measurement process in the high voltage EPS includes voltage and current transformers (VTs and CTs). In the measurement process, the sine wave of the high voltage (HV) side of the voltage and current transformers will be converted to the low voltage (LV) side with the error in both the signal amplitude and angle [16]. However, these transformers have some frequency limitations. The construction parameters and the operating and environmental conditions can have a significant impact on the frequency characteristic of the VTs and CTs. Many researchers [17-20] have analyzed the impact of the frequency to the voltage and current transformers characteristics. The conclusions are that the measurements in the HV EPSs can lead to errors in the high frequency range. Also, authors in [20] have proposed the recommendations for the reliable measurement in specific frequency ranges for each voltage level, as shown in Table 1. When it comes to measurements in 110 kV voltage level, the measurements are reliable up to 9th or 10th voltage and current harmonic. The proposed algorithm uses the first 9 voltage and current harmonics, and the DC component of the voltage and current. This approach avoids the error and provides reliable and accurate measurements that will contribute to the proposed method accuracy.

Table 1 Reliability of harmonics measurements in different voltage levels

Network	Voltage level	Harmonics		
		2nd to 7th	8th to 20th	21st to 50th
MV	10 kV	OK	OK	OK
	20 kV	OK	OK	Uncertain
	30 kV	OK	NO	NO
	60 kV	OK	OK	Uncertain
HV	110 kV	OK	Uncertain	NO
	220 kV	Uncertain	NO	NO

C. Artificial Neural Networks

In the backpropagation neural network (BPNN) the output is feedback to the input and is used to calculate the change in the values of the weights [21]. The weights of the back-error-propagation algorithm for the neural network are chosen randomly to prevent a bias towards any particular output. The first step in algorithm of BPNN is forward propagation [21]:

$$a_j = \sum_{i}^{m} w_{ji}^{(1)} x_i \tag{1}$$

$$z_j = f(a_j) \tag{2}$$

$$y_j = \sum_{i}^{M} w_{kj}^{(2)} z_j \tag{3}$$

where a_j represents the weighted sum of inputs, w_{ij} weight associated with the connection, x_i inputs, z_j activation unit of (input) that sends a connection to unit j and y_i i-th output. The second step is calculation of the output difference [21]:

$$\delta_k = y_k - t_k \tag{4}$$

where δ_k represents a derivative of the error at k-th neuron, y_k activation output of unit k and t_k corresponding target of the input. The next step is backpropagation for hidden layers [20]:

$$\delta_j = (1 - z_j^2) \sum_{k=1}^{K} w_{kj} \delta_k \tag{5}$$

where δ_j is derivative of error w_{kj} to a_j.

Afterwards, the gradient of error with respect to the first layer weights and the second layer weights are calculated, and the previous weights are being updated. The MSE for each output in each iteration is calculated by [21]:

$$MSE = \frac{1}{N} \sum_{1}^{N} (E_i - E_o)^2 \tag{6}$$

where N is the number of iterations, E_i is actual output and E_o is out of the model. After each step, the weights are updated with the new ones and the process is repeated for the entire set of inputs-outputs combinations available in the training data set, and this process is repeated until the network converges for the given values of the targets for a predefined value of error tolerance [22].

Since in this paper there are 2 and 4 PQMs installed in the systems in case of 2-bus and 8-bus test system respectively (with 120 and 240 measured values in every fault scenario), there are 120 and 240 input neurons for each system. The rest of the ANN design is same for both systems. The ANNs have two outputs that indicate the fault location and fault resistance. The number of hidden neurons (11 neurons) is empirically selected in order to provide the balance between learning accuracy and training time. In this case the network training function that updates weight and bias values according to Levenberg-Marquardt optimization is used. The structure of the ANN is shown in Fig. 1.

D. Outline of the computational procedure

After simulating the fault, for each fault and different values of fault location and resistance, the voltage and current waveforms are measured. The fault is sustained during the entire simulation interval. When the voltage and current waveforms are generated and collected, the PQM device calculates the voltage and current harmonics. These data are collected and grouped into one long sequence of voltage and current harmonics data. This

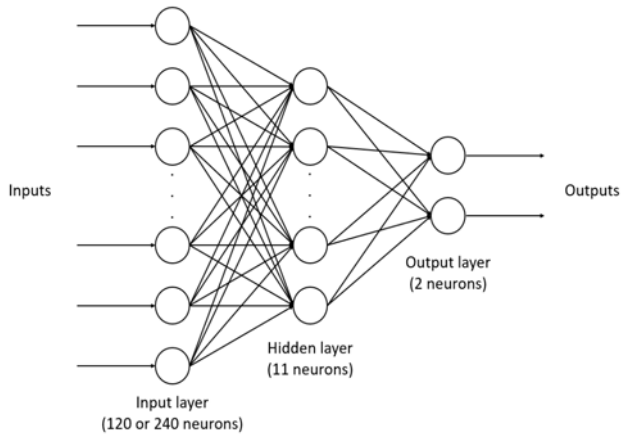

Fig. 1 Artificial neural network

signal components give a good insight into system behavior during the fault conditions. For this reason, they are used as representative signals for each fault scenario, which represents the input to the ANN. Once trained ANN is capable of fault location, according to the algorithm shown in Fig. 2.

With the PQM devices installed in power system, voltage waveforms and current harmonics can be measured, and sent to the industrial computer with proposed algorithm software. In the case of fault, appropriate following actions can be undertaken.

III. Experimental Setup

Two new, 2-bus and 8-bus systems are developed in order to test and analyze the proposed algorithm. The developed 8-bus test system is a part of a real EPS. The PQMs installed in the systems are set to record the voltages and currents up to the 9th harmonic (including the DC component).

Slack bus and system generators were modelled with voltage sources behind Thevenin equivalent. The Three-Phase Source block implements a balanced three-phase voltage source with an internal R-L impedance. The three voltage sources are connected in Y with a neutral connection that can be internally grounded or made accessible [23]. The Three-Phase PI Section Line block implements a balanced three-phase transmission line

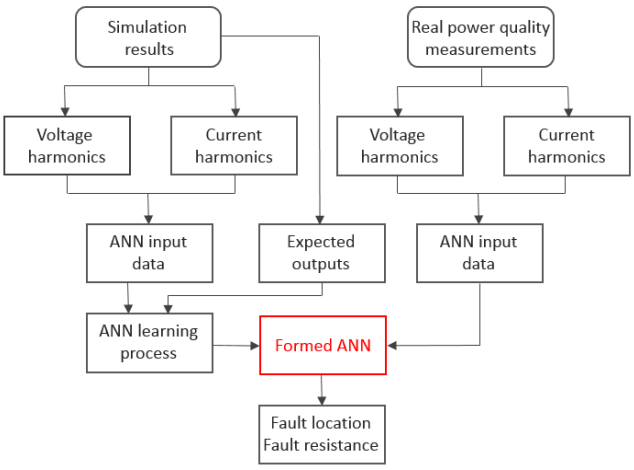

Fig. 2 Proposed method algorithm

model with parameters lumped in a PI section The line parameters R, L, and C are specified as positive- and zero-sequence parameters that take into account the inductive and capacitive couplings between the three phase conductors, as well as the ground parameters. This method of specifying line parameters assumes that the three phases are balanced. The self and mutual resistances (Rs, Rm), self and mutual inductances (Ls, Lm) of the three coupled inductors, as well as the phase capacitances Cp and ground capacitances Cg, are deduced from the positive- and zero-sequence RLC parameters [23]. The loads are modelled as the three-phase series RLC load, which implements a three-phase balanced load as a series combination of RLC elements. At the specified frequency, the load exhibits a constant impedance. The active and reactive powers absorbed by the load are proportional to the square of the applied voltage. Short circuits occur through the transition resistance which consist of two main components: arc resistance and soil resistance. There are two major categories of earth faults [1]. In the first category, the fault resistances are mostly below a few hundred Ohms and circuit breaker tripping is required [1]. These faults are most often flash-overs to the grounded parts of the network. Thus, the fault resistance will be simulated in the range of 0 – 100 Ω, for various fault locations.

Test systems are developed in MATLAB Simulink software, and represent a EPSs with 2 and 8 busbars, while the PQM are installed in 2 busbars in the 2-bus system and in 4 busbars in 8-bus system, i.e. in the places of energy exchange. Test systems are shown in Fig 3 and Fig 4. In both systems, the red busbars are the ones with the installed PQMs. In the 2-bus system, the PQMs are installed in the busbars BB1 and BB2. In the 8-bus system the PQMs are installed in the busbars: BB1, BB4, BB7 and BB8. The PQM algorithm developed in MATLAB calculates harmonics in the 200 ms time frame (10 cycles in the 50 Hz EPS). The procedure of harmonics calculation is carried out according to the IEC 61000-4-7 standard [24].

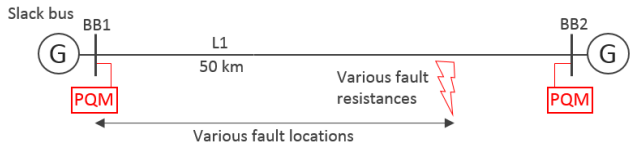

Fig. 3 2-bus test system

Before the simulation, a power load flow is carried out, to ensure that all busbar voltages are set to the values that provide the optimal power load flow, and to make the fault scenarios more real. Faults will be simulated in different places in the system, in the range of 0% to 100% length of the lines, over various fault resistance values in the range of 0.1 -100 Ω. As a result of these simulations, the voltage and current harmonics in three phases up to 9th harmonic, with DC component, which results in 120 measured values in the 2-bus system, and 240 values in the 8-bus system. The total of 573 fault scenarios are simulated in both test systems.

IV. Results and Discussion

The method presented in the section II is applied to the both test systems. After 573 simulation scenarios, the vector that contains all measured values is created. This vector presents a unique signature of the EPS and describes a specific fault scenario. In the case of 2-bus test system, the measurements are carried out in 2 busbars as shown in Fig. 3.

After that the ANN is created, by providing the appropriate inputs and desired outputs for each fault scenario. After the training process, the ANN is capable to successfully estimate the fault location and the fault resistance, based on the inputs that contain only voltage and current harmonics. The mean squared error (MSE) of the proposed ANN locator is 7.4 m in the case of fault location, and 0.0151Ω in the case of resistance estimation. Absolute error of this fault locator in various fault locations (from 0% to 100% of line length) is shown in Fig. 5 – (a) and Fig. 5 – (b). These results show that the proposed

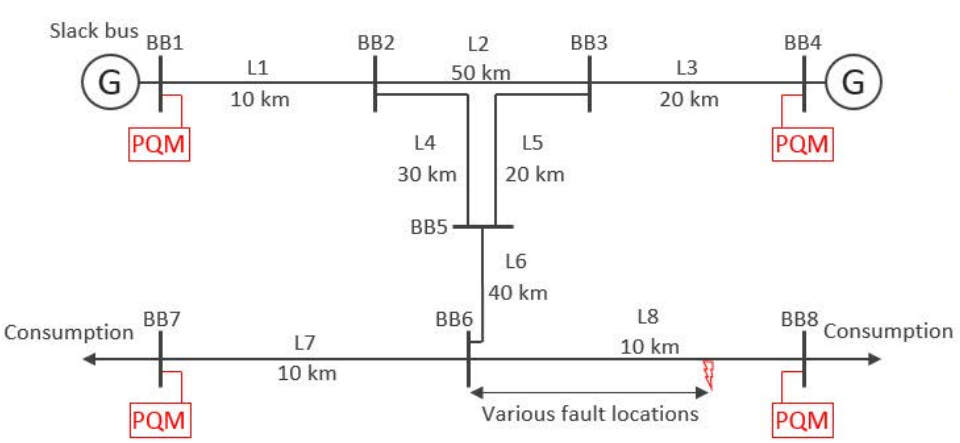

(a)

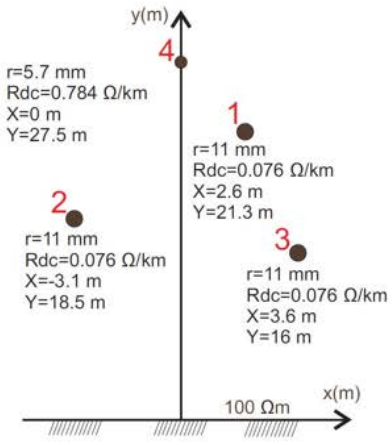

(b)

Fig. 4 (a) 8-bus power system model
(b) Transmission lines parameters

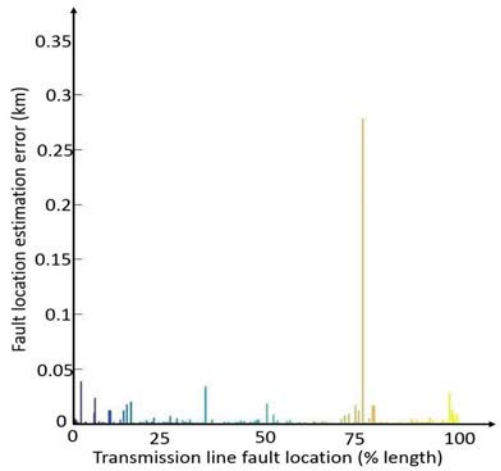

(a)

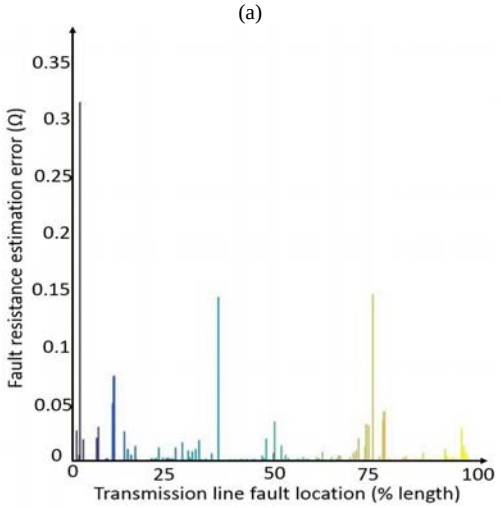

(b)

Fig. 5 (a) Fault location estimation error in 2-bus test system
(b) Fault resistance estimation error in 2-bus test system

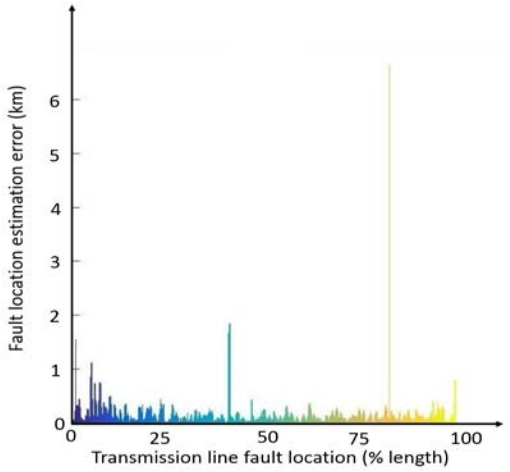

(a)

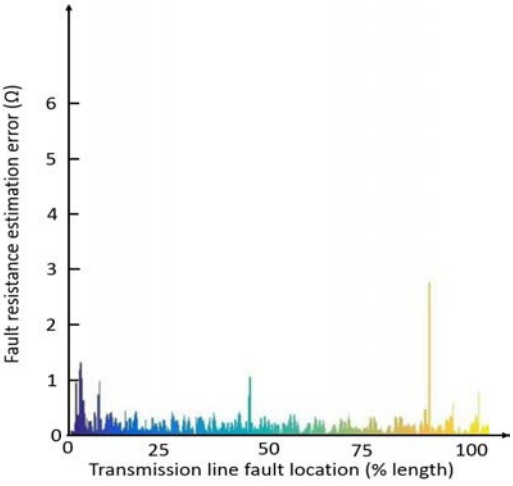

(b)

Fig. 6 (a) Fault location estimation error in 8-bus test system
(b) Fault resistance estimation error in 8-bus test system

algorithm can successfully estimate the fault location and fault resistance value. Unlike in the 2-bus test system case, the PQMs are not present in every busbar in the 8-bus test system, which is a more common setup in the real EPS. Since the PQMs are installed in 4 places in the system, the ANN input vector will contain 240 values, that represent the voltage currents and harmonics measured by the 4 PQMs.

In this case it is important to firstly detect the line where the fault occurred. For this purpose, two ANNs are created. One is used to detect the faulty line, and another to estimate the fault location and fault resistance value. After simulating the 573 fault scenarios in the system, ANN is trained and ready to use. The mean squared error (MSE) of the proposed ANN locator is 2.4196 m in the case of fault location, and 0.47913 Ω in the case of resistance estimation. Absolute error of this fault locator is shown in Fig. 6 – (a) and Fig. 6 – (b). However, to get the real picture of the proposed locator accuracy, new 7 fault scenarios are simulated, in completely different locations, and different fault resistance values. These values present the new data that ANN is not trained to. The results of the proposed ANN fault locator in the 8-bus system are presented in Table 2.

The locator could be installed in the EPS with appropriate communication infrastructure. When the fault occurs, the data can be sent to the installed industrial computer that has a

Table 2 Output of the Harmonic-ANN fault locator for different fault resistances and fault locations in an 8 – bus test system

Desired output		**Actual output**	
Fault location (% length)	**Fault resistance (Ω)**	**Fault location (% length)**	**Fault resistance (Ω)**
5	5	4,9584	4,7655
16	20	16,0169	19,6297
31	35	30,9853	35,1864
46	50	45,9688	49,9218
61	65	61,0241	64,9215
76	80	75,9458	80,1732
91	95	91,1041	94,8026

proposed ANN algorithm. Following the procedure showed in Fig. 2, the algorithm can estimate the fault location and fault resistance. This approach contributes to the operation of the EPS, by providing the more accurate fault location, and finally reducing the outage time and improving he power quality.

V. Conclusions

This paper presented a fault location algorithm based on voltage and current harmonics measurements obtained by the PQMs in the system, which are not present in every EPS busbar, and ANNs. The simulation results show the accuracy of the method, even with completely new data, which is the case possible during the operation of the EPS. The use of ANNs can be a response to all the disadvantages of current methods for fault location estimation, since the developed algorithm is noise-resistant and robust. This is primarily reflected in good behavior during various voltage and currents distortions that occur during the faults. The proposed method, together with existing PQMs, presents an upgrade to the existing equipment in the EPS that can bring large benefits, with a small initial investment.

The proposed algorithm is not immune to topology changes during the switching states in the EPS, but these changes are rare in HV EPS, and this problem can be solved by training the ANN to additional possible switching states. The possible long learning and training process of an ANN doesn't present a problem, since once created ANN has instant response.

The algorithm presents a promising solution when it comes to future heuristic power system protection devices, especially with the rising presence of PQMs in EPS. This study is a part of an ongoing research whose objective is to contribute to the development of a new fault location device that has satisfactory accuracy for fault location. An important future research direction in this area should extend the number of system elements and scenarios that can lead to the false fault location.

References

[1] T. Hubana, M. Saric and S. Avdakovic. "Approach for identification and classification of HIFs in medium voltage distribution networks." *IET Generation, Transmission & Distribution*, vol. 12, pp. 1145-1152, March 2018

[2] M. J. B. Reddy, D. V. Rajesh, P. Gopakumar and D. K. Mohanta. "Smart Fault Location for Smart Grid Operation Using RTUs and Computational Intelligence Techniques." *IEEE Systems Journal*, vol. 8, no. 4, pp. 1260-1271, Dec. 2014.

[3] D. D. Sabin, A. R. Dettloff and P. Golden. "Automatic Subtransmission Fault Location System using Power Quality Monitors." in *2016 IEEE/PES Transmission and Distribution Conference and Exposition (T&D)*, 2016, pp. 1-5

[4] K. Chen, C. Huang and J. He. "Fault detection, classification and location for transmission lines and distribution systems: a review on the methods." *High Voltage*, vol. 1, no. 1, pp. 25-33, April 2016.

[5] V. Stanojevic, G. Preston and V. Terzija. "Synchronised Measurements Based Algorithm for Long Transmission Line Fault Analysis." *IEEE Transactions on Smart Grid*, vol. PP, no. 99, pp. 1-1.

[6] A. Shaik and A. S. Reddy. "Combined classification of Power Quality Disturbances and Power System Faults." *2016 International Conference on Electrical, Electronics, and Optimization Techniques (ICEEOT), Chennai*, 2016, pp. 3796-3799.

[7] K. Yingkayun, S. Premrudeepreechacharn and K. Oranpiroj. "A power quality monitoring system for real-time fault detection." *2009 IEEE International Symposium on Industrial Electronics, Seoul*, 2009, pp. 1846-1851.

[8] B. Rathore and A. G. Shaik. "Fault detection and classification on transmission line using wavelet based alienation algorithm." *2015 IEEE Innovative Smart Grid Technologies - Asia (ISGT ASIA), Bangkok*, 2015, pp. 1-6.

[9] P. Hosein, S. Hosein and S. Bahadoorsingh. "Power grid fault detection using an AMR network." *2015 IEEE Innovative Smart Grid Technologies - Asia (ISGT ASIA), Bangkok*, 2015, pp. 1-5.

[10] M. Farajollahi, A. Shahsavari and H. Mohsenian-Rad. "Location identification of high impedance faults using synchronized harmonic phasors." *2017 IEEE Power & Energy Society Innovative Smart Grid Technologies Conference (ISGT), Washington, DC*, 2017, pp. 1-5

[11] A. Öner and M. Göl. "Fault location based on state estimation in PMU observable systems." *2016 IEEE Power & Energy Society Innovative Smart Grid Technologies Conference (ISGT), Minneapolis*, 2016, pp. 1-5.

[12] P. Y. Lin, T. C. Lin and C. W. Liu. "An intranet-based transmission grid fault location platform using synchronized IED data for the Taiwan power system." *2013 IEEE PES Innovative Smart Grid Technologies Conference (ISGT), Washington, DC*, 2013, pp. 1-6.

[13] R. Shilpa , S. S. Prabhu and P. S. Puttaswamy. "Power quality disturbances monitoring using Hilbert-Huang transform and SVM classifier." *2015 International Conference on Emerging Research in Electronics, Computer Science and Technology (ICERECT), Mandya*, 2015, pp. 6-10.

[14] A. L. da Silva Pessoa and M. Oleskovicz. "Fault location in radial distribution systems based on decision trees and optimized allocation of power quality meters." *2017 IEEE Manchester PowerTech, Manchester*, 2017, pp. 1-6.

[15] A. A. P. Bíscaro, R. A. F. Pereira, M. Kezunovic and J. R. S. Mantovani, "Integrated Fault Location and Power-Quality Analysis in Electric Power Distribution Systems," *IEEE Transactions on Power Delivery*, vol. 31, no. 2, pp. 428-436, April 2016.

[16] V. Bečirović. "Voltage Conditions Estimation Model in Frequency Domain in Part of Power System Transmission Network Without Power Quality Monitoring." PhD thesis, University of Zagreb, Faculty of Electrical Engineering and Computing, Croatia, 2017.

[17] R. Stiegler, J. Meyer, M. Elst, E. Sperling. "Accuracy of harmonic voltage measurements in the frequency range up to 5 khz using conventional instrument transformers." *21st International Conference on Electricity Distribution (CIRED)*, 2011.

[18] J. Meyer, P. Ribeiro, G. Paulillo, F. Zavoda, J.R. Gordon, J. Milanovic. "Eficient implementation of power quality monitoring campaigns.", *Europe*, vol. 40, no. 66, pp. 6-10.

[19] T. Pfajfar, J. Meyer, P. Schegner and I. Papic. "Influence of instrument transformers on harmonic distortion assessment." *2012 IEEE Power and Energy Society General Meeting*, July 2012, pp. 1-6.

[20] J. V. Milanovic, M. Bollen, N. Cukalevski. "Guidelines for monitoring power quality in contemporary and future power networks - results from cigre/cired jwg c4.112.", *CIGRE Sessions: 27/08/2014-30/08/2014. CIGRE*, 2014, pp. 1-8,

[21] M. Jamil, S. K. Sharma and R. Singh. "Fault detection and classification in electrical power transmission system using artificial neural network." *SpringerPlus*, no. 4:334, 2015.

[22] L. Teklić, B. Filipović - Grčić and I. Pavičić. "Artificial Neural Network Approach for Locating Faults in Power Transmission System." *EuroCon 2013, Zagreb*, Croatia, 2013.

[23] MathWorks, "Documentation" Internet: https://www.mathworks.com/help/physmod/sps/powersys/ref/threephasepisectionline.html [Dec, 13, 2017].

[24] International Electrotechnical Commission (IEC). "IEC 61000-4-7: Electromagnetic Compatibility (EMC) Part 4-7: Testing and Measurement Techniques - General Guide on Harmonics and Interharmonics Measurements and Instrumentation, for Power Supply Systems and Equipment Connected There

ELEKTROTEHNIŠKI VESTNIK 85(3): 109-114, 2018
ORIGINAL SCIENTIFIC PAPER

High-impedance fault identification and classification using a discrete wavelet transform and artificial neural networks

Tarik Hubana, Mirza Šarić and Samir Avdaković

Public Enterprise Elektroprivreda BiH
E-mail: t.hubana@epbih.ba

Abstract. Identification and classification of high-impedance faults (HIFs) in electric-power distribution systems (EPDSs) represent some of the most significant challenges faced by the distribution system operators (DSOs). The recent advances in signal processing and changes in the EPDS regulatory framework have prompted acceleration in the development of advanced methods used for fault identification and classification in EPDS. The paper presents a method for identification and classification of HIFs in medium-voltage (MV) EPDSs, based on the Discrete Wavelet Transform and Artificial Neural Networks. The method was tested on generated signals based on a real EPDS and it was demonstrated that it is capable to accurately detect and classify HIFs in EPDS. The paper contributes to the existing research by developing and testing, on a real EPDS, a HIF-identification and classification method which offers a better performance compared to the currently installed protection devices.

Keywords: Distribution system, faults, neural network, protection, wavelet transform

Identifikacija in klasifikacija visokoohmskih okvar z uporabo diskretne valjčne transformacije in nevronskih mrež

Identifikacija in klasifikacija visokoohmskih okvar v elektrodistribucijskih sistemih je pomemben izziv za operaterje elektroenergetskih omrežij. Napredek na področju obdelave signalov in spremembe pri regulativi elektrodistribucijskih omrežij so spodbudili razvoj naprednih metod za identifikacijo in klasifikacijo napak v elektroenergetskih omrežjih. V prispevku je predstavljena metoda za identifikacijo in klasifikacijo visokoohmskih okvar v srednjenapetostnem distribucijskem omrežju. Metoda temelji na uporabi diskretne valjčne transformacije in nevronskih mrež. Metodo smo preverili s signali na osnovi resničnih elektroenergetskih omrežij. Eksperimentalni rezultati potrjujejo, da lahko s predlagano metodo natančno in učinkovito ugotovimo visokoohmsko okvaro v elektrodistribucijskem omrežju.

1 INTRODUCTION

In the recent years, there have been historical changes in the power-system structure, organisation and management, driven by the process of market liberation and energy transition from the conventional to the renewable energy generation paradigm. As a consequence, the management and operation of the electric-power distribution systems (EPDS) have also changed. Distribution system operators (DSOs) are constantly scrutinised by regulators and customers in terms of service reliability and quality parameters [1]. Two of the major practical challenges faced by DSO are power-system fault detection and classification. In particular, fault detection and classification are very important for DSO in order to take appropriate actions and ensure that the system continues to operate safely and efficiently.

Unfortunately, many faults remain undetected due to complex physical properties of the voltage and current waveforms and lack of appropriate detection technologies which are capable to provide fast and accurate fault classification. This is particularly true in the case of high-impedance faults (HIFs), which present a special challenge. In the past, there has been an increase in the number of reported fault-detection methods, but an ideal detection and classification are still an open question and continue to be a subject of scholar efforts [2], [3]. Therefore, HIFs present a serious problem since they cannot be easily detected. For these reasons, there is a need for an ongoing investigation of new methods for the EPDS fault identification and classification, which makes this topic a vibrant research area.

The paper contributes to these efforts by presenting a new method for identification and classification of HIFs in medium-voltage (MV) EPDS based on a combination of Discrete Wavelet Transform (DWT) and Artificial Neural Networks (ANNs). The aim of the paper is to experimentally verify the new method which represents an improvement compared to operational capabilities of the protection systems currently deployed in EPDS. The method is expected to solve one of the major operational challenges faced by DSO. The paper is a part of an ongoing research into advanced power-system

Received 24 November 2017
Accepted 4 April 2018

protection, with a particular focus on HIF detection in EPDS ([1], [3] and [4]).

2 LITERATURE REVIEW

The EPDS faults can be broadly classified in two categories, based on the fault resistance. The resistances in the first category are mostly below a few hundreds of Ohms. In order to clear this type of faults, it is necessary to isolate the faulted section of the system and to trip the circuit-breaker. For this type of faults, the distance protection scheme is feasible. The resistances in the second category are very high the neutral potential is very low [4].

HIFs can generally be defined as faults with current values in the range from 0 to 75 A in an effectively grounded EPDS [5]. Their detection and classification continue to be a major challenge for DSO and is becoming even more difficult with the increase in the EPDS complexity. The existing EPDS protection systems are not completely adequate for HIF detection due to various issues such as sensitivity, selectivity and diversity [6]. The harmonic component in the zero-sequence current has been typically used in the existing detection methods [5]. Nowadays, the research into HIF detection continues to attract new interests [7], [5] and [8].

In particular, the combination of DWT and ANN appears to be a promising approach for HIF detection, because the wavelet transform (WT), which maps the time-domain signals into the time-scale domain, is capable to describe both the frequency information and the location of the frequency components. This unique feature of WT makes it a very popular method for HIF detection [8]. Further, ANNs have been tested in various engineering applications and are regarded as a fast and accurate method for classification with powerful prediction capabilities. For these reasons, DWT and ANNs are often used together in HIF identification and classification applications [8] and [9]. In conclusion, HIF identification and classification continue to be a relevant research topic and a combination of DWT and ANNs is a promising approach to an improvement of the existing EPDS protection systems.

3 THEORETICAL BASICS

WT is used in numerous engineering applications. It is regarded as a mathematical tool which has numerous advantages when compared with traditional methods in a stochastic signal-processing application, mainly because waveform analysis is performed in a time scale region [10]. WT of a signal $f(t) \in L^2(R)$, where L^2 is the Lebesgue vector space, is defined by the inner-product between $\Psi_{ab}(t)$ and $f(t)$ as [10]:

$$WT(f,a,b) = \frac{1}{\sqrt{a}} \int_{-\infty}^{+\infty} f(t)\, \Psi\left(\frac{t-b}{a}\right) dt \qquad (1)$$

where a and b are the scaling (dilation) and translation (time shift) constants, respectively, and Ψ is the wavelet function which may not be real as assumed in the above equation for simplicity [10]. The Wavelet transform of the sampled waveforms is obtained by implementing DWT given by [10]:

$$DWT(f,m,n) = \frac{1}{\sqrt{a_0^m}} \sum_k f(t)\, \Psi\left(\frac{n - k a_0^m}{a_0^m}\right) \qquad (2)$$

where a and b from equation (1) are replaced by a_0^m and ka_0^m, k and m being integer variables. In a standard DWT, the coefficients are sampled from a continuous WT on a dyadic grid, $a_0 = 2$ and $b_0 = 1$, yielding $a_0^0 = 1$, $a_0^{-1} = 2^{-1}$, etc. [10].

In the Back propagation neural network (BPNN), the output is a feedback to the input to calculate the change in the values of weights [11]. The weights of the back-error-propagation algorithm for the neural network are chosen randomly to prevent a bias toward any particular output. The first step in the BPNN algorithm is a forward propagation [11]:

$$a_j = \sum_i^m w_{ji}^{(1)} x_i \qquad (3)$$

$$z_j = f(a_j) \qquad (4)$$

$$y_j = \sum_i^M w_{kj}^{(2)} z_j \qquad (5)$$

where a_j represents the weighted sum of the inputs, w_{ij} is the weight associated with the connection, x_i are the inputs, z_j is the activation unit of (input) that sends a connection to unit j and y_i is the i-th output.

The second step is calculation of the output difference [11]:

$$\delta_k = y_k - t_k \qquad (6)$$

where δ_k represents the derivative of the error at a k-th neuron, y_k is the activation output of unit k and t_k is the corresponding target of the input.

The next step is back propagation for hidden layers [11]:

$$\delta_j = (1 - z_j^2) \sum_{k=1}^{K} w_{kj} \delta_k \qquad (7)$$

where δ_j is the derivative of error w_{kj} to a_j.

Afterwards, the gradient of the error with respect to the first- and the second-layer weights is calculated, and the previous weights are updated. MSE for each output in each iteration is calculated by [11]:

$$MSE = \frac{1}{N}\sum_{1}^{N}(E_i - E_o)^2 \tag{8}$$

where N is number of iterations, E_i is the actual output and E_o is the output of the model.

After each step, the weights are updated with the new ones and the process is repeated for the entire set of input-output combinations available in the training-data set, and this process is repeated until the network converges for the given values of the targets for a predefined value of the error tolerance [11].

4 Results, Discussion and Future Work

This section of the paper presents results of the proposed algorithm application to the problem of HIF identification and classification in MV EPDS. In order to demonstrate the practical relevance of the proposed algorithm, it is applied to a real 10 kV MV EPDS currently used in Bosnia and Herzegovina. First the EPDS test system is described, followed by an outline of the computational procedure. Next, results of the proposed method are presented and discussed. Finally, the future research directions are given.

4.1 The test system

As the MV and low-voltage (LV) distribution systems mostly operate as radial systems, the proposed algorithm is tested in a radial EPDS.

The test system developed for the purpose of algorithm testing represents a part of a real MV distribution system operating in the area of the City of Mostar (Bosnia and Herzegovina) which is similar to typical distribution systems used throughout Europe.

The MV customers are supplied from a 35/10 kV main transformer via 10 kV feeders. The LV customers are supplied via 10/0.4 kV substations. The test 10 kV network supplies electricity in an urban area and mostly consists of underground cables. Detailed test system parameters are given in Table 1.

Table 1. Power-system parameters.

Component	Parameters
System voltages	V_{MV1} = 35 kV, V_{MV2}=10 kV, V_{LV}=0.4 kV f = 50 Hz
Transmission lines	$length_{L1}$= 5.87 km, $length_{L2}$= 0.95 km, $length_{L3}$= 4.47 km, $length_{L4}$= 1.47 km, $length_{L5}$= 5.34 km, $length_{L6}$= 6.63 km, $length_{L7}$= 3.11 km Z_{L1}= Z_{L2}= Z_{L3}= Z_{L4}= Z_{L5}= Z_{L6}= Z_{L7} R_1= 0.206 Ω/km, R_0= 0.96 Ω/km L_1= 0.359x10^{-3} H/km, L_0= 1.178x10^{-3} H/km C_1= 0.254x10^{-6} F/km, C_0= 0.118x10^{-6} F/km
Transformers 35/10 kV	P_n=8 MVA, R_1=0.0802 Ω, L_1=4.028x10^{-4} H, R_2=19.64x10^{-3} Ω, L_2=9.866x10^{-5} H
Transformers 10/0.4 kV	P_n=630 kVA, R_1=0.2495 Ω, L_1=4.873x10^{-5} H, R_2=1.33x10^{-4} Ω, L_2=2.598x10^{-8} H

The simulation model is developed in MATLAB/Simulink software and presents a three-phase model of the part of the Mostar EPDS fed from two parallel 35/10 kV transformers. A schematic representation of the test system is shown in Fig. 1.

The faults and measurements are performed on a 10 kV underground cable that feeds the entire consumption area. Faults are simulated for different fault resistances (in the range from 20 Ω to 600 Ω) and at different fault locations. The simulated faults are phase A to the ground fault (AG), phase A to phase B to the ground fault (ABG) and phase A to phase B to phase C to the ground fault (ABCG).

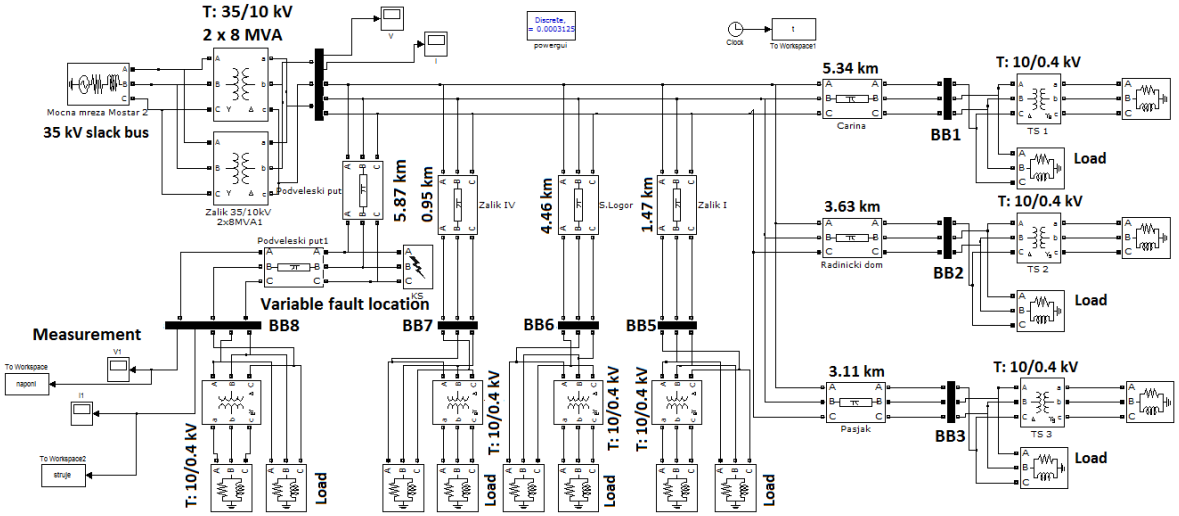

Figure 1. Test system developed in MATLAB/Simulink

The sampling frequency of the current protection relays and measuring equipment in the Bosnia and Herzegovina EPDS is 3.2 kHz. Since the existing equipment already operates with this sampling frequency, a logical upgrade would be to use this equipment coupled with the proposed algorithm. This fact is the reason for using the chosen sampling frequency.

For the proposed DWT-ANN algorithm, the condition with no fault and the conditions with three types of the fault are simulated for various resistance values and fault locations, giving a total of 1600 fault scenarios.

4.2 Computational procedure

The proposed method for fault identification and classification is based on a combination of DWT and ANN. It does not require current measurements and coefficient calculations because it performs with details and approximation waveforms rather than with calculated coefficients. The simulation model considers the fault resistance values for the unearthed MV network, based on [4].

After simulating all the possible fault scenarios, for each fault and different values of the fault location and resistance, the voltage waveforms are generated. The fault is simulated during the entire simulation interval, i.e. (0 – 0.08 s). When the voltage waveforms are generated, DWT is applied to these waveforms. A Daubechies 4 wavelet is used at a 3.2 kHz voltage signal, therefore one approximation and four details are obtained for each voltage. Four levels of decomposition are used in this paper in order to get the following frequency bands:

- First detail level - frequency band: [800, 1600] Hz,
- Second detail level - frequency band: [400, 800] Hz,
- Third detail level- frequency band: [200, 400] Hz,
- Fourth detail level - frequency band: [100, 200] Hz,
- Fourth approximation level - frequency band: [50, 100] Hz

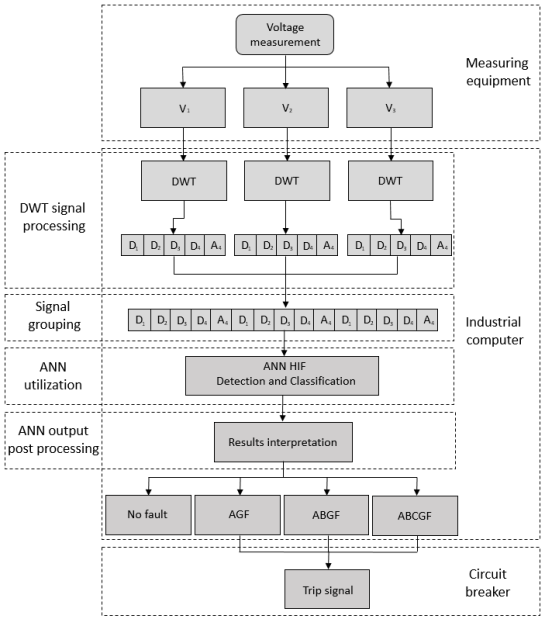

Figure 2. Algorithm of the proposed method.

The A4 waveform is a base sinusoidal wave and reflects the signal behaviour during each fault. The rest of the DWT waveforms are higher harmonic components of the voltage signal, and therefore they reflect a distinctive voltage behaviour during each fault type.

The algorithm is also tested by the Symlet 4 and Biorthogonal 4.4 wavelet families, and the output results are similar or the same. Therefore, it is not necessary to be particularly cautious regarding the choice of the wavelet family. The DWT signal components give a good insight into the system behaviour during fault conditions. For this reason, they are used as representative signals for each fault type. Afterwards, these DWT signals are combined and grouped and represent a unique „signature“ for each fault, which represents the input to ANN. After that, ANN is trained with a large set of this data, thus becoming capable to detect and identify the EPDS faults.

The ANN output consists of a set of the values that are not discrete, do not indicate an exact fault type, and do not represent a fault possibility. By adding a modification to interpret results, it is possible to convert these outputs to 0% and 100% (probability of the absence and presence of each fault). The block *Results interpretation* in Fig. 2 simply finds the highest value for the each ANN output scenario and sets it to 100%, while setting all other outputs to 0%. With this modification it is possible to get an unambiguous fault type as the algorithm output.

Once trained, ANN is capable of fault detection and classification, according to the algorithm shown in Fig. 2. With the measuring equipment installed in EPDS, the voltage waveforms can be measured and sent to an installed industrial computer with a DWT-ANN algorithm software. In the case of a fault detection, an appropriate trip signal, depending on the fault type, can be sent to the circuit breaker.

4.3 Results

In order to use the proposed algorithm in a real PDS, ANN needs to be trained to all the possible scenarios in EPDS. Since the algorithm is planned to be used in the online mode to constantly monitor the system voltages, it can constantly improve and learn new possible EPDS operating scenarios.

For the beginning, the input data for ANN need to be created. In order to get a unique EPDS signature for every fault type, a signal that reflects this state needs to be created. For this purpose, 1600 simulations for three types of the fault and normal operating conditions, with various fault resistances and fault locations, are carried out. For each fault scenario, each phase voltage is measured and transformed with DWT. By combining the DWT signals of all phase voltages for each fault scenario,

a group signal that reflects the system behaviour during each fault is created, as shown in Fig. 2.

Grouped DWT signal is a signal that is built simply by adding the start of the next signal to the end of the previous signal using the details and approximation waveforms for each fault scenario in the system, i.e. this signal is composed from the DWT waveforms of the currently measured voltage signal. A grouped signal for 400 simulations for each fault type is shown in Fig. 4.

The differences between the created signals for a particular fault type are apparently negligible, but ANN is capable to classify them correctly. Higher harmonic components, which are important for the identification process, can be efficiently identified in the DWT filters of the corresponding frequency range. Generally, DWT is widely used for the noise-removal applications [12], [13]. Moreover, since the proposed algorithm is paired with ANNs, which are known to have a high accuracy in the pattern classification and noise removal ability, this issue is addressed even more effectively [7].

After this unique signal for each fault scenario is created, the input set of data for ANN training is ready. Designed ANN takes the input set of 1600 input vectors and 1600 corresponding outputs during a training process. After that, trained ANN has four possible outputs, where each output notes the normal operating condition and three types of PDS faults. It is important to note that the ANN outputs are numerical values, that don't clearly detect or classify the PDS faults.

Because of that, a modification to the ANN output will be introduced. This modification will take the ANN output vector and set the highest value to 100%, and all other output values to 0%. This will result in an unambiguous output that clearly notes the presence of a fault and identifies the fault type. The proposed DWT - ANN algorithm is capable to accurately detect the fault and distinguish between the three possible categories of faults, regardless of the fault-resistance value and fault location. After the training and testing process, the created ANN is perfectly capable to classify faults in the EPDS.

In order to get a good insight into the algorithm efficiency, it is necessary to test it with new fault scenarios with new resistance values and different fault locations, i.e. fault scenarios that ANN is not trained to. For this purpose, new simulations with new parameters are carried out. Table 2 shows classifier results to this

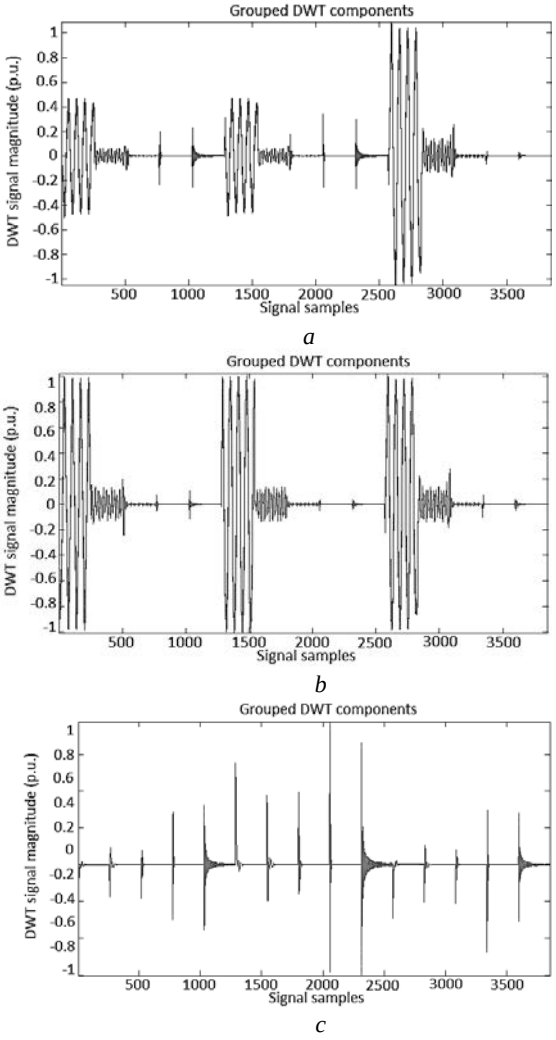

Figure 4. Grouped DWT component signals:
(a) AG HIF fault, (b) ABG HIF fault, (c) ABCG HIF fault

fault scenarios, where column *Desired output* presents a simulated-fault type and column *Actual output* an evaluated fault type. The 0% or 100% values present the absence or presence of a specific fault. Column *Actual output* presents the ANN output for each fault scenario. The proposed DWT – ANN algorithm has a 100% accuracy in the range of 20 – 600 Ω for all fault locations.

The proposed algorithm is planned to be used in the online mode. The storage method is important since the grouped DWT components take a lot of storage. A present-day industrial computer with a somewhat larger

Table 2. Output of the DWT-ANN classifier for different fault resistances, fault locations and fault types.

Resistance (Ω)	Fault location (% length)	Desired output (probability in %)				Actual output (probability in %)			
		AGF	ABGF	ABCGF	No fault	AGF	ABGF	ABCGF	No fault
20	0.01	100	0	0	0	100	0	0	0
110	0.16	0	0	0	100	0	0	0	100
200	0.31	0	100	0	0	0	100	0	0
290	0.46	0	0	100	0	0	0	100	0
380	0.61	100	0	0	0	100	0	0	0
470	0.76	0	100	0	0	0	100	0	0
560	0.91	0	0	0	100	0	0	0	100

hard drive will be enough for online monitoring. Few minutes old data can be deleted if no disturbances are recorded. However, voltage waveforms can be saved for a later analysis. The ANN output modification contributes to the algorithm speed since the ANN output matrix now consists of zeros and ones, and hence does not consume much space and makes the matrix easier to operate with.

4.4 Future research directions

The list of the EPDS fault types is not exhausted by the faults included in this paper. However, this algorithm is applicable to new scenarios since it can be easily extended by an additional training of ANN. The proposed algorithm has a potential practical application in terms of its implementation on the EPDS protection-system devices. In order to achieve that, the algorithm robustness improvement is an important part of the future research in this area. Further, an extension in the number of the system components and scenarios that can lead to a false tripping signal should be considered. Finally, an agent-based modelling of complex systems is proposed as an interesting future direction in this area.

5 CONCLUSION

EPDS faults are undesirable events and remain a serious challenge for DSO. In particular, HIF identification and classification present a particularly complex task due to physical characteristics of HIF and shortcomings of the existing protection devices. For these reasons, this topic remains an open research area. The paper proposes a method to improve the existing algorithms for identification and classification of HIFs in MV EPDS, based on DWT and ANN. This study is a part of an ongoing research into advanced power-system protection algorithms concerned mainly with the HIF identification and classification. The proposed method has a practical significance since, as demonstrated, it can be applied to a real EPDS and it accurately identifies and classifies faults in the 20 – 600 Ω range of the fault resistance for various fault locations. The proposed algorithm is believed to be a promising approach to the future implementation of the power-system protection devices.

REFERENCES

[1] T. Hubana, E. Begic and M. Saric, "Voltage Sag Propagation Caused by Faults in Medium Voltage Distribution Network," in *Advanced Technologies, Systems, and Applications II*, Springer International Publishing, Online ISBN: 978-3-319-71321-2, 2018, In press.

[2] I. Baqui, I. Zamora, J. Mazon and G. Buigues, "High-impedance fault detection methodology using wavelet transform and artificial neural networks," *Electric Power Systems Research*, no. 81, pp. 1325-1333, 2011.

[3] M. Saric, T. Hubana and E. Begic, "Fuzzy Logic Based Approach for Faults Identification and Classification in Medium Voltage Isolated Distribution Network," in *Advanced Technologies, Systems, and Applications II*, Springer International Publishing, Online ISBN: 978-3-319-71321-2, 2018, In press.

[4] S. Hanninen, Single phase earth faults in high-impedance grounded networks, Espoo: Technical Research Centre of Finland, VTT Publications , 2001.

[5] B. Wang, J. Geng and X. Dong, "High-Impedance Fault Detection Based on Non-linear Voltage-Current Characteristic Profile Identification," *IEEE Transactions on Smart Grid*, no. 99, 2017.

[6] K. Chen, C. Huang and J. He, "Fault detection, classification and location for transmission lines and distribution systems: a review on the methods," *High Voltage*, vol. 1, no. 1, pp. 25-33, 2016.

[7] T. Hubana, M. Saric and S. Avdakovic, "New approach for Identification and Classification of High-impedance Faults in MV Distribution Networks," *IET Generation, Transmission & Distribution*, DOI: 10.1049/iet-gtd.2017.0883 , Online ISSN 1751-8695, In press, available online: 06 November 2017.

[8] A. Ghaderi, H. L. Ginn III and H. A. Mohammadpour, "High-impedance fault detection: A review," *Electric Power Systems Research*, pp. 376-388, 2017.

[9] H. Laaksonen and P. Hovila, "Straightforward Detection Method for High-Impedance Faults," *International Review of Electrical Engineering*, vol. 12, no. 2, 2017.

[10] M. Choudhury and A. Ganguly, "Transmission line fault classification using discrete wavelet transform," in *International Conference on Energy, Power and Environment: Towards Sustainable Growth (ICEPE)*, Shilong, 2015.

[11] M. Jamil, S. K. Sharma and R. Singh, "Fault detection and classification in electrical power transmission system using artificial neural network," *SpringerPlus*, no. 4:334, 2015.

[12] R. K. Sarawale and S. R. Chougule, "Noise removal using double-density dual-tree complex DWT," in *2013 IEEE Second International Conference on Image Information Processing (ICIIP-2013)*, Shimla, 2013.

[13] A. R. Haider Mohamad, C. P. Diduch, Y. Biletskiy, R. Shao and L. Chang, "Removal of measurement noise spikes in grid-connected power converters," in *2013 4th IEEE International Symposium on Power Electronics for Distributed Generation Systems (PEDG)*, Shimla, 2013.

Tarik Hubana received his B.Sc. and M.Sc. degrees in electrical engineering from the Faculty of Electrical Engineering, University of Sarajevo, Bosnia and Herzegovina, in 2013 and 2015, respectively. He is currently employed with the Public Power Utility Elektroprivreda B&H, DSO Mostar. His areas of interest are power system analysis, power quality, power-system protection and distributed generation.

Mirza Šarić graduated with honours in the field of Electrical & Computer Systems Engineering at the Monash University, Australia. He holds an MA degree from the School of Economics, University of Sarajevo. He is currently with the Public Power Utility Elektroprivreda B&H, DSO Mostar. His research interests include power distribution system planning and operation, distributed generation and power-system economics.

Samir Avdaković received his Ph.D. degree in electrical engineering from the Faculty of Electrical Engineering, University of Tuzla, Bosnia and Herzegovina, in 2012. He works at the Department of strategic development at the Public Power Utility Elektroprivreda B&H. His research interests are in power-system analysis, power-system dynamics and stability, WAMPCS and signal processing.

IET Generation, Transmission & Distribution

Research Article

IET Journals
The Institution of Engineering and Technology

Approach for identification and classification of HIFs in medium voltage distribution networks

ISSN 1751-8687
Received on 5th June 2017
Revised 27th September 2017
Accepted on 3rd November 2017
E-First on 19th January 2018
doi: 10.1049/iet-gtd.2017.0883
www.ietdl.org

Tarik Hubana[1] ✉, *Mirza Saric*[1], *Samir Avdaković*[2]

[1]*Distribution System Operator Mostar, Public Enterprise Elektroprivreda of Bosnia and Herzegovina, Mostar, Bosnia and Herzegovina*
[2]*Sector for strategic development, Public Enterprise Elektroprivreda of Bosnia and Herzegovina, Sarajevo, Bosnia and Herzegovina*
✉ *E-mail: t.hubana@epbih.ba*

Abstract: The modern power system operation is faced with numerous challenges related to the power quality improvements such as identification and classification of power distribution network (PDN) faults. The recent advances in the area of signal processing allow the development of new algorithms and methods which can be used for fault identification and classification in PDN. This study presents a comparison of two approaches for identification and classification of high-impedance faults (HIFs) in medium-voltage PDN. The first approach is based on the voltage phase difference algorithm, whereas the second approach is based on the combination of discrete wavelet transform and artificial neural networks algorithm. The proposed algorithms are tested on models of a real distribution network, which represents a typical PDN currently used in Bosnia and Herzegovina. It was demonstrated that the proposed methods are capable to accurately detect and classify HIF in PDN. This study makes a contribution to the existing body of knowledge by developing, testing and comparing two methods for HIF classification and identification, whose application represents an improvement when compared with the capability of the existing protection devices.

1 Introduction

The power system is commonly regarded as one of the most complex engineering systems. Management and operation of the power systems have changed dramatically in recent years due to technological advancements and new regulatory requirements. The introduction of smart grid technologies provides a number of advantages both to end customers and the system operator. However, a number of challenges remain yet to be solved. One such challenge is power system fault detection and classification.

Recently, system operators are under the increasing amount of pressure exerted by customers and regulators to improve the power quality and reliability levels. The power system faults are particularly unwelcome events because, apart from causing the system interruption, they create numerous technical issues such as voltage sag propagation [1]. For these reasons, it is expected that faults on the power system lines are detected, classified and cleared by the protection settings as fast as possible [2]. This means that new methods for power system fault detection and classification are constantly developed. Many of the advances in this field are owned to the progress in signal processing techniques, artificial intelligence [3] and machine learning, global positioning system and communications [4], because they allow the development of new algorithms and methods which can be used for fault identification and classification in power distribution networks (PDNs) such as discrete wavelet transform (DWT), artificial neural networks (ANNs), Hilbert–Huang transform.

High-impedance faults (HIFs) are defined as faults with current values in the range from 0 to 75 A in effectively grounded distribution systems [5] and present the greatest challenge for the PDN operator in terms of fault detection and classification. HIF occurs when there is a contact of an energised conductor with a high-impedance surfaces such as dry ground, concrete, gravel, high resistance soils and asphalt road or when a live conductor makes a contact with grounded objects such as tree limbs [6]. These situations are particularly hazardous and might lead to serious dangers such as electric shock or/and fire [7]. With the increase in PDN complexity, a reliable HIF detection becomes an even more important concern for utilities [8]. HIF detection has been extensively researched for more than 30 years with harmonic component in zero-sequence current, typically used in detection algorithms, because waveform distortion is often produced by arc flash [5]. The conventional protection relays such as distance protection, overcurrent and ground fault relays are not entirely adequate for HIF detection due to the sensitivity, diversity and selectivity issues related to the low value of fault current [9]. Although many detection methods have been developed, an ideal detection and classification method is still the object of scholar efforts [6] which makes this topic a vibrant area of research.

Every method for fault detection and classification has its own advantages and disadvantages. In this paper, it is proposed that a combination of the best features of each method has a potential to achieve more accurate results. For example, considering the disadvantage of using DWT or ANN separately, the combination of the two methods is proposed as an improved approach for HIF detection in distribution power systems [10].

In particular, this paper presents a comparison of two approaches for identification and classification of HIFs in medium-voltage distribution networks. The first approach is based on the voltage phase difference (VPD algorithm), whereas the second approach is based on the combination of DWT and ANNs (DWT–ANN algorithm). Test systems developed in MATLAB/Simulink represent models of a real medium PDN in the area of the City of Mostar (Bosnia and Herzegovina).

2 Literature review

There has been a steady increase of the use of heuristic HIF detection methods over the past decade, with a ratio of classic to heuristic methods being ~50:50 [11]. This demonstrates the importance of the application of heuristic methods in HIF detection, which attract some of the most recent research efforts in this area. Some of the most recent research results in the area of fault identification and classification are presented in [7, 11, 12]. One of the most promising methods is the combination of DWT and ANNs. Time-scale analysis, also known as WT, maps the time-domain signals into time-scale domain. It catches both the frequency information and the instant (location) in a time, where these frequency components occur. This capability makes the wavelet-based methods powerful tools for analysing signals with

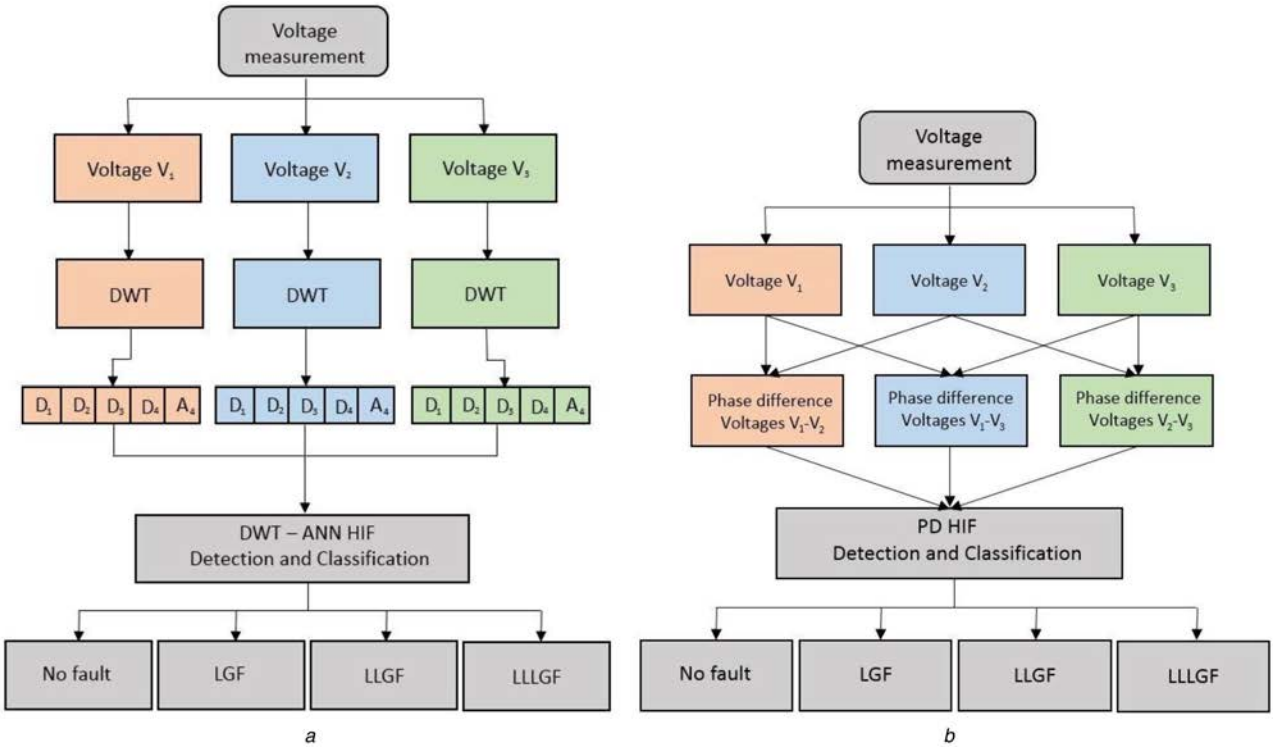

Fig. 1 *Algorithms of the proposed methods*
(a) DWT and ANN classifiers, ***(b)*** VPD classifier

time-varying spectrum such as HIF voltage and current [13]. Therefore, this unique feature of WT in HIF detection results in the increase of its popularity (about 40% of all the HIF detection techniques have been wavelet based) [7].

ANNs are known to have high accuracy in pattern classification and generalisation, fast response, noise removal ability and prediction capability. About 23% of HIF detection techniques utilise some topologies of ANN. Despite their apparent advantages, the ANN contributes significantly to the overall complexity of the fault identification and classification systems. Moreover, choosing the number of layers and number of perceptrons in each layer is the trial-and-error procedures which decrease the objectivity of the ANN-based techniques [7].

The combination of WT and ANN appears to be an acceptable approach for solving the HIF detection problem, as shown in [6, 14–16], where DWT was used as a pre-processing stage for feature extraction and then used as an input to ANN stage [11].

DWTs were initially utilised to extract distinctive features of the voltage and current signals and were transformed into a series of detailed and approximated wavelet components as shown in [10, 13, 16]. This information is used as an input to ANN to verify in order to identify and classify PDN HIF [11, 17]. It was demonstrated that only three levels of decompositions of the voltage signal were required for classification of faults [12]. The proposed system was verified with various types of faults including the symmetrical and asymmetrical faults for different locations and resistances. High-speed and accurate fault classification techniques for new feature selection of WT and probabilistic NN are presented in [12]. The coefficients calculated from the DWT details and approximations of voltages and currents are also used in [10, 13, 16]. In conclusion, the accumulated body of evidence suggests that PDN fault identification and classification continue to be an important area of research in which various advanced methods and models are constantly developed.

3 Proposed methods algorithms

The first algorithm proposed in this paper is based on DWT paired with ANN, whereas the second is based on the VPD as shown in Figs. 1*a* and *b*, respectively. The algorithms proposed in this paper do not perform with the calculated coefficients, but with the details and approximation waveforms, and thus do not require current measurement and coefficients calculations.

3.1 DWT and ANN approaches

WT is a mathematical method used for many signal processing applications. Wavelets have many advantages over the conventional method in processing the stochastic signal, because of the waveform analysis in time-scale region [18]. The WT of a signal $f(t) \in L^2(R)$, where $\boldsymbol{L}^2$ is Lebesgue vector space, is defined by the inner-product between $\Psi_{ab}(t)$ and $f(t)$ as [18]

$$\mathrm{WT}(f, a, b) = \frac{1}{\sqrt{a}} \int_{-\infty}^{+\infty} f(t) \Psi\left(\frac{t-b}{a}\right) \mathrm{d}t \tag{1}$$

where a and b are the scaling (dilation) and translation (time shift) constants, respectively, and Ψ is the wavelet function which may not be real as assumed in the above equation for simplicity [18]. WT of sampled waveforms can be obtained by implementing the DWT which is given by [18]

$$\mathrm{DWT}(f, m, n) = \frac{1}{\sqrt{a_0^m}} \sum_k f(t) \Psi\left(\frac{n - k a_0^m}{a_0^m}\right) \tag{2}$$

where a and b from (1) are replaced by a_0^m and ka_0^m, k and m being integer variables. In a standard DWT, the coefficients are sampled from the continuous WT on a dyadic grid, $a_0 = 2$ and $b_0 = 1$, yielding $a_0^0 = 1$, $a_0^{-1} = 2^{-1}$ etc. [18].

DWT is applied to the measured voltage signals; therefore, one approximation and four details are obtained for each voltage. Four levels of decompositions are used in this paper in order to get the following frequency bands:

- *First detail level*: Frequency band: [800, 1600] Hz.
- *Second detail level*: Frequency band: [400, 800] Hz.
- *Third detail level*: Frequency band: [200, 400] Hz.
- *Fourth detail level*: Frequency band: [100, 200] Hz.
- *Fourth approximation level*: Frequency band: [50, 100] Hz.

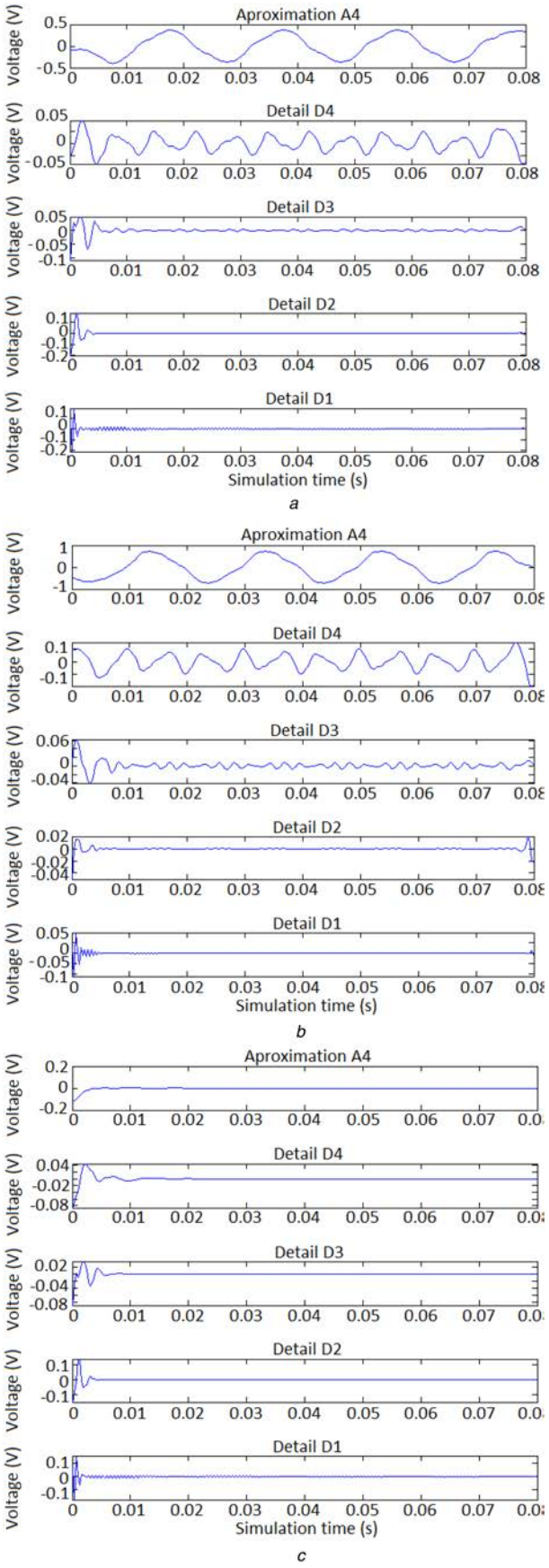

Fig. 2 *DWT of the faulty phase voltage signal*
(a) LG HIF fault, ***(b)*** LLG HIF fault, ***(c)*** LLLG HIF fault

Fig. 2 shows that the A4 waveform is the base sinusoidal wave and reflects the signal behaviour during each fault. The rest of the DWT waveforms are higher-harmonic components of the voltage signal, and therefore reflect the distinctive voltage behaviour during each fault type.

In the back propagation NN (BPNN), the output is the feedback to the input to calculate the change in the values of weights [2]. The weights of the back-error-propagation algorithm for the NN are chosen randomly to prevent a bias toward any particular output. The first step in algorithm of BPNN is forward propagation [2]

$$a_j = \sum_i^m w_{ji}^{(1)} x_i \tag{3}$$

$$z_j = f(a_j) \tag{4}$$

$$y_j = \sum_i^M w_{kj}^{(2)} z_j \tag{5}$$

where a_j represents the weighted sum of inputs, w_{ij} is the weight associated with the connection, x_i are inputs and z_j is the activation unit of input that sends a connection to unit j and y_i ith output.

Second step is calculation of the output difference [2]

$$\delta_k = y_k - t_k \tag{6}$$

where δ_k represents derivative of error at the kth neuron, y_k is the activation output of unit k and t_k is the corresponding target of input.

Next step is BP for hidden layers [2]

$$\delta_j = (1 - z_j^2) \sum_{k=1}^{K} w_{kj} \delta_k \tag{7}$$

where δ_j is the derivative of error w_{kj} to a_j.

Afterwards, the gradients of error with respect to the first-layer weights and the second-layer weights are calculated, and the previous weights are being updated. The mean square error for each output in each iteration is calculated by [2]

$$\text{MSE} = \frac{1}{N} \sum_1^N (E_\text{i} - E_\text{o})^2 \tag{8}$$

where N is number of iterations, E_i is the actual output and E_o is out of the model.

After each step, the weights are updated with the new ones and the process is repeated for entire set of inputs–outputs combinations available in the training data set, and this process is repeated until the network converges for the given values of the targets for a predefined value of error tolerance [2].

In the proposed algorithm, DWT signals are combined and grouped and represent a unique ‘signature’ for each fault. After that, the ANN is trained with a large set of this data, and becomes capable to detect and identify PDN faults. It is important to note that the proposed classifier is fully customisable, very flexible and can be extended to include additional parameters and criteria.

3.2 VPD approach

Hilbert transform has a wide range of applications, but one of its best features is the instantaneous frequency which represents the time rate of change of the instantaneous phase angle. Hilbert transform, $\hat{y}(t)$, which can be written for any function $x(t)$, of L^P class, where $\boldsymbol{L}^P$ is Lebesgue vector space, is [19]

$$H[x(t)] \equiv \hat{y}(t) = \frac{1}{\pi} \text{PV} \int_{-\infty}^{\infty} \frac{x(\tau)}{t - \tau} \, \text{d}\tau \tag{9}$$

where the PV denotes Cauchy's principle value integral.

It is determined that an analytic function can be formed with the Hilbert transform pair as shown in (10) [19]

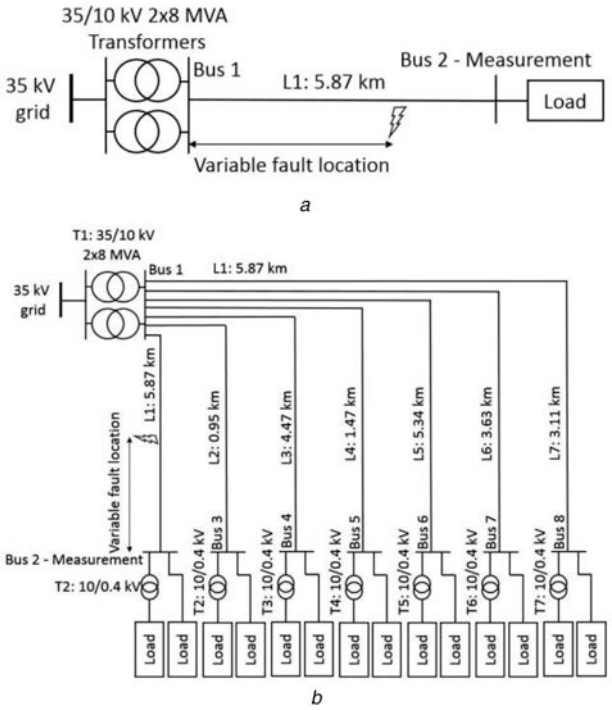

Fig. 3 *Single line diagram of the developed test systems*
(a) 2-Bus test system, ***(b)*** 8-Bus test system

$$z(t) = x(t) + i\hat{y}(t) = A(t)\mathrm{e}^{i\theta(t)} \tag{10}$$

where

$$A(t) = \left(x^2 + \hat{y}^2\right)^{1/2} \quad \theta(t) = \tan^{-1}\left(\frac{\hat{y}}{x}\right) \quad i = \sqrt{-1} \tag{11}$$

where $A(t)$ and $\theta(t)$ are the instantaneous amplitudes and phase functions, respectively [19].

PD is calculated as difference between two instantaneous phases of voltage signal, for example, between voltage V_1 instantaneous phase θ_1 and voltage V_2 instantaneous phase θ_2, as showed in (12)

$$\mathrm{PD}_{12} = (\theta_1 - \theta_2)\frac{180}{\pi} \tag{12}$$

Hilbert transform is used in this paper to obtain the VPD, as shown in (9)–(12). For a pure sinusoid, the instantaneous amplitude and frequency should be constant. However, during the fault conditions this parameter is changed, and represents an appropriate input for fault classification.

4 Experimental setup

There are two major categories of earth faults. In the first category, the fault resistances are mostly below a few hundred ohms and circuit breaker tripping is required. These faults are most often flashovers to the grounded parts of the network [20].

Distance computation is possible for these faults. In case of the second category, the fault resistances are in the order of thousands of ohms. In this case, the neutral potentials are usually so low that continued network operation with a sustained fault is possible [20].

However, HIFs present a serious problem since they cannot be easily detected. Hanninen [20] shows the unearthed medium voltage (MV) network fault resistance distribution during the 2 year measurement. Hence, the simulation model developed in this paper considers the values of fault resistance from the 20 to 600 Ω range.

To compare the two proposed approaches, their performances will be tested in two test systems, developed in MATLAB/Simulink, using the real PDN data.

4.1 Test model

MV and low-voltage (LV) distribution systems mainly operate as radial systems, in opposition to the high-voltage systems that have a meshed topology. For this reason, the proposed algorithms are applicable in a radial PDN.

There are two test systems which are developed for the purpose of algorithm testing and comparison. Both systems represent a part of a real MV distribution system in the area of the City of Mostar (Bosnia and Herzegovina), which is similar to typical distribution systems used throughout the Europe.

The first test system is a simple 2-bus test system which consists of one 10 kV feeder fed by 35/10 kV transformer. This system is shown in Fig. 3*a*.

In the second, more complex system, end customers are supplied from 35/10 kV main transformer, via 10 kV feeders. LV end customers are supplied via 10/0.4 kV substations. The 10 kV network is in an urban area and consists of predominantly underground cables. Test system parameters are given in Table 3 in the Appendix.

A simulation model is developed in MATLAB/Simulink software, and presents a three-phase model of the part of the Mostar distribution network. This system is shown in Fig. 3*b*.

The faults and measurements are performed on 10 kV underground cable that feeds the entire load area. Faults are simulated for different fault resistances (in the range of 20–600 Ω), and at different fault locations. The simulated faults are line-to-ground fault (LG), double LG (LLG) and triple LG (LLLG).

Current protection relays and measuring equipment in the Bosnia and Herzegovina PDN have the sampling frequency of 3.2 kHz. Since this equipment already runs with this sampling frequency, the logical upgrade would be to use this equipment coupled with proposed algorithms. This fact is the basis for the choice of this sampling frequency.

For the proposed DWT–ANN algorithm, no fault and three types of faults conditions are simulated, for various resistance range and fault locations, giving a total of 1600 fault scenarios.

The simulation model for VPD classifier is performed with same fault resistance and fault location range and total of 2000 fault scenarios are obtained.

4.2 Outline of the computational procedure for DWT–ANN algorithm

After simulating the fault, for each fault and different values of fault location and resistance, the voltage waveforms are generated. Since the fault resistance rises up to the 600 Ω, voltage waveforms in the range of high impedance will be considerably damped. The fault is sustained during the entire simulation interval, i.e. (0–0.08 s). When the voltage waveforms are generated and collected, DWT can be applied. In this case, a Daubechies 4 wavelet is used on a 3.2 kHz signal, and thus one approximate and four details of components are obtained. The algorithm is also tested by Symlet 4 and Biorthogonal 4.4 wavelet families, and output results are the same or similar. Therefore, it is not necessary to be particularly cautious regarding the choice of wavelet family. The signals shown in Figs. 2*a–c* represent a DWT for faulty phase voltage in every fault type (for one value of fault location and resistance). These signal components give a good insight into system behaviour during the fault conditions. For this reason, they are used as representative signals for each fault type. Afterwards, these signals are used to create the grouped DWT signal, which represents the input to the ANN. Once trained ANN is capable of fault detection and classification, according to the algorithm as shown in Fig. 1*a*. This procedure is further discussed in Section 5.

With the measuring equipment installed in PDN, voltage waveforms can be measured and sent to the industrial computer with DWT–ANN algorithm software. In the case of fault, the trip signal is sent to the circuit breaker.

4.3 Outline of the computational procedure for VPD algorithm

After simulating the fault in the PDN for different fault locations and different values of fault resistance, the voltage waveforms are

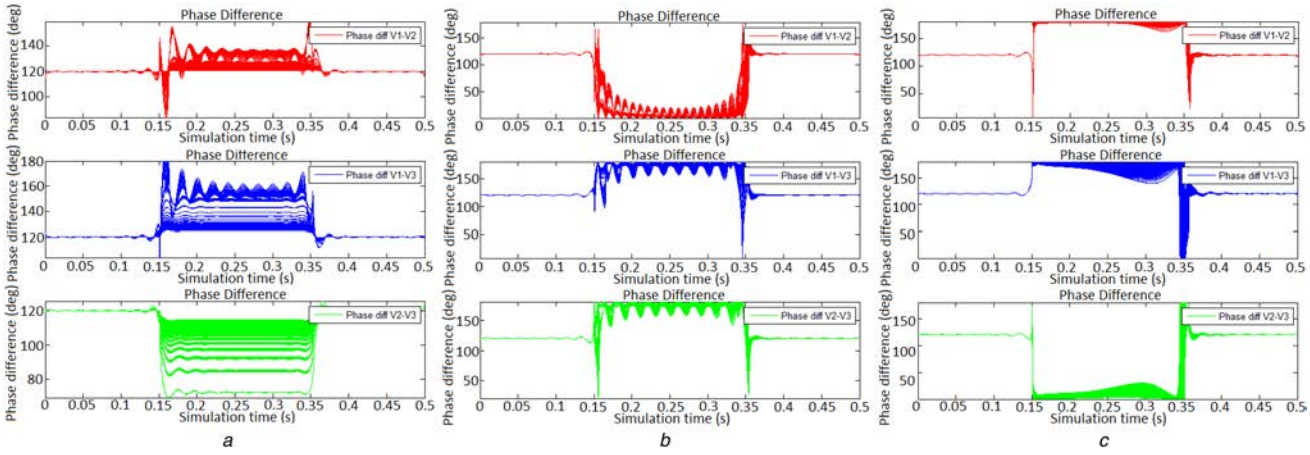

Fig. 4 *VPDs*
(a) LG HIF fault, ***(b)*** LLG HIF fault, ***(c)*** LLLG HIF fault

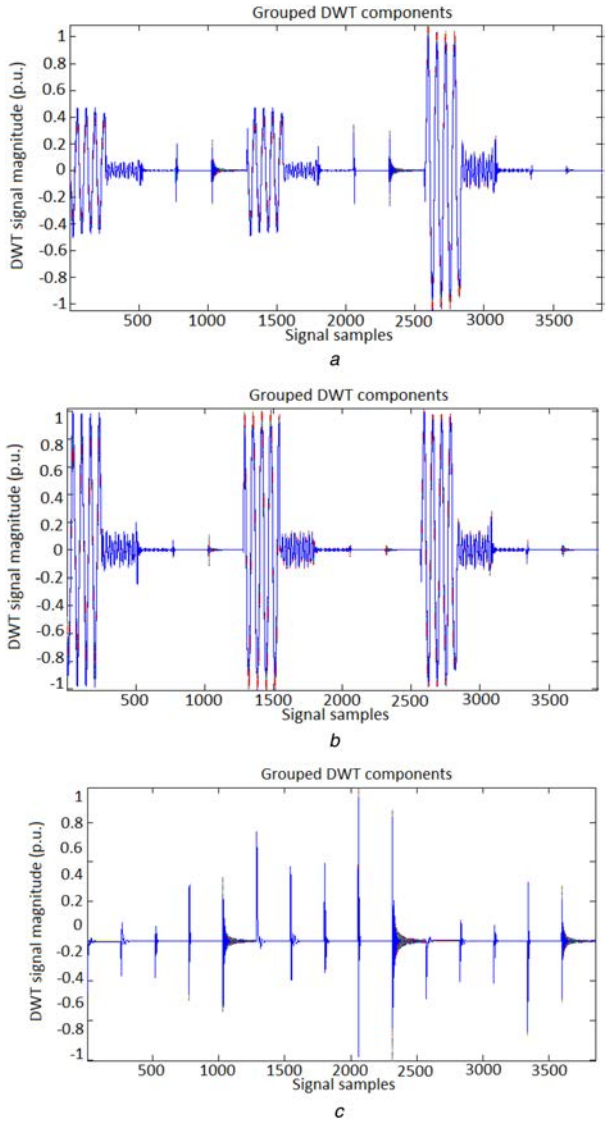

Fig. 5 *Grouped DWT components signal*
(a) LG HIF fault, ***(b)*** LLG HIF fault, ***(c)*** LLLG HIF fault

generated. A total of 500 fault scenarios for each fault type (2000 in total) are simulated. As a result of a Hilbert transform applied to the voltage signals, instantaneous frequencies can be obtained, as explained in Section 3. This data is used to calculate the PD between the system voltages over time. Fault start is simulated in the 0.15 s of the simulation, lasting until the 0.35 s. VPDs for 500 scenarios recorded during the fault in the case LG, LLG and LLLG faults are shown in Fig. 4. This data is used to set the range of VPD values that are characteristics for each fault scenario. As a result of this method, faults can be detected and classified, by monitoring the VPD value change in every voltage phase, according to the algorithm shown in Fig. 1*b*. This procedure is further discussed in Section 5.

Similarly to the DWT–ANN algorithm, with the measuring equipment integration in the PDN, voltage waveforms can be obtained and sent to the industrial computer with VPD algorithm software. In the case of fault, the trip signal is sent to the circuit breaker.

5 Results and discussion

This section of this paper presents the results of the proposed algorithms application. First, the DWT–ANN algorithm application results are presented and discussed, followed by presentation of the results and discussion of the VPD algorithm application. The advantages and disadvantages of both algorithms are compared and discussed.

5.1 Results and discussion of the DWT–ANN algorithm

During the PDN faults identification and classification process, it is necessary to observe the behaviour of the DWT components and PDs in all voltage phases, because each phase components reflect certain behaviour under fault conditions.

First, it is necessary to create input data for ANN training. To get a real insight into the system behaviour under the fault conditions, it is necessary to create a signal that contains DWT components from all three voltage phases.

The grouped DWT signal presents a signal that is built simply by adding the start of the next signal to the end of the previous signal, using the details and approximation waveforms for each fault scenario in the system. This signal is not equivalent to the actual signal; it is composed from the DWT waveforms of the currently measured voltage signal. By adding all these signals into one specific signal, a unique signal that provides the insight into the specified fault scenario in the system is created. Fig. 5 presents the grouped signals for all LGF, LLGF and LLLGF fault scenarios. The fault is simulated with different fault resistance values, and different fault locations; therefore, every figure shows 400 scenarios for each fault type. Differences between signals for particular fault type are apparently negligible, but ANN will be capable to classify them correctly. Higher-harmonic components which are important for identification process can be efficiently identified in the DWT filters of the corresponding frequency range. Generally, DWT is widely used for the noise removal applications [21, 22]. Moreover, since the proposed algorithm is paired with ANNs, which are known to have high accuracy in pattern classification and noise removal ability, this issue is addressed even more effectively.

Table 1 Output of the DWT–ANN classifier for different fault resistances, fault locations and fault types in an 8-bus test system

Resistance, Ω	Fault location (% length)	Desired output				Actual output			
		LGF	LLGF	LLLGF	No fault	LGF	LLGF	LLLGF	No fault
20	0.01	1	0	0	0	0.9997	0.0052	0.0011	0
110	0.16	0	0	0	1	0.0029	0.0023	0.0018	0.9959
200	0.31	0	1	0	0	0.002	0.9969	0.0013	0.0015
290	0.46	0	0	1	0	0.0012	0	0.9999	0.0001
380	0.61	1	0	0	0	0.9992	0.0014	0.0013	0.0001
470	0.76	0	1	0	0	0.0021	0.9969	0.0013	0.0015
560	0.91	0	0	0	1	0.0029	0.0023	0.0018	0.9959

Table 2 Output of the VPD classifier for different fault resistances, fault locations and fault types in an 8-bus test system

Resistance, Ω	Fault location (% length)	Desired output				Actual output			
		LGF	LLGF	LLLGF	No fault	LGF	LLGF	LLLGF	No fault
20	0.01	1	0	0	0	1	0	0	0
110	0.16	0	0	0	1	0	0	0	1
200	0.31	0	1	0	0	0	1	0	0
290	0.46	0	0	1	0	0	0	1	0
380	0.61	1	0	0	0	1	0	0	0
470	0.76	0	1	0	0	0	1	0	0
560	0.91	0	0	0	1	0	0	0	1

When the grouped signals presented in Fig. 5 are created, they present the input data for the ANN training. The designed ANN takes in the sets of 1600 inputs, and 1600 corresponding outputs. The ANN has four outputs, each of them corresponding to the three types of faults and the normal operating conditions. Hence the outputs are either 0 or 1 denoting the absence or presence of a fault, and the various possible permutations can represent each of the various faults accordingly. The proposed ANN should be capable to accurately detect the fault, and distinguish between the three possible categories of faults, regardless of the fault resistance and fault location. After the training and testing processes, the created ANN is perfectly capable to classify faults in the distribution network.

To obtain a real insight into the work of the created classifier, it is necessary to test the algorithm with new signals, i.e. signals that the AN is not trained to. For this purpose, different fault simulations with different fault locations and fault resistance values are carried out. Table 1 shows the classifier results to this fault scenarios, where column *Desired output* presents simulated fault type and *Actual output* the evaluated fault type. Zero or one presents absence or presence of a specific fault. *Actual output* column presents the ANN output for each fault scenario, with evaluated values representing the each fault presence possibility. Furthermore, the highest value for each ANN output scenario could be set to 1, while setting all other outputs to 0 in order to get unambiguous fault type as output. The proposed DWT–ANN algorithm has a 100% accuracy in the range of 20–600 Ω, for all fault locations, in both 2-bus and 8-bus simulated distribution systems.

The proposed algorithm is suggested to be used in online mode. The storage method is important, since the grouped DWT components take a lot of storage. One present-day industrial computer with a somewhat larger hard drive (over 500 GB) would be enough for online monitoring. About 10 min old data could be deleted if no disturbances are recorded. However, voltage waveforms could be saved for later possible analysis.

Fault classifier based on the proposed algorithm does not take other possible faults that can occur in network; however, it is possible to take additional parameters and apply the same algorithm to train the NN to these new scenarios. This research is ongoing and additional fault parameters incorporation is part of the future research in this area.

5.2 Results and discussion of the VPD algorithm

The VPD method calculates the VPD between the normal operation scenario and fault scenario. In the normal condition, PD between phases should be 120°, as shown in Fig. 4, but during specific fault, this parameter is changed. Change of the PD is specific for every fault type, and therefore this parameter is used for fault detection and classification. This change for range of fault locations, and fault resistances is shown in Fig. 4, where the PD changes in the fault conditions (for 0.15–0.35 s), and goes back to the 120° after fault. Each subfigure in Fig. 4 presents a 500 fault scenarios for each fault type, and PDs V_1–V_2, V_1–V_3 and V_2–V_3. Using the PD change during the fault, an appropriate detection and classification algorithm is developed.

Table 2 contains the created classifier output for different fault simulations with different fault locations and fault resistance values. Zero or one present absence or presence of a specific fault.

The proposed classifier uses PD values calculated from the simulation. Real power system data may slightly vary, i.e. PD values may change even in normal operating conditions, and bring in an error in the current decision-making algorithm. Owing to that it is necessary to determine the boundary values for decision-making algorithm according to the system normal operating conditions. This algorithm performs well in a wide range of fault locations and fault resistances.

The phase shifts in unbalanced networks are present (and they are not the ideal 120°), but they are constant during certain period. The VPD algorithm tracks the change in the phase shift in a very short time (characteristic to the faulty conditions – fast PD changes), so the unbalanced network will not lead to the maloperation of circuit breakers.

In the 2000 fault scenario sample tests, the algorithm has a detection and classification accuracy of 92.5% in the 2-bus test system, where all misclassified scenarios come from the high-impedance distant faults. In the more complex 8-bus test system, 2000 fault scenario sample tests are simulated, and the algorithm has a detection and classification accuracy of 90.19%.

The VPD algorithm is suggested to be used in online mode. Similarly to the DWT–ANN algorithm, an industrial computer connected to the measuring equipment can be used for online monitoring.

6 Conclusion

HIFs in the PDN present a serious problem and need to be detected, classified and cleared by protection devices as soon as possible. However, the existing protection devices are not

completely reliable in performing these tasks, which open numerous research opportunities in this area.

This paper proposed two approaches for identification and classification of HIFs in medium-voltage PDN. Results demonstrated that both algorithms present a good solution for detection and identification of HIFs in the PDN. Accuracy of the DWT–ANN algorithm is 100% in the 20–600 Ω range of fault resistances and different fault locations. The ANN is not immune to the large load and switching state changes, and in order to overcome this, further ANN training is required.

Accuracy of the VPD algorithm is 92.5% on a 2-bus simulated model, and 90.19% on an 8-bus simulated model for various ranges of resistances and fault locations. Both algorithms proved to be promising methods for the future implementation of power system protection devices.

The VPD algorithm is more immune to parameter changes in the distribution network, but in real distribution systems, there are many dynamic changes that may affect the accuracy of the proposed algorithm, especially in the range of very high-fault resistances (>400 Ω). The VPD algorithm is less effective in the region of the very high-fault resistances, since very high resistance makes small or barely notable PDs that are not always detectable by the algorithm. For lower resistance values, the VPD algorithm is immune to any changes in the network, and thus presents a competitive fault detection and identification tool.

This paper is a part of an ongoing research, whose objective is to contribute to the development of an HIF detection device that has satisfactory accuracy for detection and classification of the HIFs. Moreover, important future research direction in this area should extend the number of system elements and scenarios that can lead to the false tripping signal.

7 References

[1] Hubana, T., Begic, E., Saric, M.: 'Voltage sag propagation caused by faults in medium voltage distribution network', in Hadzikadic, M., Avdaković, S. (Eds.): '*Advanced technologies, systems, and applications II (lecture notes in networks and systems)*' (Springer International Publishing AG, Switzerland), 2018 in press

[2] Jamil, M., Sharma, S.K., Singh, R.: 'Fault detection and classification in electrical power transmission system using artificial neural network', *SpringerPlus*, 2015, **4**, (334), pp. 1–13

[3] Saric, M., Hubana, T., Begic, E.: 'Fuzzy logic based approach for faults identification and classification in medium voltage isolated distribution network', in Hadzikadic, M., Avdaković, S. (Eds.): '*Advanced technologies, systems, and applications II (Lecture notes in networks and systems)*' (Springer International Publishing AG, Switzerland, 2018), in press

[4] Chen, K., Huang, C., He, J.: 'Fault detection, classification and location for transmission lines and distribution systems: a review on the methods', *High Volt.*, 2016, **1**, (1), pp. 25–33

[5] Wang, B., Geng, J., Dong, X.: 'High-impedance fault detection based on non-linear voltage-current characteristic profile identification', *IEEE Trans. Smart Grid*, 2017, **PP**, (99), p. 1

[6] Baqui, I., Zamora, I., Mazon, J.*, et al.*: 'High impedance fault detection methodology using wavelet transform and artificial neural networks', *Electr. Power Syst. Res.*, 2011, **81**, (7), pp. 1325–1333

[7] Ghaderi, A., Ginn, H.L.III, Mohammadpour, H.A.: 'High impedance fault detection: a review', *Electr. Power Syst. Res.*, 2017, **147**, (1), pp. 376–388

[8] Ferdowsi, F., Vahedi, H., Edrington, C.S.: 'High impedance fault detection utilizing real-time complexity measurement'. 2017 IEEE Texas Power and Energy Conf. (TPEC), College Station, USA, March 2017, pp. 1–5

[9] Routray, P., Mishra, M., Rout, P.K.: 'High impedance fault detection in radial distribution system using S-transform and neural network'. 2015 IEEE Power, Communication and Information Technology Conf. (PCITC), Bhubaneswar, India, October 2015, pp. 545–551

[10] Michalik, M., Rebizant, W., Lukowicz, M.*, et al.*: 'High-impedance fault detection in distribution networks with use of wavelet-based algorithm', *IEEE Trans. Power Deliv.*, 2006, **21**, (4), pp. 1793–1802

[11] Sedighizadeh, M., Rezazadeh, A., Elkalashy, N.I.: 'Approaches in high impedance fault detection – a chronological review', *Adv. Electr. Comput. Eng.*, 2010, **10**, (3), pp. 114–128

[12] Prasad, A., Edward, J.B., Ravi, K.: 'A review on fault classification methodologies in power transmission systems: part – I', *J. Electr. Syst. Info. Technol.*, 2017, **151**, doi: 10.1016/j.jesit.2017.01.004, early access

[13] Bakar, A.H.A., Ali, M.S., Tan, C.*, et al.*: 'High impedance fault location in 11 kV underground distribution systems using wavelet transforms', *Int. J. Electr. Power Energy Syst.*, 2014, **55**, (1), pp. 723–730

[14] Mishra, M., Rout, P.K., Routray, P.: 'High impedance fault detection in radial distribution system using wavelet transform'. 2015 Annual IEEE India Conf. (INDICON), New Delhi, India, December 2015, pp. 1–6

[15] Singh, S., Vishwakarma, D.N.: 'Application of DWT and ANN for fault classification and location in a series compensated transmission line'. 2016 IEEE Sixth Int. Conf. Power Systems (ICPS), New Delhi, India, March 2016, pp. 1–6

[16] Nag, A., Yadav, A.: 'Fault classification using artificial neural network in combined underground cable and overhead line'. 2016 IEEE First Int. Conf. Power Electronics, Intelligent Control and Energy Systems (ICPEICES), Delhi, India, July 2016, pp. 1–4

[17] Mokhtari, H., Aghatehrani, R.: 'A new wavelet-based method for detection of high impedance faults'. 2005 Int. Conf. Future Power Systems, Amsterdam, Netherlands, November 2005, pp. 1–6

[18] Choudhury, M., Ganguly, A.: 'Transmission line fault classification using discrete wavelet transform'. 2015 Int. Conf. Energy, Power and Environment: Towards Sustainable Growth (ICEPE), Shillong, India, June 2015, pp. 1–5

[19] Barnhart, B.L.: 'The Hilbert–Huang transform: theory, applications, development'. PhD thesis, University of Iowa, 2011

[20] Hanninen, S.: 'Single phase earth faults in high impedance grounded networks'. PhD thesis, Helsinki University of Technology, 2001

[21] Sarawale, R.K., Chougule, S.R.: 'Noise removal using double-density dual-tree complex DWT'. 2013 IEEE Second Int. Conf. Image Information Processing (ICIIP-2013), Shimla, India, December 2013, pp. 219–224

[22] Haider Mohomad, A.R., Diduch, C.P., Biletskiy, Y.*, et al.*: 'Removal of measurement noise spikes in grid-connected power converters'. 2013 Fourth IEEE Int. Symp. Power Electronics for Distributed Generation Systems (PEDG), Rogers, USA, July 2013, pp. 1–5

8 Appendix

A list of test system parameters are given in Table 3 (overleaf).

Table 3 Power system parameters

Component	Parameters
system voltages	$V_{MV1} = 35$ kV, $V_{MV2} = 10$ kV, $V_{LV} = 0.4$ kV and $f = 50$ Hz
transmission lines	$\text{length}_{L1} = 5.87$ km, $\text{length}_{L2} = 0.95$ km, $\text{length}_{L3} = 4.47$ km, $\text{length}_{L4} = 1.47$ km, $\text{length}_{L5} = 5.34$ km, $\text{length}_{L6} = 6.63$ km and $\text{length}_{L7} = 3.11$ km $Z_{L1} = Z_{L2} = Z_{L3} = Z_{L4} = Z_{L5} = Z_{L6} = Z_{L7}$ $R_1 = 0.206$ Ω/km and $R_0 = 0.96$ Ω/km $L_1 = 0.359 \times 10^{-3}$ H/km and $L_0 = 1.178 \times 10^{-3}$ H/km $C_1 = 0.254 \times 10^{-6}$ F/km and $C_0 = 0.118 \times 10^{-6}$ F/km
transformers 35/10 kV	$P_n = 8$ MVA, $R_1 = 0.0802$ Ω, $L_1 = 4.028 \times 10^{-4}$ H, $R_2 = 19.64 \times 10^{-3}$ Ω and $L_2 = 9.866 \times 10^{-5}$ H
transformers 10/0.4 kV	$P_n = 630$ kVA, $R_1 = 0.2495$ Ω, $L_1 = 4.873 \times 10^{-5}$ H, $R_2 = 1.33 \times 10^{-4}$ Ω and $L_2 = 2.598 \times 10^{-8}$ H